RPL-TDR-64-110 R-5638

TOTAL IMPULSE MEASURING SYSTEM FOR SOLID-PROPELLANT ROCKET ENGINE

FINAL REPORT

APRIL, 1964

SECOND PRINTING
AUGUST 1964

AIR FORCE ROCKET PROPULSION LABORATORIES
AIR FORCE SYSTEMS COMMAND
UNITED STATES AIR FORCE
EDWARDS, CALIFORNIA

PROJECT NO. 3850, TASK NO. 3850306

PREPARED UNDER CONTRACT NO. AF04 (611) - 8515

BY

V. C. PLANE

ROCKETDYNE
A DIVISION OF NORTH AMERICAN AVIATION, INC.
6633 CANOGA AVENUE, CANOGA PARK, CALIFORNIA

CLEARINGHOUSE FOR FEDERAL SCIENTIFIC AND TECHNICAL INFORMATION CFSTI
DOCUMENT MANAGEMENT BRANCH 410.11

LIMITATIONS IN REPRODUCTION QUALITY

ACCESSION # 605-491

☒ 1. WE REGRET THAT LEGIBILITY OF THIS DOCUMENT IS IN PART UNSATISFACTORY. REPRODUCTION HAS BEEN MADE FROM BEST AVAILABLE COPY.

☒ 2. A PORTION OF THE ORIGINAL DOCUMENT CONTAINS FINE DETAIL WHICH MAY MAKE READING OF PHOTOCOPY DIFFICULT.

☐ 3. THE ORIGINAL DOCUMENT CONTAINS COLOR, BUT DISTRIBUTION COPIES ARE AVAILABLE IN BLACK-AND-WHITE REPRODUCTION ONLY.

☐ 4. THE INITIAL DISTRIBUTION COPIES CONTAIN COLOR WHICH WILL BE SHOWN IN BLACK-AND-WHITE WHEN IT IS NECESSARY TO REPRINT.

☐ 5. LIMITED SUPPLY ON HAND: WHEN EXHAUSTED, DOCUMENT WILL BE AVAILABLE IN MICROFICHE ONLY.

☐ 6. LIMITED SUPPLY ON HAND: WHEN EXHAUSTED DOCUMENT WILL NOT BE AVAILABLE.

☐ 7. DOCUMENT IS AVAILABLE IN MICROFICHE ONLY.

☐ 8. DOCUMENT AVAILABLE ON LOAN FROM CFSTI (TT DOCUMENTS ONLY).

☐ 9.

PROCESSOR:

TSL-107-10/64

NOTICES

When government drawings, specifications, or other data are used for any purpose other than in connection with a definitely related government procurement operation, the United States Government thereby incurs no responsibility nor any obligation whatsoever; and the fact that the government may have formulated, furnished, or in any way supplied the said drawings, specifications or other data is not to be regarded by implication or otherwise as in any manner licensing the holder or any other person or corporation, or conveying any rights or permission to manufacture, use, or sell any patented invention that may in any way be related thereto.

Copies of this report should not be returned to the Air Force Laboratories unless return is required by security considerations, contractual obligations, or notice on a specific document.

This report is releasable to the Office of Technical Services, Department of Commerce.

RPL-TDR-64-110

TOTAL IMPULSE MEASURING SYSTEM FOR SOLID-PROPELLANT ROCKET ENGINE

FINAL REPORT

APRIL, 1964

SECOND PRINTING
AUGUST 1964

TECHNICAL DOCUMENTARY REPORT NO. RPL-TDR-64-110

AIR FORCE ROCKET PROPULSION LABORATORIES
AIR FORCE SYSTEMS COMMAND
UNITED STATES AIR FORCE
EDWARDS, CALIFORNIA

PROJECT NO. 3850, TASK NO. 3850306

PREPARED UNDER CONTRACT NO. AF04 (611)-8515

BY

V. C. PLANE

ROCKETDYNE
A DIVISION OF NORTH AMERICAN AVIATION, INC.
6633 CANOGA AVENUE, CANOGA PARK, CALIFORNIA

ACKNOWLEDGMENTS

The Instrumentation Research Group gratefully acknowledges the valuable efforts and contributions made by the following Groups and individuals to the overall program effort:

Mathematics and Statistics Group

J. M. Zimmerman - Group Scientist

M. R. Dubman - 1 degree of freedom dynamic analysis (general)

I. Mirsky - 2 degree of freedom dynamic analysis

R. Van Wyck - Computer program study of 2 degree of freedom system

D. Rothman - Statistical analysis of static test results of actual system

Research Design Group

R. R. Doubleday - Supervisor

J. L. Greening - Mechanical design of entire test stand and its components

A. B. Fabunan - Design detail of all test stand components

G. A. McMahon - Dynamic tester design

FOREWORD

This report was prepared by Rocketdyne, A Division of North American Aviation, Inc., Canoga Park, California, on Air Force Contract AF04(611)-8515 under Task No. 3850306 of Project No. 3850, "Total Impulse Measuring System for Solid-Propellant Rocket Engine (Research)." Contract AF04(611)-8515 consists of a program for the analysis and design (Phase I), fabrication and testing (Phase II), and installation and testing (Phase III), of an accurate (0.1%) solid-propellant total impulse measurement system for Edwards Air Force Base. This report is submitted to present the entire development of the system and constitutes the final report in the over-all program. It was prepared by the Research Instrumentation Group of the Rocketdyne Research Department.

ABSTRACT

Discussion and results of all main considerations comprising the three phases of program effort are presented: (1) preliminary considerations consisting of study of the EAFB use site and thrust integration system existing at the beginning (November 1962) of the Rocketdyne program, (2) new and original analyses of spring-mass systems to obtain sufficient information to ensure a satisfactory design for the Rocketdyne system, (3) mathematical analyses of a parallelogram compression-type engine suspension flexure system, (4) determination of specifications and performance requirements of all measurement system components consistent with the required overall system accuracy, (5) new and original design concepts and considerations of a remotely-operated high-precision hydraulic calibrator, (6) the Rocketdyne design of the solid propellant engine test stand, (7) technical negotiations with manufacturers to obtain components with the desired performance, (8) fabrication, inspection, and testing

of all critical components prior to system assembly to determine conformance with specifications, (9) construction of the test stand and alignment of critical components, (10) system tests and calibrations at Rocketdyne, (11) statistical analyses of Rocketdyne calibrations, (12) installation, tests, and calibrations at EAFB, and (13) witness of initial engine test firings at EAFB as well as general assistance to EAFB personnel in the measurement system operation, data acquisition and interpretation activities associated with the initial tests.

CONTENTS

ILLUSTRATIONS

SUMMARY

The culmination of all efforts in the program was the operational emplacement of a solid propellant total impulse measurement system with a total error less than 0.1% in the thrust range 1500 - 10,000 pounds and propellant burning time range 2 - 10 seconds. The achievement of this objective not only supplied the apparatus needed to obtain significant advances in the field of solid propellant performance determinations, but also clearly demonstrated that a considerable improvement is realizable in general test stand design, where accuracy of measurements is the primary concern.

INTRODUCTION

PROGRAM NEGOTIATION

The need for an accurate and dependable solid propellant total impulse measurement system has been apparent, for a number of years, to personnel working in the rapidly-expanding field of solid propellant development and application. This need resulted in a request from AFFTC Edwards Air Force Base, California to Rocketdyne (PR 186543, 19 April 1962), and other industrial firms, to propose a program leading to the construction and installation of a complete measurement system with an overall error not exceeding 0.1% at the 95% confidence level.

Rocketdyne's proposed system was described in report number R-3612P, 18 May 1962, and the contractual effort was begun 25 October 1962.

GENERAL DESCRIPTION OF MEASUREMENT SYSTEM

The preliminary study involved in the proposal indicated that the most satisfactory approach to the technical objective consisted of a statically and dynamically simple engine support and restraint, a remotely-operated precision calibration system, and accurate and dependable electronic measurement equipment. Serious consideration of measurement accuracy requirements showed that departures from conventional equipment and operational methods would be required. Accordingly, it was

seen that the motor should be supported on a simple, but effective, flexure system and restrained in operation by a stiff and dynamically uncomplicated concrete abutment. It was also anticipated that rapid and very accurate static calibrations of the entire system would be essential just prior to, and immediately after, an engine test, if the stringent accuracy requirement was to be met. Prior experience and study had indicated that this pre-operational feature could be realized by a remotely-operated hydraulic system consisting of a dead-weight tester and a precision hydraulic piston. The accuracy of such a system would be directly related to machined weights, and calibration of the system by the Bureau of Standards would provide the knowledge of the true accuracy of the overall calibration equipment.

Accurate production and utilization of the electrical counterparts of calibration forces and engine thrusts was expected to require not only a simple method but also electrical components with quality superior to the best commercially-available equipment. Accordingly, it was anticipated that the most suitable electrical system would utilize a precision strain-gage load cell energized by a very stable D.C. power supply, to produce D.C. signal voltages to a voltage-controlled oscillator whose output pulses are electronically counted to obtain total impulse of the solid propellant.

Detailed descriptions, specifications, and test results of all components of the system are contained in a later section of this report.

PHASE I: ANALYSIS AND DESIGN

STUDY OF EAFB SITE AND EXISTING SYSTEM

Discussions and use-site inspections with EAFB personnel resulted in agreement regarding the general measurement system approach previously taken by EAFB in the design and construction of equipment and facilities for solid-propellant evaluation studies (BATES). The basic method was identical to that proposed by Rocketdyne, namely, a load cell analog signal supplied to a voltage-controlled oscillator to produce a proportional pulse repetition rate whose pulses are cumulatively registered by an electronic counter. However, very substantial improvement over the previous application of this method appeared to be realizable through concentrated analytical and design efforts directed at component and system refinement, and by careful instrumentation engineering. As a result, specific design, installation and operational features of the existing EAFB system appeared to be undesirable and incompatible with the measurement objectives in this contract and are briefly listed as follows:

1. Calibration system

   The mechanical loading calibrator uses mechanical linkages to convert a vertical force to a horizontal force and appeared to be susceptible to an error of about 0.25%. Errors of this amount were intolerable in the present contractual effort.

2. Load cell

This component is a conventional unit and did not appear to possess the superior quality that would be needed in the Rocketdyne effort.

3. Instrumentation wiring

Conversations with EAFB operating personnel indicated the presence of four or five connections between the load cell, at the test stand, and the electronic integrator in the control room. This type of wiring is very susceptible to environmental interferences and was not compatible with the technical objectives in the proposed system.

4. Intermediate circuitry

The EAFB system in use at the start of the present effort also employed circuitry between the load cell output and the integration equipment to provide flexibility of operation with one-, two-, and four-arm bridges. The use of such extraneous equipment provides a possible source of additional errors.

5. Integration equipment

The equipment employed possessed performance capabilities satisfactory for most purposes, but was not considered suitably linear and stable enough to yield measurements with errors less than 0.1%.

The afore-mentioned parts of the EAFB system existing in Nov. 1962, and others, while providing flexible equipment and methods also provided errors considered too large for the Rocketdyne system. Consequently, the EAFB system demonstrated that high accuracy and flexibility are incompatible, and that some improvement in accuracy could be obtained by the sacrifice of some circuitry flexibility. Also, it was seen that additional accuracy could be obtained by component improvement and refinement.

MATHEMATICAL ANALYSIS OF SPRING-MASS SYSTEMS

Mathematical analysis was an essential part of the effort to design and build a total impulse measurement system possessing the accuracy required in the contractual effort. Its application ranged from its use to determine both general and specific guide-lines during the system design phase to its use in an accurate and detailed evaluation of the system after its construction. The objective of all mathematical analysis undertaken in this contractual effort was the mathematical characterization of the system for the purpose of a quantitative determination of its behavior in the performance of its measuring function. The analyses consisted not only of static equilibrium considerations needed in motor suspension flexure system design and constructional alignment operations, but also of dynamic response determinations of the mechanical system to transient force excitations similar to thrust outputs encountered in rocket motor propellant

tests. Accordingly, the range and type of analyses reflected the variety of inquiries directed, at various times, to the design aspects of the over-all constructional problem, and the following sequence of Phase I mathematical efforts corresponds to their actual chronological occurrence.

1. General treatment of the relationship between the actual and measured impulse for certain linear dynamic systems, including a preliminary discussion of the impulse errors incurred by less-than-infinite integrations of indicated displacements. No numerical examples were undertaken in this initial effort because its purpose was a general discussion and elaboration of the basic idea underlying the measuring function.

2. Determination of errors in the measurement of impulse by a viscously-damped one-spring, one-mass (one-degree) system excited by rectangular and trapezoidally-shaped force-time inputs. Its purpose was to obtain some numerical results with a system-excitation combination which approximated an actual thrust-measuring system and rocket motor. The results of this undertaking provided the initial quantitative indication of the adequacy of the mechanical system design.

3. Determination of errors in the measurement of impulse by a two-spring, two-mass (two-degree) system. Its purpose was a more accurate and detailed study of the actual Rocketdyne measurement

system, consisting of a series-connected massive concrete block, a thrust-measuring load cell, and the motor and mount assembly. The representation of the system in this study was the most advanced model undertaken in the Phase I effort. Its purpose was the determination of the effects on the impulse measurement error of such characteristics as concrete-block compliance, variable motor mass (propellant burning), non-viscous damping, and nonlinear force-displacement calibrations because of load-cell aging and/or imposed bending moments. The results of this advanced study provided the greater part of the justification of the design employed in the designed system.

FLEXURE SYSTEM DESIGN ANALYSIS

The purpose of this effort was to effect a compatible design of a flexure system engine support with a load cell spring and abutment restraint. The method consisted of the determination of translational stiffness, in the three coordinate directions, of a parallelogram, compression type, flexure system used for the motor suspension, and of its rotational stiffnesses about the three coordinate axes. The result of this effort was the determination of a suitable combination of flexure system and load cell mechanical stiffnesses that effectively isolated the load cell from extraneous forces and moments that would degrade its basically linear performance. The application of the results to the flexure system design thereby

minimized both the problem of nonlinearities in the system calibration and the problem of incorrect measurement of off-axis motor thrusts.

DESIGN OF ROCKETDYNE MEASUREMENT SYSTEM

The result of all Phase I effort was the detailed design of the Rocketdyne total impulse measurement system. This system provides measurements, with errors not exceeding 0.1%, of solid propellant motor thrusts, and its time-integral, total impulse, at thrust levels in the 1500 - 10,000 pound range, and for propellant burning times in the range of 2 - 10 seconds. Descriptions of the system are provided by the functional, physical, and electrical discussions that follow.

Functional

The solid propellant motor, when fired, produces a thrust force which compresses a strain-gage load cell to obtain a dc voltage which is linearly proportional to the thrust force. This dc voltage-equivalent of the motor thrust controls the generation of a train of voltage pulses by a voltage-controlled oscillator, and the repetition rate of the pulses is linearly proportional to the dc voltage and, hence, motor thrust. An electronic counter totalizes the number of pulses produced during the propellant burning time, and the number so produced is, consequently, linearly proportional to the time-integral of the thrust, or total impulse, of the burned propellant. Figure 1 shows a block diagram of the described measurement system.

The calibration of the entire system is accomplished by the use of a force calibration system which utilizes a dead-weight tester to provide a hydraulic pressure standard within a piston-cylinder assembly of precisely known effective cross-sectional area. The product of the pressure and the area gives a known force. The piston cylinder assembly is essentially a dead-weight tester operated in reverse. In order to resolve very small pressure increments into a resultant force with essentially zero hysteresis, a lapped fit between the piston and cylinder is provided. Either the piston or the cylinder is rotated with respect to the other and the hydraulic oil provides the lubrication. In this manner no packing glands or O-rings are required to effect a seal. The forces produced by the calibrator are mechanically transmitted to the motor support by rods extending through clearance holes in a massive concrete retaining abutment. The total impulse calibration of the entire system is accomplished by counting the number of pulses generated in one second by one of the specific static calibration forces. The calibration constant is obtained by the division of this number by the value of the static force. The units of the calibration constant obtained by this method are consequently the number of pulses per pound-second of impulse. In order to obtain the most accurate use of the measurement system, static calibrations are made immediately before and after each propellant test to eliminate the effects of long-term drifts in the determination of the calibration constant used in data reduction operations.

Physical

The general configuration of the mechanical system and components of the 20' x 5' x 5', approximately 22,000 pounds, two-piece, test stand is shown in Fig. 2 and in several of the accompanying photographs. The larger, 13' long, approximately 18,000 pounds forward section consists of: (1) a motor support section, (2) a thrust collector and distributor section, (3) a concrete abutment and I-beam base frame, and (4) the calibration piston assembly and tie-rods. The smaller, 7' long, approximately 4000 pounds, rear section of the two-piece test stand consists of: (1) the master pressure standard, consisting of precision dead-weights and hydraulic cylinder (dead-weight gage), pump, valves, and oil reservoir; (2) an electronic calibration control box, (3) a weather-tight enclosure for the protection of the calibration system, and (4) the primary and secondary I-beam base frames.

The installation provisions on the test stand include lifting-eye bolts on both sections, six tiedown bolt locations on the larger, forward section (two each at the fore and aft ends of the concrete abutment and two at the motor end) and four tiedown bolt locations on the smaller, rearward section (two at each end). Elevation adjustment bolts are provided at the sides of both sections to facilitate level installation when used in conjunction with suitable shims located adjacent to the tiedown bolts (see Fig. 22 and 25 for details).

The general mechanical configuration of the electronic equipment cabinet located in the control room is shown in Fig. 27 and 28. The enclosure contains the integrating digital voltmeter which performs the electronic integration of the thrust-time curve, the load cell power supply and bridge balances, and the control panel for the remote operation of the calibration system. Not shown is a pulse modifier to enable the accurate counting during the playback of the tape recording of the voltage-controlled oscillator pulses.

Electrical

The electronic measurement system consists of two specially constructed metal foil strain gage bridges, in a single load cell, powered and balanced, respectively, by an all-transistor supply and Kelvin-Varley voltage dividers designed and constructed specifically for use in this system. The bridge output signals are supplied directly to a precision integrating digital voltmeter, with no intermediate attenuating circuitry. To reduce electrical noise to a minimum, the system features a floated and completely shielded measuring circuit extending from the strain gage load cell on the test stand to the electronic integrator, power supply, and bridge balances in the remotely located control room. The circuitry in the power supply and bridge balances are isolated from their respective chassis, which are, in turn, isolated from their respective front panels. In this manner, these units are insulated from their common mounting rack in order that their separate ground wires would provide maximum versatility in grounding problems invariably encountered in precision electronic measurements.

The measurements of total impulse are presented as a direct reading digital display and also as a pulse train output which, if suitably recorded and played back at a later time, provides the basic information needed in any delayed integration. A very wide range of measurement sensitivity, along with very high resolution, is provided by the dual means of digitally selectable input power to the thrust transducer and the multi-range input circuit of the integrator. Identification of specific components of the measurement circuit includes a Baldwin-Lima-Hamilton Corporation special type C3P2S load cell, Systems Research Corporation special Model 3512A digital power supply and Model 4700A bridge balances, and a Dymec (Hewlett-Packard Company) Model DY-2401A integrating digital voltmeter. Complete specifications for stability, linearity, hysteresis, and temperature effects are given in a later discussion of all electrical measurement system components.

Simplicity, maximum accuracy, and utility of equipment is provided by the single integrating digital voltmeter employed at the strain gage output. Its use provides (1) the necessary high-accuracy bridge balance indicator during pre-calibration procedures, (2) the high-accuracy one-second integrator needed in static calibrations of the system, and (3) the externally-gated integrator necessary for extended-time integrations of motor thrust-time curves.

The electrical features of the hydraulic calibration system are associated with both its remote operation and its accuracy. Geared-down electric motors rotate the cylinder of the piston assembly and the support of the

pressure-producing weights in the master pressure standard to eliminate static friction forces otherwise present. Associated with the remote programming of static forces are solenoids to actuate the weight-holding pins, electric motor drive of the hydraulic pump, and photocell weight-position detecting circuits.

PHASE II: FABRICATION AND TESTING AT ROCKETDYNE

COMPONENT DESCRIPTIONS

Concrete Abutment and Support Bases

Motor thrust forces are transferred to a welded I-beam supporting base frame by a reinforced-concrete block 5 feet long, 4 feet high, and 4 feet wide, weighing approximately 6 tons. Figure 30 shows the block during its curing period. The block serves the dual purposes of a rigid restraint and an accurate reference for alignment of critical calibration and measurement components. Its weight also provides restraint against overturning moments produced on it by motor thrust forces. The motor thrust forces enter the block through a 12" x 12" x 2" steel plate and are transferred to the welded I-beam support frame by a 2-inch-thick steel base plate extending under the entire block. Reinforcing rods, $\frac{3}{4}$-inch diameter, are spaced at 6 inch intervals from top to bottom and are welded to the base plate.

The reaction forces associated with the static calibration forces enter the block through an identical rear plate, and both imbedded plates are internally secured to the concrete by horizontal reinforcing rods. Figure 31 and 32 show the internal details of the reinforcing steel prior to concrete pouring, and Fig. 33 and 34 show, respectively, the form design for the concrete abutment and its pouring. All internal steel surfaces of the base

plate and forward and rear mounting plates were bonded to the concrete by thiopoxy cement. Accurate installation and alignment of the hydraulic calibration piston and the load cell assembly were obtained by accurate machining of the fore and aft mounting plates after dimensional stability of the concrete was obtained by a full 28-day curing time. A pattern of ¼-inch holes was accurately machined in each mounting face in which dowel pins are placed during test stand leveling operations. Twenty-two ¾-inch-diameter bolts secure the concrete block base plate to the forward I-beam base assembly, 10 of which are visible along its edges. 5 on each side of the block (see Fig. 25).

Both of the forward and rear I-beam base assemblies consist of 3 lengthwise sections of 10-inch-high beams welded together by cross beams. Figure 35 shows the detail of the forward base assembly. The forward base frame is connected to the EAFB test pad by 6 tiedown bolts of the design previously utilized in the BATES program, and the rear base frame by 4 tiedown bolts, 2 on each end. Leveling adjustments on both I-beam base assemblies is accomplished by the use of elevation bolts located along their sides (see Fig. 22 and 25). Detailed specifications and test results of the concrete abutment are contained in a later section of this report.

Motor Mount Assembly

The entire motor mount assembly consists of two aluminum support blocks (containing adjustable buttons) on a horizontal platform, 2 supporting flexures and a secondary mount assembly which connects the platform to the

load cell assembly (see Fig.24). The adjustable buttons enable the alignment of the motor and load cell axes. The platform consists of a welded aluminum I-beam and plate assembly and the secondary mount assembly includes a braced thrust plate in direct contact with the head end of the motor. The motor is secured to the support blocks by adjustable chains and to the thrust plate by a clamp ring and a long bolt through the motor head flange. The secondary mount assembly provides connections for the calibration tierods and alignment of the assembly with the load cell assembly is accomplished by a close fitting recess in its mating face. The steel compression-type parallelogram flexure system, which supports the motor and platform assembly, features one-piece flexures designed to be compatible with load cell transverse force sensitivity, in order that motor thrust force measurements are not degraded by response to bending moments incurred by off-axis thrusts.

Load Cell Assembly

The load cell assembly, shown in detail B of Fig. 2 and in Fig.24, consists of the series combination of the thrust dome, load cell, and distributor. The conical shapes of the dome and distributor, respectively, collect and distribute the motor thrust force to, and from, the load cell. Coaxial alignment of the components of this assembly, is accomplished by the use of centerline holes in the load cell into which fit integral centerline pins on the dome and distributor. Symmetrical minimum-size slots enable the installation and removal of propellant igniters in the motor head. The

entire load cell assembly is aligned with the front mounting face center hole by an integral pin machined on the load distributor.

The load cell component of this assembly is a specially designed and constructed unit obtained from the Baldwin-Lima-Hamilton Corporation, Waltham, Massachusetts. Technical negotiations between Rocketdyne and Baldwin-Lima-Hamilton resulted in the design and construction of a load cell with an accuracy exceeding that of their precision units. Important additional calculated data and actual test results were obtained for this unit concerning mechanical stiffness and electrical sensitivity to transverse loads, bending and twisting moments. These mechanical and electrical data enabled an adequate design analysis to be made of a suitable motor suspension flexure system. Figure 3 shows the external features and dimensions of the load cell, and Fig. 4 is its electrical schematic drawing. A discussion of the specifications and performance of this load cell is given in a later section of this report.

Calibration System

The hydraulic, remotely-operated, force calibrator utilized in the total impulse measurement system is a specially designed and constructed unit obtained from the Ruska Instrument Corporation, Houston, Texas. Technical negotiations between Rocketdyne and Ruska resulted in the design and construction of a force-production system whose performance is believed to be unmatched in systems of this type.

The entire hydraulic calibration system was calibrated by the National Bureau of Standards, Washington, D.C. prior to its shipment to Rocketdyne. It is operable either locally at the test stand or remotely in the test control room. The remote-operation feature of the calibration system permits its use immediately before and after a propellant test to obtain the most timely system calibrations possible.

The hydraulic force calibrator consists of the combination of a master pressure standard and a precision hydraulic cylinder. Precise hydraulic pressures, produced in the pressure standard by accurate dead-weights supported on an oil column, are transmitted to a precision piston-cylinder assembly to produce the accurate calibration forces. The dead weights were accurately machined to produce forces of 1000, 2000, 4000, 6000, 8000, and 10,000 pounds at locations where the local value of gravity acceleration is 979.477 gals (the value at test pad No. 5, Solid Motor Test Area, Rocket Propulsion Laboratory, EAFB on January 18, 1963). More specifically, the calibration system is essentially a hydraulic lever with which a large force may be compared to a smaller force in such a manner and with such precision as to economically justify the hydraulic method of comparison as opposed to other methods presently in use. The hydraulic lever system consists of two loaded pistons of unequal areas against which a common fluid may be pressurized to obtain equilibrium of the larger and smaller forces. The system is considered to be in equilibrium or in balance when the axial load on one piston divided by the piston area is equal

to the load on the other piston divided by its area. In the described calibrator, the smaller piston and a set of standardized masses constitute the dead-weight tester portion of the entire apparatus, while the larger piston, independent of the loading mechanism, is referred to as the cell or as the force cell. The remote control of the selection of prescribed static forces is accomplished by the programming of solenoid-actuated weight-holding pins which, at a given calibration test point, support all weights not desired and allow the pressure-producing weights to be supported by the oil column. Figures 25 and 26 show the major components and installation configuration of the system and Fig. 5 and 6 show component configuration and design features. Figure 36 shows the calibration system during its calibration at the National Bureau of Standards, Washington, D.C.

Load Cell Power Supply

The Systems Research Corporation, Van Nuys, California, Model 3512A digital power supply used for the load cell excitation is a highly stable and electrostatically isolated power supply specifically designed for applications where precision and resettable dc voltages are required. Its primary function in the system is to provide a precise and accurate setting of the range of the strain-gage load cell. The selection of voltages is accomplished from the front panel by means of 5 switches, and any particular value selected is supplied to 2 identical outputs at the rear panel for the excitation of the two strain-gage load cell circuits. The selected value of voltage also appears at the front panel binding posts to accommodate an external monitoring voltmeter, if desired. The circuit of the power supply is a

transistorized, regulated and isolated configuration producing 0 - 18 vdc output up to 200 ma. Referring to the schematic diagram shown in Fig.7 , 115 vac, 60 cps power is applied through the rear line cord to the input transformer T1. T1 is a laminated double-shielded type transformer providing two secondaries, S1 and S2. S2 is tapped to provide a reference voltage supply and connects to a full wave bridge and filter network to produce a dc voltage. This dc voltage is fed through Q1, the series regulator transistor and hence to the output. Regulation is achieved by comparing the output voltage to a stable zener diode reference circuit Z5. Q7, Q8, Q9 and Z4 comprise a regulator that stabilizes the reference voltage across Z5. The output voltage and reference voltage are compared by the difference amplifier Q5 and Q6. The stability of the difference amplifier is maintained by holding the collector voltage constant through the regulator circuit of Z2, Z3, and Q4.

The output of the difference amplifier then serves as the controlling voltage to bias the series regulator transistor Q1 and must be amplified through Q2 and Q3. The gain of this feedback loop controls the response and sensitivity of the overall regulation. The S1 secondary of T1 feeds a separate full wave rectifier and filter to produce the operating voltages for Q2 and Q3.

Figures 28 and 29 show details of the front and rear panels. Specifications and test results of this component are contained in a later section of this report.

Bridge Balances

The Systems Research Corporation model 4700 A digital bridge balance units associated with each load cell strain gage circuit employs decade switching of precision voltage dividers connected in a Kelvin-Varley arrangement. By accurate selection of close tolerance resistors, superior accuracy is obtained and resolution to 5 significant figures, or 1 part in 100,000 is realized. Six front panel mounted controls allow nulling with bridge unbalances as high as ±5%. The precision resistors possess excellent repeatability. Terminals are provided for a limiting resistor, if desired, otherwise these terminals are jumpered. Connections are supplied at the rear panel of each bridge balance unit to its associated strain gage circuit, power supply output, and recorder or indicator. A schematic diagram of these units is contained in Fig. 8 .

Integrating Digital Voltmeter

A Dymec (Hewlett-Packard Company) model 2401 A integrating digital voltmeter is employed for all electrical measurements performed in the calibration and use of the Rocketdyne total impulse measurement system. Its versatility and range provide the means for obtaining very close bridge balance prior to calibration of the system, the accurate indication of load cell output signals during calibration, and the electronic integration of the voltage-time characteristic supplied by the load cell during propellant test operations.

All measurements are indicated on a 5-digit display, and a sixth position on the display is provided to indicate the engineering units of each measurement and the polarity of dc voltages. An internal ±1 volt standard is provided for self-calibration. In addition to visually-displayed measurements, means are provided at the rear panel for recording of the basic test data in digital form, namely, a pulse-train output whose pulse repetition rate is directly proportional to motor thrust. A separate Rocketdyne-designed system, used in conjunction with the Dymec unit, will provide satisfactory tape recording playback of the pulses in the output. By this means, propellant test data can be stored and processed at a later time.

A full description of the design and use of this instrument is contained in a separate handbook prepared by the Dymec Division of the Hewlett-Packard Company. The external appearance of the instrument is shown in Figures 27, 28, and 29.

SPECIFICATIONS AND TEST RESULTS OF CRITICAL COMPONENTS

1. CONCRETE ABUTMENT

A. Specifications

(1) Concrete - 4000 psi crushing strength

(2) Machining of forward and rear mounting faces

Each surface flat within 0.001 inch total

Each surface normal to a common axis within 0.005 inch total

Surfaces parallel to each other within 0.005 inch total

(3) Mounting surface reference holes: $\frac{1}{4}$ inch holes

5.250 inches apart

B. Measurements

(1) Concrete - 5400 psi crushing strength: see Fig. 9

(2) Machining of forward and rear mounting faces

Forward mounting surface flat within 0.001 inch

Rear mounting surface flat within 0.0008 inch

Each surface normal to a common axis within 0.0045 inch

Surfaces parallel to each other within 0.003 inch

(3) Mounting surface reference holes: see Fig. 11

2. LOAD CELL

A. Specifications (to be met by test results)

(1) Full scale load: 10,000 lbs compression

(2) Full scale output: 3 mv/v input (±0.15%)

(3) Input volts: 18 vdc

(4) Bridge resistance: 350 ohms nominal, each bridge

(5) Nonlinearity: less than 0.03% full scale

(6) Hysteresis: less than 0.02% full scale

(7) Repeatability: less than 0.01% full scale

(8) Temperature effects:

(a) On zero output: less than 0.15% F.S./100 F

(b) On sensitivity: less than 0.08% of load per 100 F

(9) End-plate pilot and mounting holes: see Fig. 3

B. Additional Specifications (to be met by a combination of calculations and tests)

(1) Mechanical

(a) The transverse stiffness is to be in the order of 1×10^6 (one million) lbs per inch in any direction, assuming the load is supplied at the top of the cell (5 inches from base).

(b) The torsional stiffness is to be in the order of 20×10^6 (20 million) pound-inches per radian or less.

(c) The bending stiffness for a couple applied to the end of the cell tending to bend the axis of the cell is to be in the order of 25×10^6 (25 million) pound-inches per radian in any direction.

(2) Electrical

(a) The cell response to a 500 lb transverse load is to be a maximum span change of $\pm 0.15\%$ of full scale, and this change increases and decreases sinusoidally as the direction of loading is rotated about the cell.

(b) Cell response to torsion is to be negligible within a limit of 1000 pound-inches.

(c) A moment of 2500 pound-inches applied at the end of the cell is to have the same effect as item (a).

(3) Test Results

(a) Capacity: 10,000 lbs

(b) Full scale output: 3.0010 mv/v input

(c) Input volts: 25 vdc recommended maximum

(d) Bridge resistances: 350.2 and 350.3 ohms

(e) Nonlinearity: 0.01% full scale: see Fig. 12

(f) Hysteresis: 0.003% full scale: see Fig.12

(g) Repeatability: 0.013% full scale: see Fig. 12

(h) Temperature effects: same as required

(i) End plate pilot and mounting holes: as required

(j) Response to 500 lb transverse load: 0.15% full scale: see Fig. 13

(k) Response to 2500 pound-inches moment applied at the end of the cell: 0.15% full scale: see Fig. 14

3. HYDRAULIC CALIBRATOR

A. Specifications

(1) Six calibration points required: 1000, 2000, 4000, 6000, 8000, and 10,000 pound force.

(2) Accuracy of each force point: ±0.05%

(3) Resolution: 0.02% of full scale

(4) Float time of dead-weight gage and force-piston cylinder shall be at least one minute for each calibration point.

(5) Hydraulic pump capacity shall be sufficient to provide at least one complete calibration (ascending and descending), including any leakage without refilling.

(6) The dead-weight gage must be capable of being remotely operated.

(7) Visual means shall be provided at the control console to indicate when the dead-weight gage is floating and a calibration point may be taken.

(8) Weights shall be applied in ascending or descending order selectable through a multi-position switch.

(9) The piston cylinder of both the dead-weight gage and force-piston cylinder shall be of the same material.

B. Test Results

(1) All specifications were met and exceeded; specific numerical data as follows:

(a) Accuracy of each point: ±0.02%, by reference to the dead weights used at the National Bureau of Standards.

(b) Resolution: 0.01 lb at 10,000 lbs (equivalent to one part in 10^6 or 0.0001% FS).

(c) Float time of dead-weight gage and force piston exceeds 10 minutes, provided that air is properly excluded from the hydraulic lines.

4. LOAD CELL POWER SUPPLY

A. Specifications

(1) Type: digitally programmable (decade switching)

(2) Input power: 95 - 135 vac, 60 cycles

(3) Output: digitally selectable 0 - 18 vdc, 0 - 200 ma. Two excitation outputs are required.

(4) Regulation: 0.01 percent NL-FL and 95-135 vac

(5) Ripple: 0.05 mv rms

(6) dc isolation: 10 K meg

(7) Stability: 0.005 percent/°C, and +0.01% in any 8-hour period

(8) Noise at bridge (350 ohm): 2 microvolt

(9) Overload protection: fused

(10) Overvoltage protection: limits output voltage to 18 vdc

(11) Current regulation: available by jumpering at rear chassis

(12) Size: $3\frac{1}{2}$" x 19" x 10" for rack mounting

B. Test Results

(1) All specifications were met or exceeded with the minor exception given as follows:

(a) Stability: 0.007 percent/°C: see Fig. 15. Long term stability of this component is shown in Fig. 16.

5. BRIDGE BALANCES

A. Specifications

(1) Type: decade switching of precision voltage dividers connected in a Kelvin-Varley arrangement

(2) Input: 3 wires to strain-gage bridge

(3) Resolution: balance to one microvolt with 350 ohm bridge

(4) Size: 3½" x 19" x 6" for rack mounting

(5) General: 6 front panel mounted controls to allow nulling with bridge unbalances of ±5%. Precision tolerance resistors of long term stability are to be used throughout. Quality switches of low contact resistance are to be used in order to assure excellent repeatability. Terminals are to be provided for a limiting resistor if desired. All switch positions in each decade are to be numbered to enable repeatable settings.

6. INTEGRATING DIGITAL VOLTMETER

A. Specifications (quoted by Dymec Div. of Hewlett-Packard)

(1) dc voltage measurements

(a) Noise rejection: overall common mode 140 db at all frequencies

(b) Accuracy specifications for ±10% line voltage change. Stability (at constant temp): ±0.03% of full scale. (0.1 volt range)

Linearity: ±0.005% of full scale (zero to full scale)

Temperature effects: (+10 C to +50 C)

Scale factor: ±0.002% of reading per °C

Zero ±0.002% of full scale per °C (0.1 volt range)

Internal calibration source: ±0.002% per °C

(2) dc voltage integration

(a) Accuracy same as for dc voltage measurement, with exception that errors given as percent of full scale must be multiplied by the integration time in seconds.

B. Test Results

(1) Laboratory tests, at the Rocketdyne Research Instrumentation Laboratory, of the integration capability of the Dymec 2401A integrating digital voltmeter, show correlation, within 0.02%, of theoretical input and measured values of area with pulses 1 volt high, pulse rise/fall times as fast as 500 microseconds, and durations in the range 20 to 200 milliseconds.

SYSTEM ASSEMBLY, ALIGNMENT, AND CHECKOUT

Test Stand

Assembly and alignment of the components of the larger, forward, section presented a problem readily solved by the use of tooling telescopes. The accurate machining of alignment and reference holes in the abutment forward and rear mounting faces established the measurement system axis of the concrete abutment. Mounting and alignment of the load cell assembly on the forward side, and the hydraulic calibrator force cell and tierod crossbar and flexure support, on the rear side, was accomplished by the use of these holes and tooling telescopes in the following sequence of operations:

1. Abutment leveling

   Using dowel pins in reference holes number 4 on both the forward and rear mounting faces, along with vertical alignment scales and a leveled telescope, the concrete block was leveled about a transverse axis by means of its elevation adjustment bolts. Leveling of the abutment about its longitudinal (thrust measurement) axis was accomplished by the use of dowel pins in the forward mounting face reference holes number 1 and 3 and an accurate spirit level.

2. Load cell assembly alignment

   Coaxial alignment of the components of this assembly is obtained by the accurate machining of integral center pins on both the load distributor and load collector which mate with the center holes machined in the load cell end bearing faces. Coaxial alignment of this assembly with the abutment axis is accomplished by the mating of an integrally-machined pin on the load distributor and the center hole in the abutment forward mounting face.

3. Hydraulic force cell forward bearing alignment

   Alignment of the force cell forward bearing is accomplished by the use of a close-fitting plug, half of which mates with the hole containing the force cell forward bearing plate, the other half of which mates with the abutment rear mounting face center hole.

4. Motor secondary mount assembly alignment

   This unit, also called the motor thrust plate, contained a machined recess which mated with the end of the load collector, and holes

equidistant from its centerline to accommodate the forward ends of the calibration tierods.

5. Hydraulic force cell rear bearing alignment

   Alignment of the force cell rear bearing is accomplished by the alignment of the calibration tierod crossbar which contains the rear bearing plate. The crossbar, with tierods and flexure support attached, is aligned with the abutment rear mounting face center hole by means of tooling telescopes and scales, using the machined edge of the abutment base plate for a horizontal reference plane and an arbitrary horizontal plane obtained by a leveled telescope. Figure 10 and Figure 37 show the reference dimensions and the equipment and methods used for alignment operations.

6. Motor platform and flexure suspension alignment

   Final alignment of this assembly, minus motor, was accomplished by the use of the elevation bolts at the foot of each motor suspension flexure. The vertical positioning of the platform and flexure suspension system by this method prevented bending loads from being imposed on the load cell during the installation of bolts to secure the platform to the secondary mount assembly.

Electrical wiring to the test stand consisted of two instrumentation cables to the load cell, (one for each strain gage bridge), and five cables for operation and control of the hydraulic calibrator. The load cell cable

connectors can be seen in Fig. 24 on the bottom of the load cell. The calibrator control cable connectors were installed on the rear end of the weathertight enclosure, and are shown in Fig. 38.

Measurement System Electronic Equipment

Figure 17 is a block-schematic diagram of the entire total impulse measurement circuitry. Examination of this diagram shows all pertinent information regarding the use of cable shields and ground wires, along with full identification of connector pin numbers. It shows the direct connection of the load cell output wiring to the electronic integrator through the bridge balance, the common ground wire for all cable shields, and the floating end of the load cell shield at the test stand. Remote calibration wires were provided in the event that electrical calibrations with a shunting resistor became desirable.

Figure 18 shows the negligible electrical zero drift of the entire measurement system with 50 foot cables to the load cell. The results of all zero drift tests demonstrated the interference-free capabilities of the electronic measurement system.

SYSTEM CALIBRATIONS AND EVALUATION

A series of complete static calibrations was performed on the entire system over a period of 8 calendar days. The calibrations were performed in accordance with the procedure stated in the Operation and Mainentenance Manual, R-5575.

The test series was composed of 8 "daily test sequences" for 10 days skipping the week-end day of Sunday. Each daily test sequence was composed of 4 calibration test cycles of 0, 1, 2, 4, 6, 8, 10, 8, 6, 4, 2, 1, 0 kilopound steps noting the system signal output for each force increment. On alternate days the ambient air temperature of the test area was in the normal room temperature range (68 - 73 F) and in a somewhat cooler range (60 - 64 F).

The parameters noted were: Date, ambient temperature, humidity, barometric pressure, range or span settings (strain gage power supply), balance settings, time at the start and finish of each calibration test cycle of the daily test sequence, applied calibration force, and the system output voltage as measured using the system Dymec integrating digital voltmeter.

The pre-calibration procedure followed during the series of calibrations included the following sequence of operations at the beginning of each day's test series:

1. Turn the equipment on
2. Vent the Ruska calibrator by depressing execute button with force selector switch at zero pounds.
3. Record the time of day the equipment was turned on.
4. After a 1½ hour warmup start the pre-test.
   a. Record time of day, ambient temperature, barometric pressure, and relative humidity.
   b. Vent the Ruska calibrator as above.

c. Re-zero and calibrate the Dymec integrating digital voltmeter (DIDVM) model No. 2401 A.

d. Check load cell strain gage power supply voltage and setting (span or range).

e. Set the load cell strain gage balance unit for zero signal output.

f. Record d and e

g. Exercise the Ruska calibrator by pushing the execute switch with the force selector at 1000 pounds and after the "Ruska" cycle is complete return the force selector to 0 pounds and execute again.

h. Repeat items c and e and record the final bridge balance unit setting.

The foregoing test data were statistically analyzed by the Mathematics and Statistics Group of the Rocketdyne Research Department to determine the linearity and precision variational properties. The instantaneous (short term) variational properties of the system were studied as well as the long term variational or "drift" properties of the measuring system.

Although both outputs (A gage and B gage) of the load cell were monitored, they were so similar that only the B gage data were analyzed.

Not all of the data from test sequences 2 through 8 were actually used in the final analysis. All of the data from sequences 2 and 8 were used, but, for sequences 3 through 7, the 1, 4, 8, 8, 4, and 1 points from

cycles 1 and 4 were used. For sequences 2, 4, and 6, the 2 and 2 points from cycle 2 and the 6, 10, and 6 points from cycle 3 were used. For sequences 3 and 5, the points used were: the 2, 10, and 2 points from cycle 2, and the 6 and 6 points from cycle 3. Thus, a 184 point sample of the tabulated 308 points was analyzed.

Each cycle was divided into an "up-half" (0,1,2,4,6,8, and 10) and a "down-half" (8,6,4,2,1, and 0). The zero-reading for each half of the data was subtracted from each of the other readings in that half of the cycle. The model used for regression was:

For up data:

$$(y-0)/xV_0 = A+B + CxT+Dx + Ex^2 + F(V_0-17.990) + \epsilon \qquad (1)$$

For down data:

$$(y-0)/xV_0 = A+CxT + F(V_0-17.990) + \epsilon \qquad (2)$$

where x denotes force (thousands of pounds)

T denotes ambient temperature (F)

V_0 denotes bridge voltage (volts), and

y denotes the load cell system output (millivolts)

ϵ denotes random error involved in each measurement

Many additional terms were tried, including the cycle number (a test for short term drift) and for extended time (a test for long term drift), but they were not significant and were therefore discarded.

Only one term in the above expression was unexpected, and that was the term in V_0. It was thought that V_0 variations (± 0.005 about 17.990), although small, would be sufficiently corrected by dividing the load cell output by V_0, but this apparently is not the case.

The standard deviation of residuals was estimated to be $\sigma_\epsilon = 0.000043$, and since the average value of the expression is 0.2984, this represents an estimated coefficient of variation of 0.0144%, a rather low figure. The worst points were in sequence 2 at the beginning of cycle 3 and at the end of cycle 4, and in sequence 3 at the beginning of cycle 1. They deviated roughly 4, 6, and 4 standard deviations, respectively, from the above regression.

The estimates of the parameters were

$$\hat{A} = 0.298,667$$
$$\hat{B} = -0.000,462$$
$$\hat{C} = -0.000,000,592$$
$$\hat{D} = 0.000,088,2$$
$$\hat{E} = -0.000,003,867$$
$$\hat{F} = -0.004,76$$

Since a calibration curve must be used for both up and down data, it is obtained by taking 0.5 of the B, D, and E coefficients in equation (1), giving

$$(y-0)/xV_0 = (0.298,436)-(0.000,000,59)xT + (0.000,044)x - (0.000,001,93)x^2 - (0.004,76)(V_0-17.990) + \epsilon + \Delta \qquad (3)$$

The hysteresis bias term in the regression was

$$= \pm \tfrac{1}{2} \left[B + Dx + Ex^2 \right]$$

and therefore the hysteresis error in $(y-0)/V_0$ was $+ x\Delta$. This is maximized when

$$3Ex^2 + 2Dx + B = 0,$$

for which the solution is

$$x = \frac{-D + \sqrt{D^2-3BE}}{3E}$$

$$= 3.36$$

$$+ x \quad = + 1.68 \left[B+Dx+Ex^2 \right] \simeq \pm \ 0.000353$$

Now $(y-0)/V_0$ at full scale is roughly 2.984, and therefore the maximum hysteresis error as a percentage of full scale was 0.012%.

The overall linearity can most easily be tested <u>non statistically</u> by examining the up data directly. By using the 10,000 lb point to represent the slope determining point, a value for the calibration constant (K_c) in volts per lb can be determined.

$$(y-y_0)/x = K_c = \frac{\text{millivolts (at 10,000 lbs)}}{\text{10,000 lbs}}$$

Examining all of the B gage up data on this basis and comparing K_c with the corresponding value at 1000 lb yields the following conclusion:

The worst case error observed was in test sequence number 2, cycle number 4 where the error was $\frac{0.0035 \times 100}{5.364} = 0.066\%$. The typical error for sequences 4 through 8 was about $\frac{0.001 \times 100}{5.365} = 0.02\%$ of actual value.

Statistically, all of the data was considered to have demonstrated a single calibration factor of 0.298,407 ± a Standard Deviation of 0.000,127,505 or 0.298,407 millivolts per volt excitation per thousand pounds ±0.08% at the 95% confidence level (2 σ). Alternatively, the data agreed with equation (3) ±0.0288% at the 95% confidence level, in addition to which an error of ±0.012% due to hysteresis is present, to produce an overall error of 0.031% for this case.

The system evidenced no significant short term or long term drift.

DYNAMIC EVALUATION

Description of Technique and Apparatus

Early in the Phase I effort it was determined that an elastic-collision or impulse type of dynamic calibration would involve unnecessary expense and extremely large, and, possibly, destructive forces. Therefore, this method was discarded in favor of a "step-unloading" of force produced by a break-link. This technique is described as follows:

1. A force was gradually applied to the test stand through the "break-link" which was fabricated to fracture at approximately 5000 lbs of force. The force was applied by means of a manually-operated hydraulic jack and a mechanical lever (Fig. 19).

2. The electrical circuit including the automatic gating circuit, is depicted in Fig. 20. On-line integration of the load cell's response to the step excitation was accomplished by means of two Dymec digital integrating voltmeters - one connected to integrate the positive signal and the other to integrate the negative signal. This latter is necessary because the load cell was resonated at the zero force level. Total impulse measurements after the break were obtained by subtracting the negative value from the positive value. This empirically derived value was then compared with the calculated value of the impulse associated with a one-spring-mass system's initial response to the stepped unloading, and to the value theoretically obtained by an <u>infinite-time</u> integration, after the break, of the response of a one-spring-mass system to the stepped unloading.

3. The output of the load cell bridge was simultaneously recorded on tape to provide natural frequency and dynamic linearity information. Figure 21 is a reproduction of the actual record of the load cell output.

Calculations

The calculated value of the total impulse of a one-spring-mass system's initial response to the step is as follows:

Given: $\frac{650 \text{ lbs}}{g}$ = dynamic mass of test stand = m

24×10^6 lbs/ft = load cell's spring constant = k

5152 lbs = fracture force = F

$\frac{5152}{24 \times 10^6 \text{ ft}}$ = displacement = x_o

$F = kx$ with $\dot{x} = 0$ at instant of fracture

$$\text{Energy} = \int_0^{x_c} F dx = k \int_c^{x_o} x dx = \underbrace{\tfrac{1}{2} k x_o^2}_{\text{P.E.}} = \underbrace{\tfrac{1}{2} m v_{max}^2}_{\text{K.E.}}$$

and $v_{max} = \sqrt{\frac{k x_o^2}{m}}$

$$\text{Impulse} = I = m v_{max} = m \sqrt{\frac{k x_o^2}{m}} = x_o \sqrt{km}$$

$$I = \frac{5152}{24 \times 10^6} \sqrt{24 \times 10^6 (20.2)} = 4.77 \text{ lb-sec}$$

This calculated value is the area under the load cell response curve from the "break" time to the first intersection of the decay curve with the zero reference line ($\frac{1}{4}$ cycle of the decayed response curve).

The calculated value of the impulse measured by a one-spring-mass system responding to a stepped-unloading is obtained from the use of equation (85), p 45 of the Phase I report, R-5162. It is restated as follows:

$$I_M = \frac{F_o}{n^2+w_1^2}\left[\left(\frac{w_1^2 - n^2}{w_1}\right) e^{-nt} \sin w_1 t - 2ne^{-nt} \cos w_1 t + 2n\right]$$

in which

F_o = force level of the step

w_1 = damped natural frequency (circular) of the system

n = damping factor

t = time of integration after the step

A suitable value of the impulse for a very long integration time is obtained by letting $t \to \infty$ in the above equation:

$$\lim_{t\to\infty} I_M = I_M^1 = \frac{2 F_o n}{n^2 + w_1^2}$$

From Fig. 21 and the height of the step, the following values are obtained:

F_o = 5152 lbs

w_1 = 1000 rad/sec

n = $wh \doteqdot 5.5$ (h = damping ratio)

Substitution of the values in the equation yields:

$I_M^1 \doteqdot 0.01$ lb/sec

Consequently, it is seen that the theoretical measured value of total impulse by the constructed system (assuming one-degree) is a negligible amount and is well below the impulse resolution of the equipment, since the one-count ambiguity of the equipment represents approximately 0.2 lb/sec.

Results

1. Integration

   a. The empirically measured value of impulse obtained by the two-Dymec system used with the alternating-polarity load cell signal was 5.2 lb sec. This value was considered to be sufficient for the intended purpose. The necessarily poor accuracy of the integration is explained by the following statements:

      (1) Integration by the Dymec integrators must be terminated in a short time after the fracture-link break in order that the integration of very small "zero-bias" signals are not integrated longer than necessary.

      (2) A counter ambiguity is risked each time the load cell signal passes through the zero reference level in its polarity excursions.

   b. The significance of the dynamic integration can be summed up as follows:

(1) The measured value of impulse was small, namely, about 5 lb sec, and although the measurement possessed poor accuracy, the value obtained is about 0.025% of the minimum total impulse anticipated in propellant testing.

(2) A measured value equal, or less, than the calculated initial response of the system to a step is considered to be an adequate demonstration of the system's capability to integrate transient forces.

2. Frequency Response Characteristic

a. As shown in Fig. 21 the system can be described as a linear, second-order system, having two degrees of freedom. The frequency of oscillation within the envelope agrees well with the mathematical model established during the Phase I effort (175 cps). Also the model provided for two degrees of freedom.

A rather surprising aspect of the response function, however, was the relative amplitude of the second resonance (modulation envelope), and the apparent low damping factor associated with it.

Detailed examination of the modulated oscillation showed in Fig. 21 shows that the measurement system is a coupled two degree-of-freedom system in which the load cell oscillation frequency varies between its two mode frequencies as its amplitude of oscillation varies between its maximum and minimum.

Further experimental investigation of this phenomenon was delayed until the demonstration testing phase (Phase III) at AFRPL, for two reasons: (1) The on-line dynamic calibration demonstrated that no significant errors were attributable to this second degree of freedom, and (2) the experiment at Rocketdyne was performed without the test stand being bolted or secured firmly to earth, whereas the testing phase at AFRPL will be accomplished with the test stand securely affixed to a concrete deadman and earth.

An expanded discussion of dynamic test results of this two degree-of-freedom system related to test stand performance is contained in the second part of the Appendix, page 111.

PHASE III: INSTALLATION AND TESTING AT EAFB

INSTALLATION

Concrete Test Pad

The Rocketdyne system was installed at EAFB on a thick, reinforced concrete pad whose levelness was constructed to be within $\frac{1}{4}$ inch over its area. Imbedded beams and tiedown bolts, of a similar type already used in the BATES program, were utilized.

Wiring

Two instrumentation cables for the load cell circuits were installed in a separate conduit in order to minimize electrical interference from the wiring used for test stand operation and control. The load cell cables were routed through a waterproof junction box for the purpose of practical wiring and checkout operations. The remainder of the load cell cables were unbroken between the test stand and control room equipment.

Roof

A steel roof was installed over the Rocketdyne test stand and supplied a degree of shading of the system from the direct sun. Additional statements concerning shading from the sun are contained in a later section of this report.

STATIC CALIBRATIONS AND EVALUATION

A series of twenty static calibrations were performed at EAFB to determine its operational suitability and precision following installation operations. The accumulated test data is contained in Fig. 39. A non-statistical examination of this data resulted in the following statements regarding the performance of the system:

The first five calibrations exhibited linearity, hysteresis and repeatability entirely consistent with necessary performance specifications (0.1%). The second five calibrations, for the most part, exhibited good linearity and hysteresis, but somewhat poorer repeatability. However, the difference between the lowest and highest system sensitivity was 0.03% of full scale. The third five calibrations exhibited characteristics entirely suitable, with repeatability error only 0.02%. The last five calibrations showed excellent performance with linearity 0.01%, hysteresis 0.03%, and repeatability 0.01% of full scale being typical values. It was felt that a statistical analysis of the data was not needed for system verification.

DYNAMIC EVALUATION

A fracture-link dynamic test was performed on the installed system at EAFB. The load-cell delay curve and the associated integrator on-off signal are pictured in the Fig. 40 tracings of the polaroid camera pictures of the oscillographic traces obtained by playback of the taped recording of the

signals. It is seen that the integrator was "on" for only about 3½ cycles of the electrical oscillation, due to an electrical short at the break-link. The numerical value of total impulse obtained during this integration time(about 17 milliseconds) was 3 lb.sec. Although the integration time was considerably less than intended, it was sufficient to show the same general result that was obtained at Rocketdyne, namely, a total impulse value near the calculated initial response to the step. Since the measured and calculated impulse values associated with the initial response to a stepped-unloading are approximately 0.025% of the minimum total impulse anticipated in propellant test operations at EAFB, any further investigation into the transient measurement capabilities of the system was considered superfluous and unnecessary.

TEST FIRING RESULTS

Four solid propellant motor tests were conducted with the Rocketdyne measurement system at EAFB Test Pad No. 5, Solid Motor Test Area, on 13 and 16 April 1964 with an EAFB-furnished propellant whose performance was well established by previous testing on the pre-Rocketdyne BATES measurement system. In each of these four tests, the dual-bridge load cell was utilized to provide two simultaneous impulse measurements, one employing the Rocketdyne electronic integrator system and the other employing the electronic integrator system used in the pre-Rocketdyne BATES system. In the latter system, integration of motor thrust was performed over the

time interval between the two instants of time at which 10% of maximum thrust occurs. In the Rocketdyne system, the entire thrust was integrated from the initial to the final zero thrust level. The post-run termination of thrust integration was manually controlled during these four tests since it was intended to integrate any oscillatory response of the test stand that might have occurred with a sharp motor cutoff, without any prolonged integration of a small non-zero signal after cutoff.

The results of these tests, uncorrected in any way for various operational test conditions, is given below:

Run No.	Rocketdyne System lb.sec.	EAFB System lb.sec.	Difference lb.sec.	% Difference
1	16,982	16,860	122	0.72
2	16,923	16,890	33	0.19
3	16,928	16,895	33	0.19
4	16,904	16,840	64	0.32

The data obtained in these test firings was considered to be reasonable and it verified, in a qualitative way, the various operational and test conditions associated with the firings as follows:

1. Numerical results agreed well with previous measurements of the test propellant.

2. The Rocketdyne-system measured values of impulse were more than those obtained by the parallel EAFB electronic equipment, since the latter were obtained between the 10% thrust levels.
3. The values obtained in run No. 4 were less than those obtained in run Nos. 1, 2, and 3, due to motor nozzle wear experienced in the preceding tests.

A thermal expansion effect occurred in the motor suspension and/or retaining system due to heat generated in the motor during firing operations. It resulted in load cell indications of force subsequent to motor thrust cutoff. Immediately upon motor cutoff, a negative force indication, corresponding to a load-cell tensile force, of approximately 15 pounds was immediately followed by a sloped change toward zero force indication over a time period of approximately 30 seconds followed by a slower change and level-off at about 7 pounds of indicated thrust, or compressive force. Subsequent slow cooling of the motor and its suspension and retaining system, over a period of 2½ hours, reduced the load cell indication to essentially zero level.

Statements regarding the operation of the system under these post-run conditions are made in a later section of this report.

RECOMMENDED ADDITION TO MOTOR INSTALLATION

The post-run thermal expansion effect, experienced at the end of each of the four motor firings witnessed by Rocketdyne personnel, appeared

to be a problem capable of solution by the use of thermal insulators installed at suitable locations on the motor suspension and retaining system. The need for elimination, or at least reduction, of this thermal effect on the test stand is necessitated by its adverse effect on post-run calibrations of the measurement system and also by its effect on the zero thrust reference base during the motor firing and hence, on the accurate measurement of propellant total impulse. Accurate calibrations of, and measurements by, the system can be obtained only when the system "zero" reading is stable but the transient thermal expansion produced circuit zero instability for about two hours after a motor test.

In order to obtain information leading to the elimination, or at least reduction, of this effect it is recommended that surface temperature and strain gages be installed on the motor mount, platform, and flexure assemblies to determine the temperature-time history at each gage location subsequent to a motor test. In this manner a suitable temperature distribution and strain history can be obtained to reveal the most effective locations for thermal insulation needed to reduce the passage of heat from the motor to the test stand.

The head and nozzle closures of the motor attain temperatures of several hundred degrees after a motor firing. The motor mount assembly is in direct metallic contact with the motor head and, subsequently, suggests

that thermal insulation between these butted members would effectively reduce heat transmission at this location. The motor chamber exterior does not become very hot and heat transmission from it to its four supporting buttons does not appear to be great. However, any decision regarding the location and amount of insulators would best be made by reference to actual temperature-time measurements obtained by surface temperature gages. It is felt that a short-term effort in this direction would result in more accurate and useful measurement data.

An expanded discussion of the post-run thermal effect and the recommended program for its reduction or elimination is contained in the second part of the Appendix, page 111.

OPERATIONAL CONSIDERATIONS

In order that the maximum accuracy, utility, and efficiency of operation are obtained with the total impulse measurement system, the following operational policies and procedures are recommended.

TEST STAND

Motor Heat

The transmission of motor heat to the motor support and restraining assemblies must be reduced to a level of non-interference with the load cell indication of force. The accuracy of impulse measurements will be degraded if this is not accomplished.

Enclosure Condensation

The cooling of moist air within the weathertight enclosure has been observed to result in condensation on metal surfaces of the calibration system. The total impulse measurement system can detect the force produced by a layer of water about 0.0015 inch thick on an area equal to that of one side of a calibrating weight. Consequently, it is imperative that condensation within the enclosure be kept to a minimum. Suggested methods to accomplish the removal of condensation include the use of sacks of desiccant placed within the enclosure and/or the use of electric light bulbs to provide heat for the evaporation of the water.

Force Cell Bleeding

It is recommended that accumulated air within the hydraulic force cell be removed by bleeding it at least once a month until sufficient experience dictates otherwise. This is accomplished by loosening the set screw in the force cell assembly, the latter rotated until the screw is at its highest point during a revolution of the cylinder. With the force cell assembly not rotating, the calibration system is operated to produce hydraulic pressures within the cell to drive out the accumulated air. Bleeding of the air from the force cell should be accomplished at both low and high pressure levels, say at the 1000 and 8000 pound calibration levels.

Leveling Check

A check of the levelness of the test stand, both longitudinally and transversely, should be made periodically in order to ensure proper alignment with the horizontal. The system measurement axis should be horizontal within 0.2° in order that motor thrust indications are accurate. A check of levelness should be made at least once a month.

Bolt Tightness

A check of the tightness of all bolts and screws should be made at least once a week to ensure against inaccuracies and malfunction of

system components. Particular emphasis should be placed on the tightness of all components of the motor mount platform and flexure system, hydraulic force cell and rear flexure assemblies. Vibration of the test stand experienced during motor test operations will tend to loosen all bolts and screws and vigilance is required to maintain their tightness.

Dynamic Test

A dynamic test with the fracture-link apparatus should be performed at least once every six months, in order to detect any major departure of test stand dynamic behavior due to component malfunctions not readily discernible (e.g., concrete abutment internal cracks, loose abutment mounting faces, or loose motor installation). The appearance of the load cell delayed response is directly relatable to secure component installations and the "cleanness" of the dynamic response curve is indicative of satisfactory system fabrication and assembly.

Enclosure Air Temperature

The temperature of the air within the weathertight enclosure should be monitored during all calibration and test operations. It is anticipated that the calibration equipment may experience malfunction during the high ambient air temperatures encountered during summer months, particularly in electronic components of the calibration system (transistors, condensers, etc.). Records of enclosure air temperatures would be useful in the event of such malfunction.

CONTROL ROOM ELECTRONIC EQUIPMENT

Dymec Integrator

The calibration of the Dymec integrator is important to the accurate acquisition of calibration and propellant test data. The instruction manual for this unit contains the procedure for accomplishing this operation. Calibration checks and adjustments of the Dymec integrator should be made just prior to every calibration and use of the entire total impulse measurement system.

TEST PAD ENVIRONMENT

Gravity Check

The accuracy of the static calibrations of the entire measurement system is directly related to the accuracy of the assigned value of the earth's acceleration due to gravity at the test site. The calibration weights were machined to produce the calibration forces at locations where $g = 979.477$ cm/sec^2, the value at Test Pad No. 5, Solid Motor Test Area, Edwards Rocket Propulsion Laboratory on 18 January 1963. It is recommended that this measurement be repeated at six-month intervals in order to detect any changes in its value necessitating corrections in the values of the calibration forces.

Sun Shielding

It is felt that satisfactory performance of the hydraulic calibration system will require adequate shielding of its weathertight enclosure from the direct sun.

Air temperature inside the enclosure during summer months are expected to become too high unless adequate measures are taken to minimize the heating of critical components. It is recommended that all direct incidence of the sun upon the enclosure be eliminated by whatever means is suitable to EAFB. If sun shielding measures are inadequate to prevent calibration system malfunction, recourse must necessarily be made to blowers or air-conditioners installed in the enclosure itself.

Ambient Air Temperature

In order to relate overall system calibration and performance parameters to environmental conditions, over comparatively long periods of time, it is recommended that test pad ambient air temperature be recorded.

CONCLUSIONS

The most important technical conclusion derivable from the overall program effort was that a significant advance was made in research and developmental test equipment which will enable substantial improvement to be made in solid propellant development. It is felt that this advance was directly due to a reversal of accepted test stand design practices and procedures. Prolonged and exhaustive mathematical analysis was followed by careful design activities, the two efforts encompassing eight months, almost half of the calendar time of the entire program. The second phase of the effort consisted of original engineering and design efforts by competent component manufacturers to produce the superior products needed to obtain the required system performance, followed by careful fabrication, assembly, and testing of the components and assembly. The third, and last, phase consisted of cooperative efforts at all levels between Rocketdyne and EAFB personnel to effect the installation of the equipment without degradation of accuracy and performance. An important non-technical conclusion of the effort was the realization by both Rocketdyne and EAFB personnel that an effective government-industry cooperative effort had been demonstrated in the field of instrument development engineering.

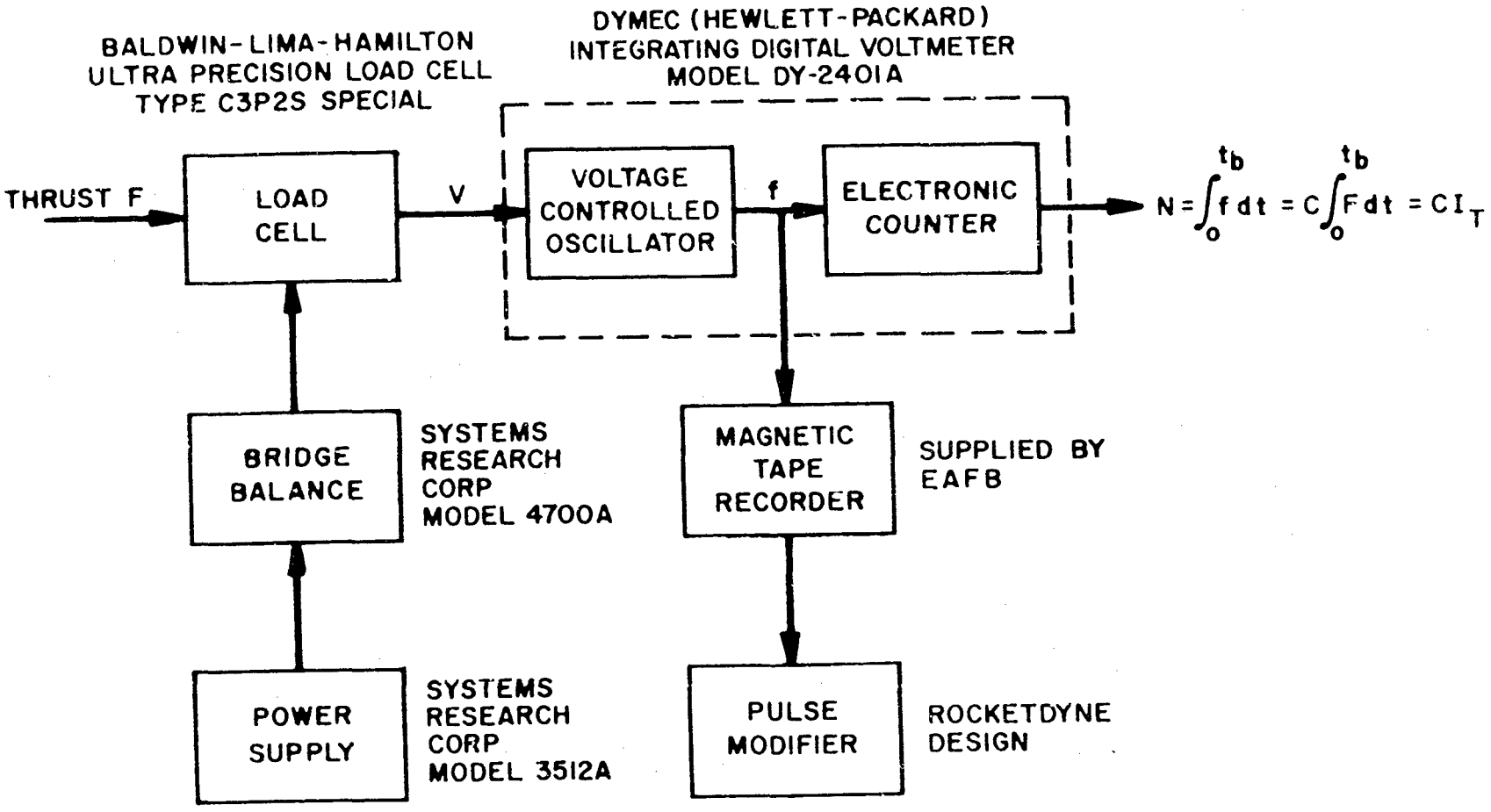

Figure 1. Block Diagram of Measurement System

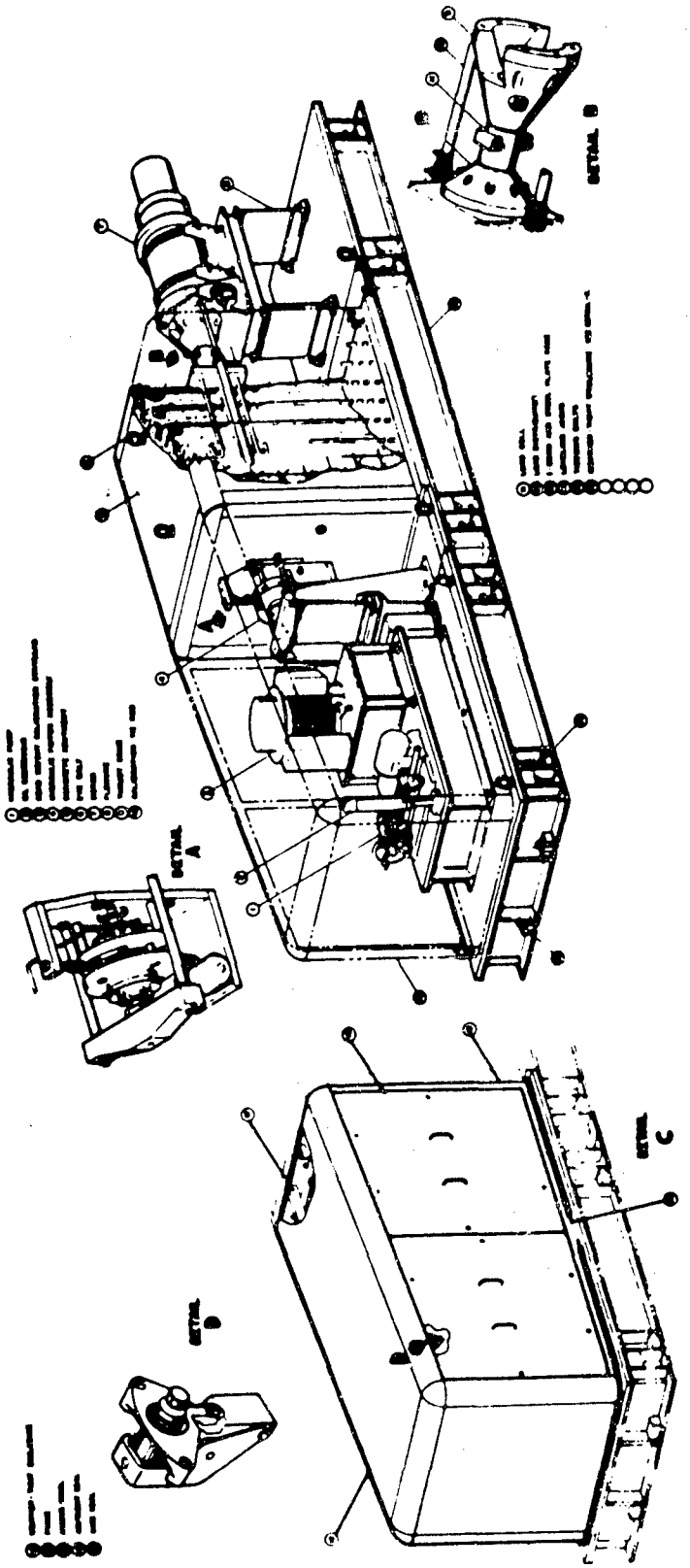

Fig. 2. Test Stand of Rocketdyne Total Impulse Measurement System

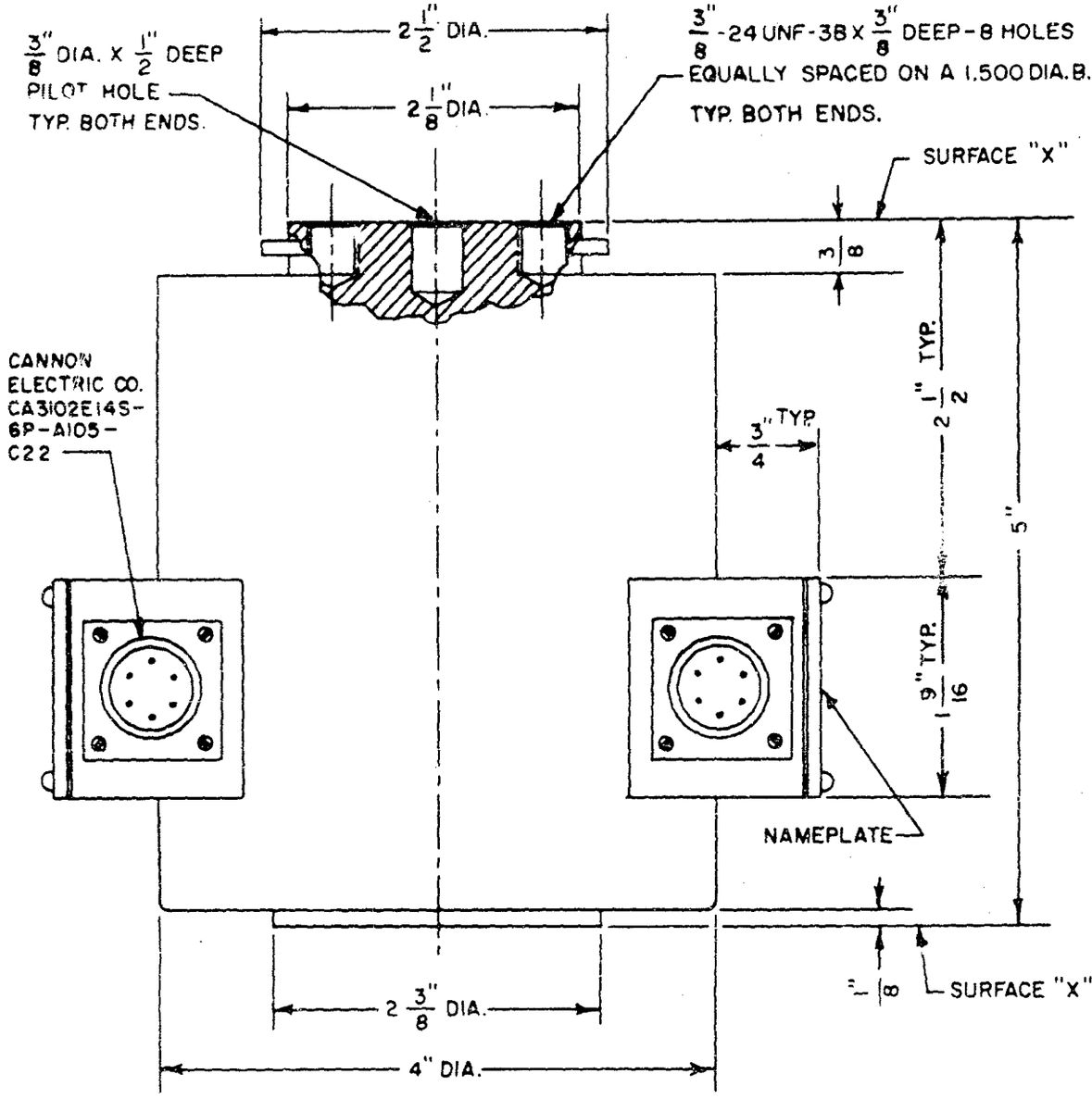

GENERAL NOTES

1. BEARING SURFACES "X" ARE LAPPED AND ELECTROPLATED WITH LEAD .001/.002 THK.

Fig. 3. Dimensional Drawing of Load Cell

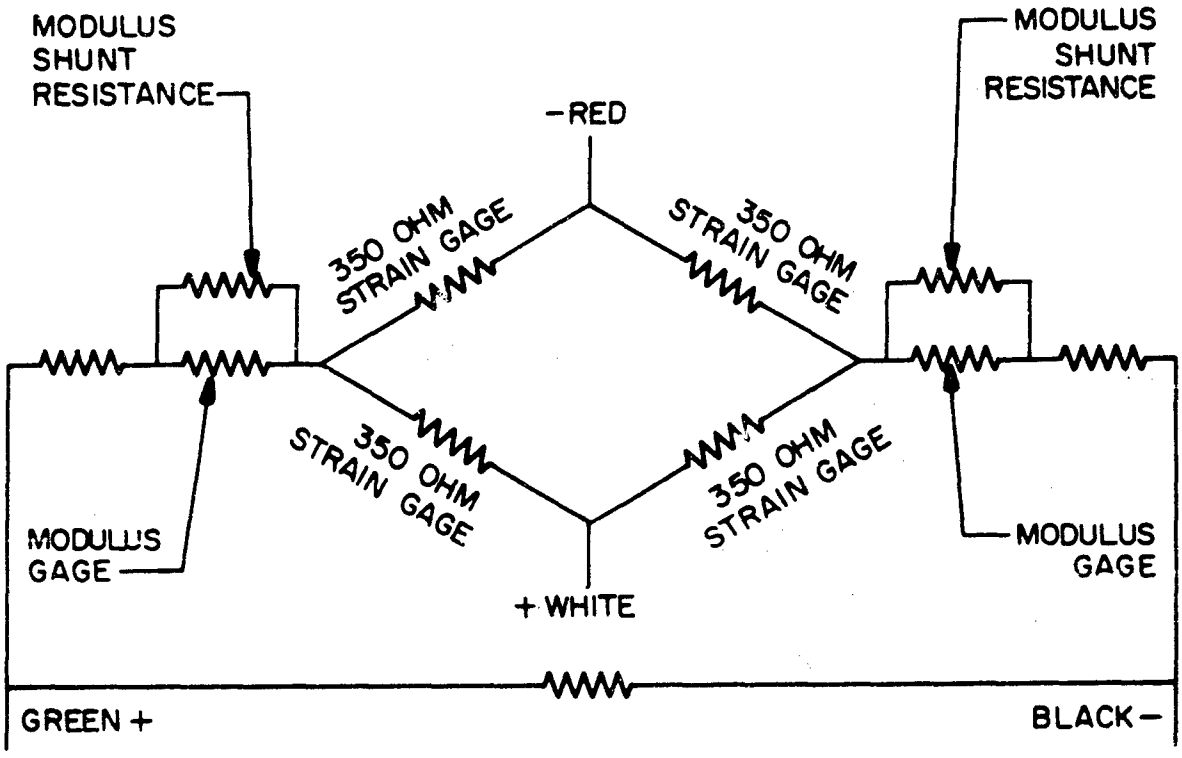

INPUT - BLACK TO GREEN - RESISTANCE 350±3.0 OHMS AT 70°F
INCREASES 3.5 OHM FOR 50°F RISE

OUTPUT - RED TO WHITE - RESISTANCE 350±3.0 OHMS AT 70°F

PICKUP	CHANGE IN OPEN CIRCUIT OUTPUT VOLTAGE FOR RATED CAPACITY	OUTPUT VOLTAGE AT ZERO LOAD
C3P T3P	3.000 ± .003 MV/V INPUT	NOT OVER .030 MV/V INPUT
U3G	3.000 ± .0075 MV/V INPUT	NOT OVER .020 MV/V INPUT
C2K T2K	2.400 ± .006 MV/V INPUT	NOT OVER .024 MV/V INPUT
U-1A U-3XXA (COMP.)	3.000 ± .009 MV/V INPUT	NOT OVER .030 MV/V INPUT

1. MOD. GAGE VARIES WITH TEMPERATURE TO COMPENSATE FOR THERMOELASTIC COEFFICIENT OF PICKUP METAL
2. RECOMMENDED INPUT 12 VOLTS AC OR DC. MAX. INPUT 25V AC OR DC
3. POLARITY IS SHOWN FOR COMPRESSIVE LOAD.

Fig. 4. Schematic Diagram of Load Cell

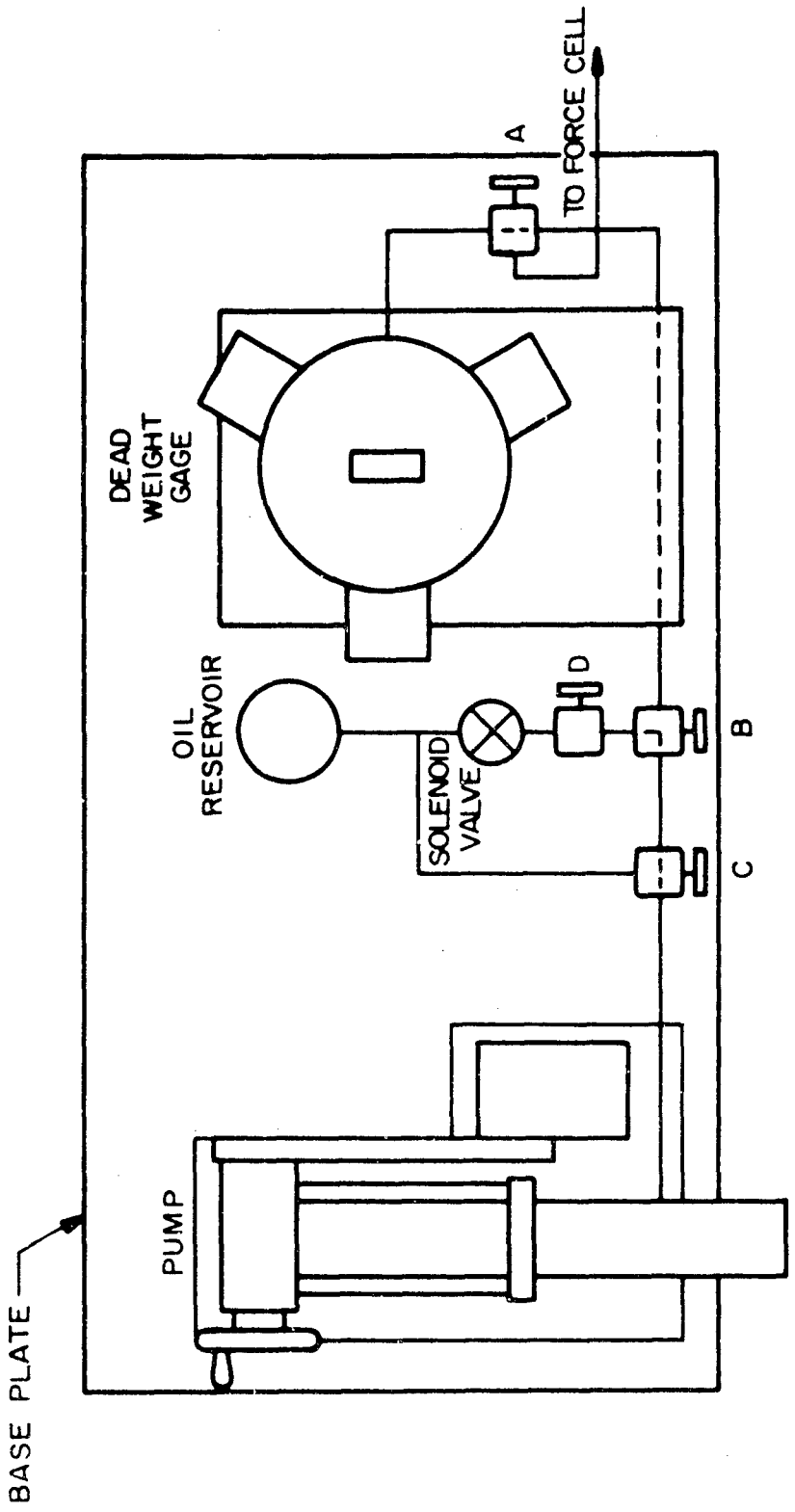

Fig. 5. Ruska Master Pressure Standard

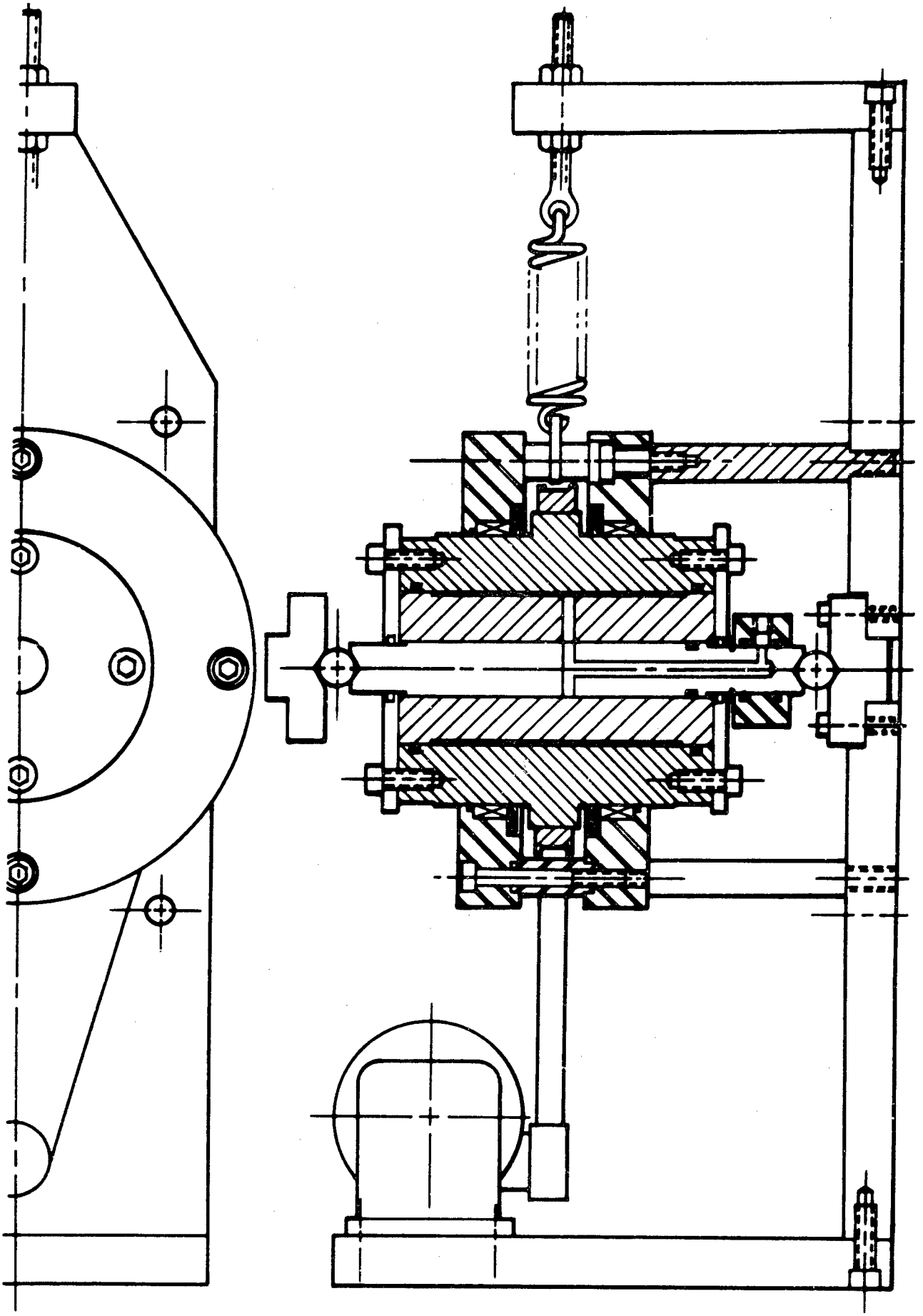

Fig. 6. Ruska Force Cell

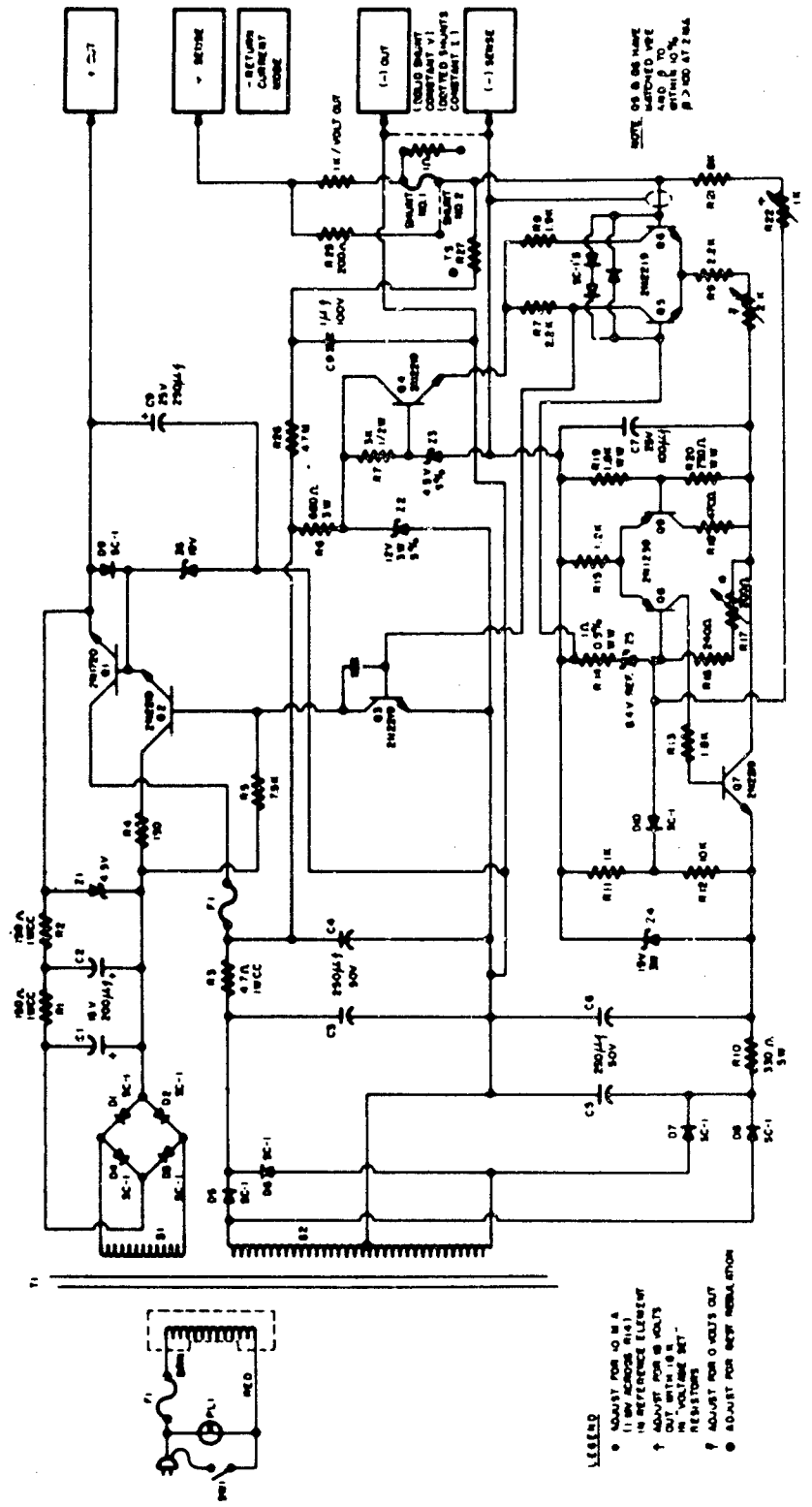

Fig. 7. Schematic Diagram of Load Cell Power Supply

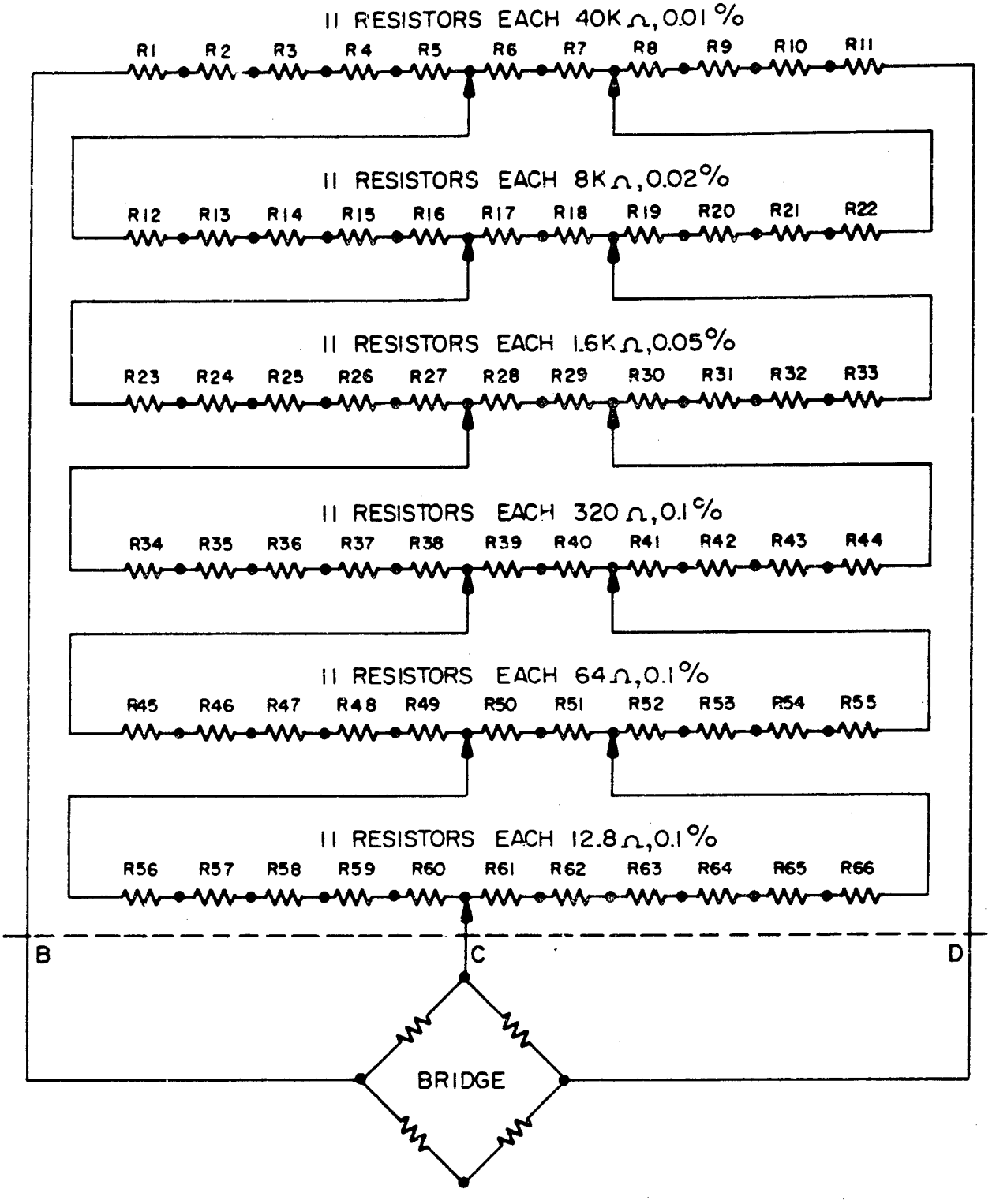

Fig. 8. Schematic Diagram of Bridge Balance

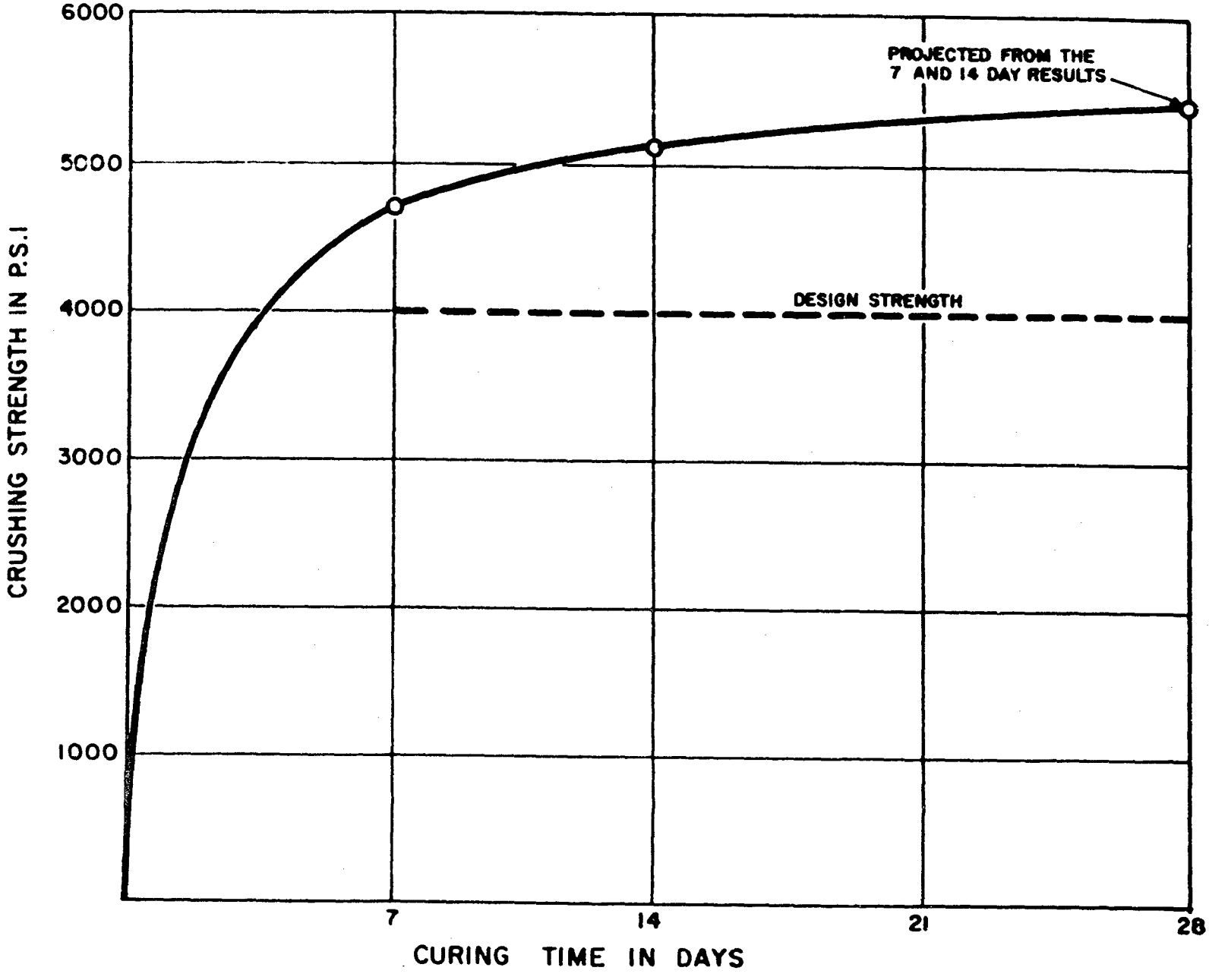

Fig. 9. Concrete Strength Curve

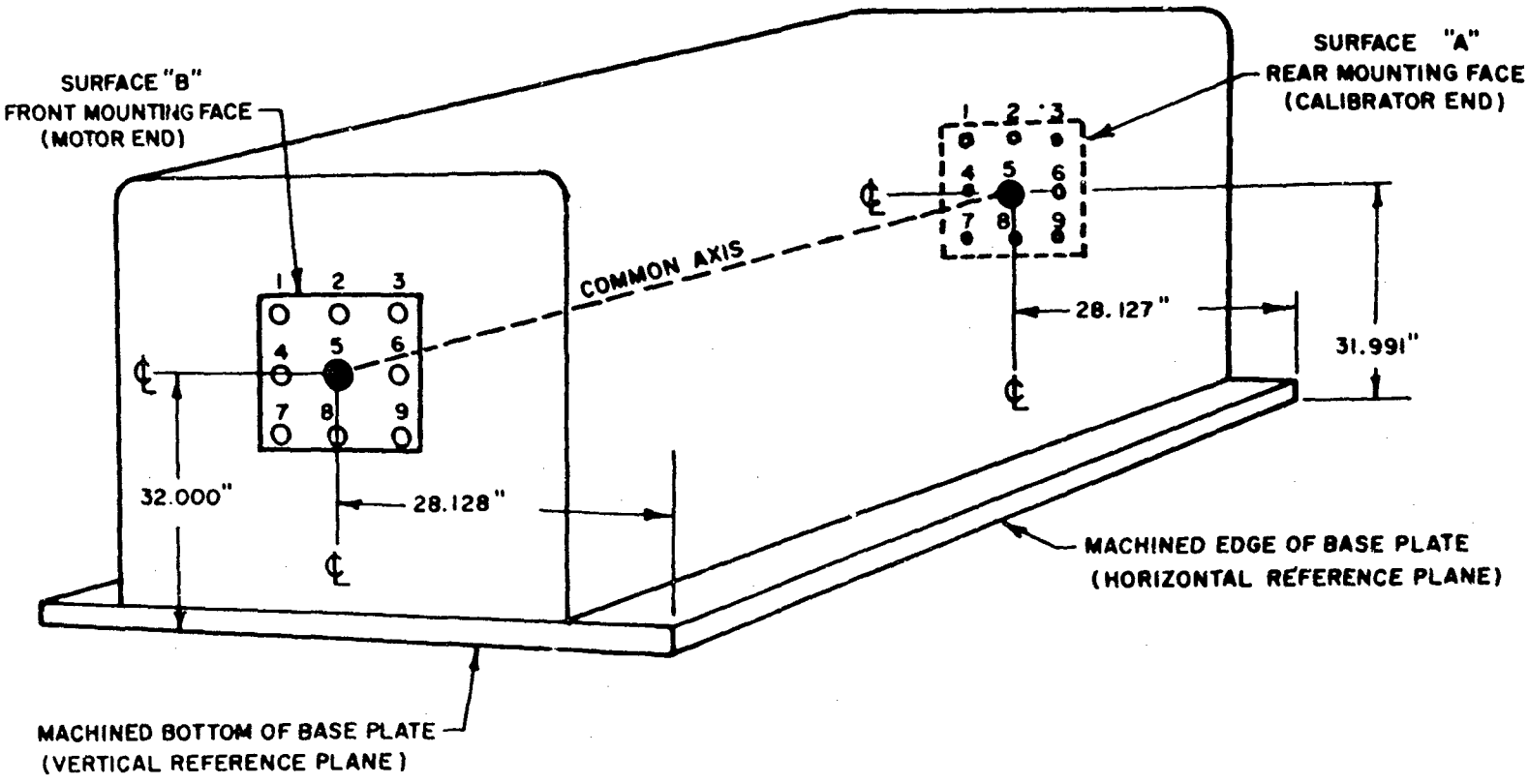

MOUNTING FACES MEASUREMENTS:

1. SURFACE "A" FLAT WITHIN 0.001 INCH, SURFACE "B" WITHIN 0.0008 INCH.
2. SURFACES "A" AND "B" NORMAL TO COMMON AXIS WITHIN 0.0045 INCH.
3. SURFACES "A" AND "B" PARALLEL WITHIN 0.003 INCH.

Fig. 10. Measurement of Concrete Abutment Alignment

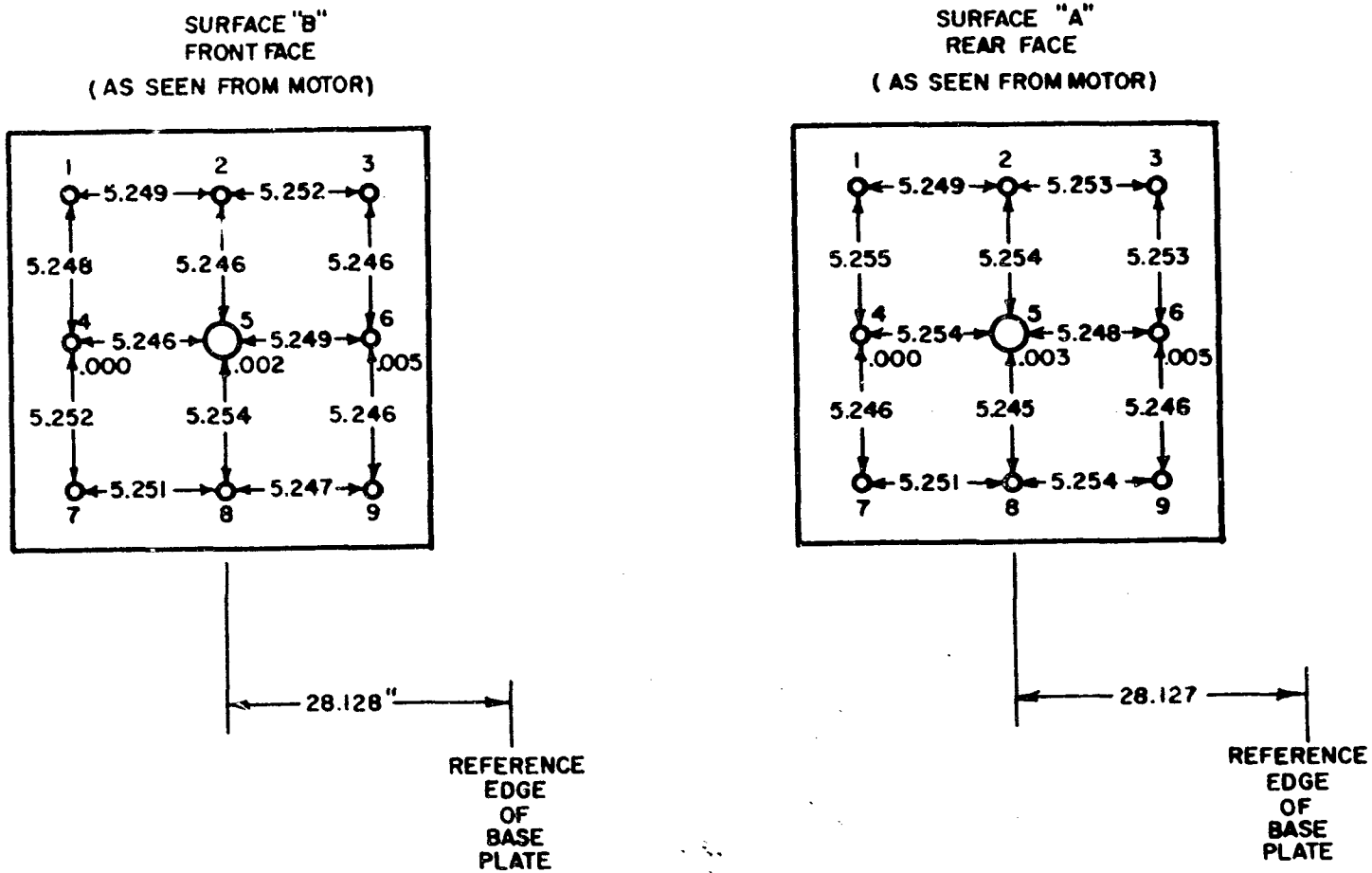

Figure 11. Abutment Mounting Face Reference Holes

COMPRESSION CALIBRATION DATA

CHANGE IN OPEN CIRCUIT OUTPUT VOLTAGE PER VOLT INPUT @ 75°F IN MV/V

% CAPACITY	BRIDGE "A"			BRIDGE "B"		
	1	2	3	1	2	3
0	0.0000	0.0000	0.0000	0.0000	0.0000	0.0000
10						
20	0.6000	0.6002	0.6002	0.5999	0.6001	0.6001
30						
40	1.2000	1.2002	1.2001	1.2000	1.2003	1.2002
50						
60	1.8002	1.8006	1.8004	1.8002	1.8006	1.8006
70						
80	2.4005	2.4009	2.4009	2.4005	2.4008	2.4007
90						
100	3.0008	3.0010	3.0008	3.0009	3.0009	3.0010
60	1.8001	1.8007	1.8003	1.8002	1.8007	1.8007
0	0.0002	0.0003	0.0003	0.0002	0.0002	0.0003

LOAD CELL TYPE C3P2S SERIAL NO. 32318 CAPACITY 10,000 LBS
INPUT RESISTANCE (OHMS @ 75°F): BRIDGE "A" 350.2 - BRIDGE "B" 350.3
OUTPUT RESISTANCE (OHMS @ 75°F): BRIDGE "A" 347.0 - BRIDGE "B" 347.4
ZERO BALANCE (MV/V. @ 75°F): .0135 BRIDGE "A" >20
.0160 BRIDGE "B" >20 BRIDGE TO GROUND RES. (MEGOHMS @ 75°F)

CALIBRATION STANDARD: DEAD WEIGHTS
DATE OF CALIBRATION: 10/2/63
PLACE OF CALIBRATION:

BALDWIN-LIMA-HAMILTON
ELECTRONICS DIVISION
WALTHAM 54, MASSACHUSETTS

Fig. 12. Load Cell Calibration Data (B-L-H)

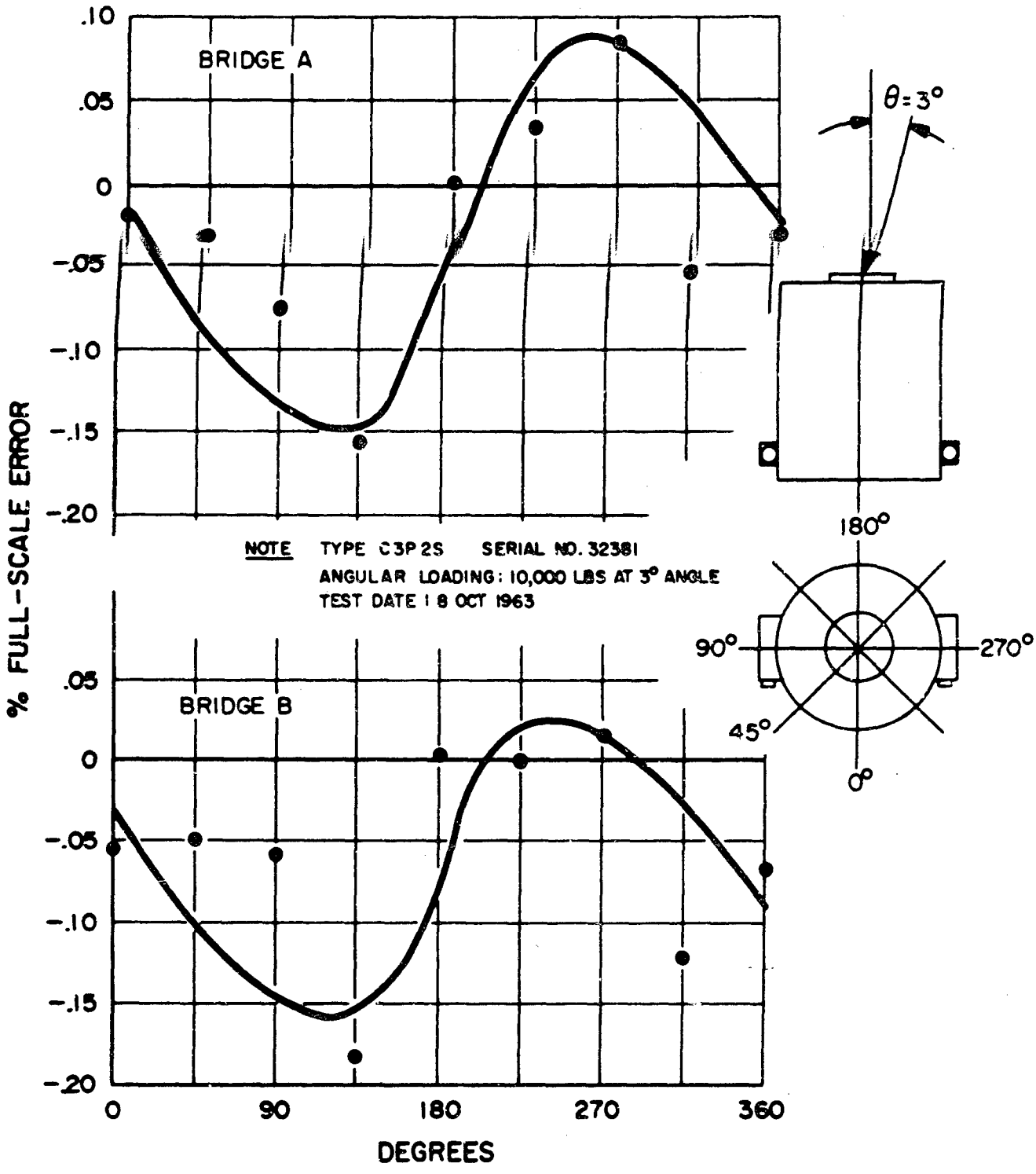

Fig. 13. Load Cell Test Data (B-L-H)

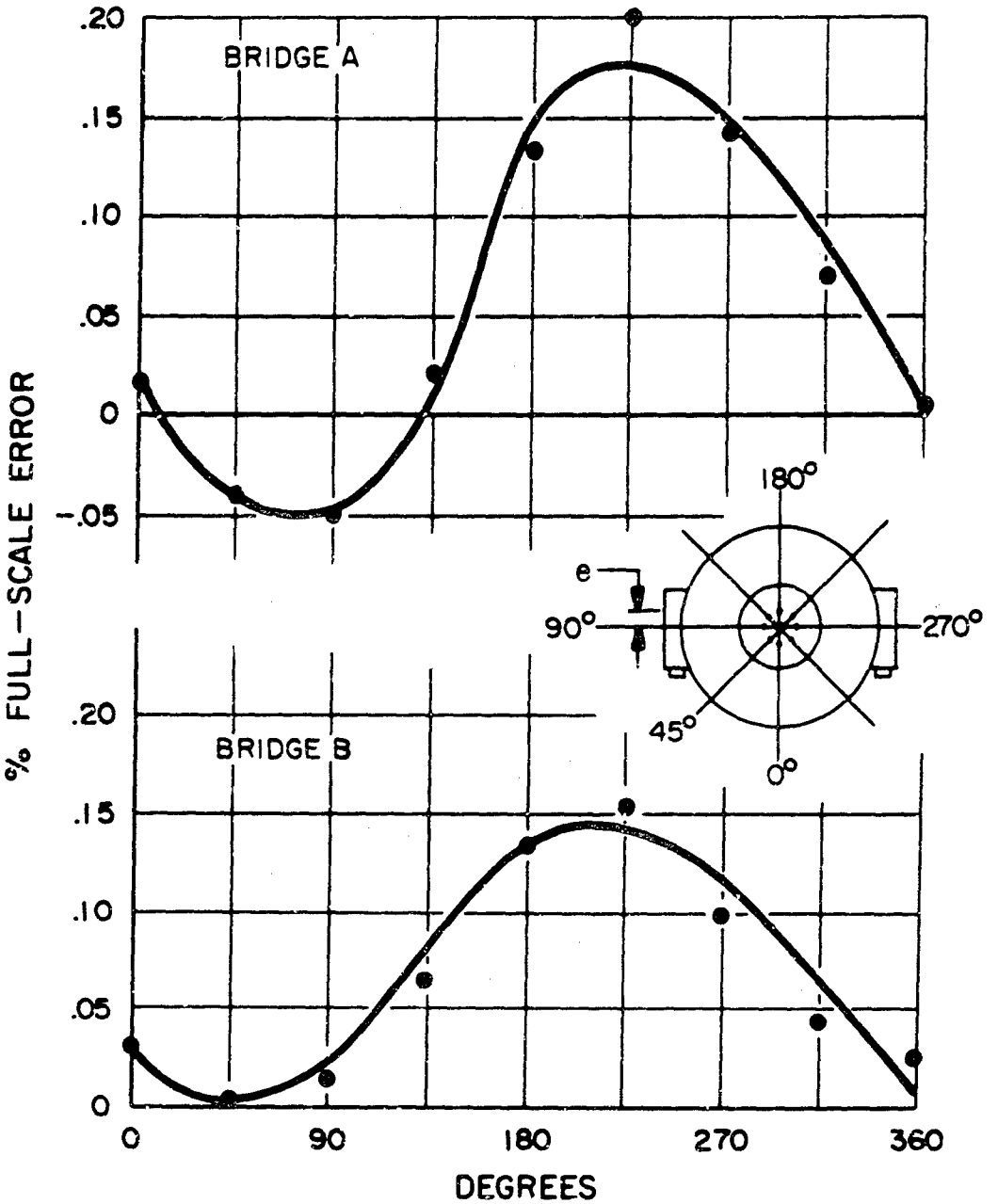

NOTE TYPE C3P2S SERIAL NO. 32381
CALIBRATION STANDARD - DEAD WEIGHTS
ECCENTRIC LOADING: 10,000 LBS AT 0.25 INCH OFF-AXIS
TEST DATE: 8 OCT 1963

Fig. 14. Load Cell Test Data (B-L-H)

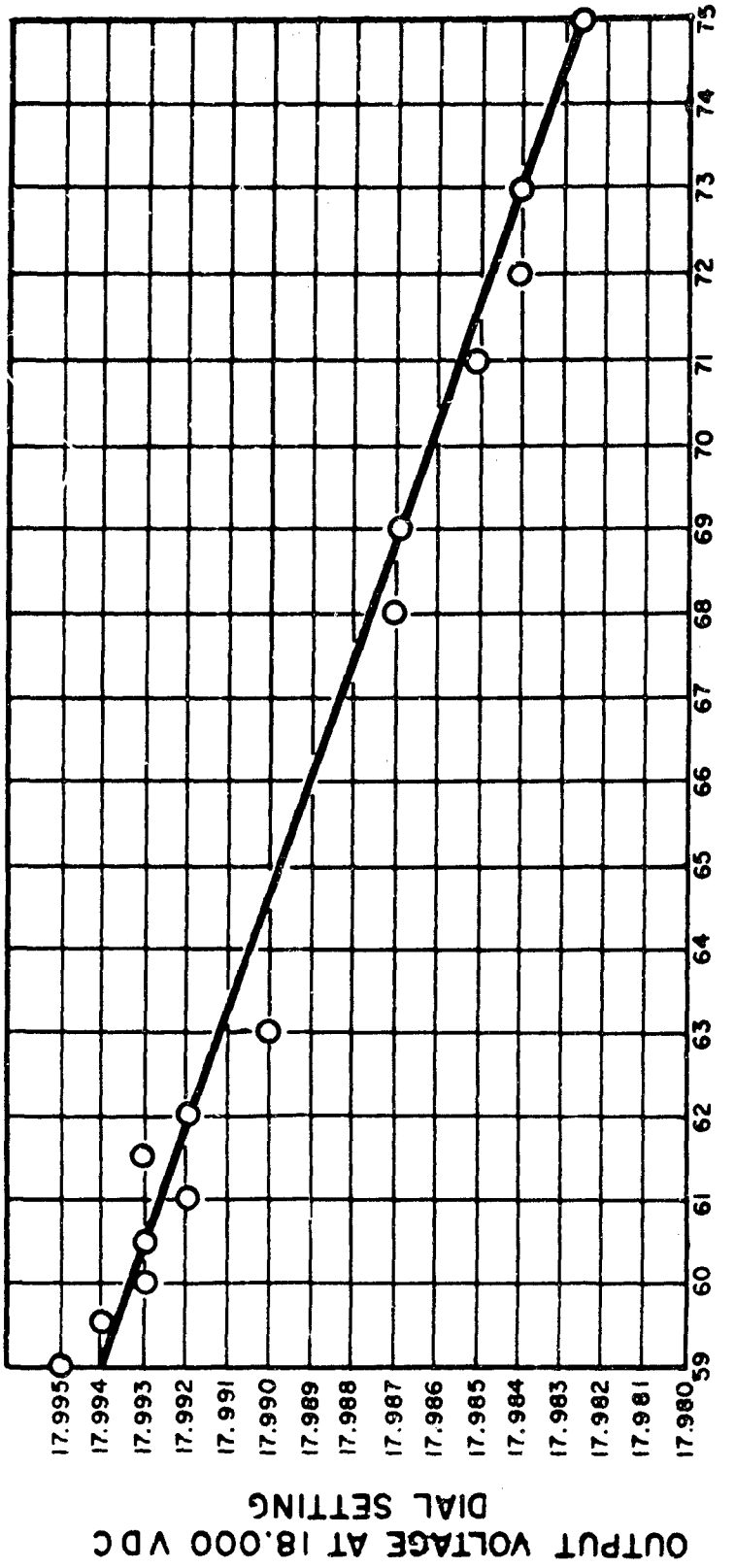

Fig. 15. Load Cell Power Supply Temperature Sensitivity

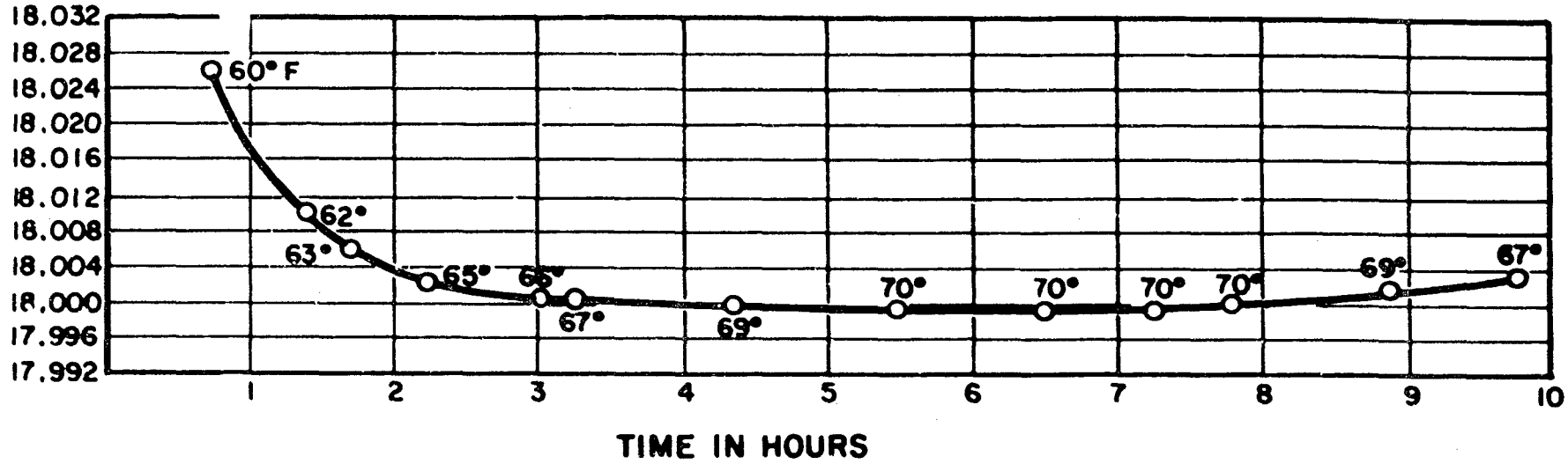

Fig. 16. Load Cell Power Supply Long-Term Drift

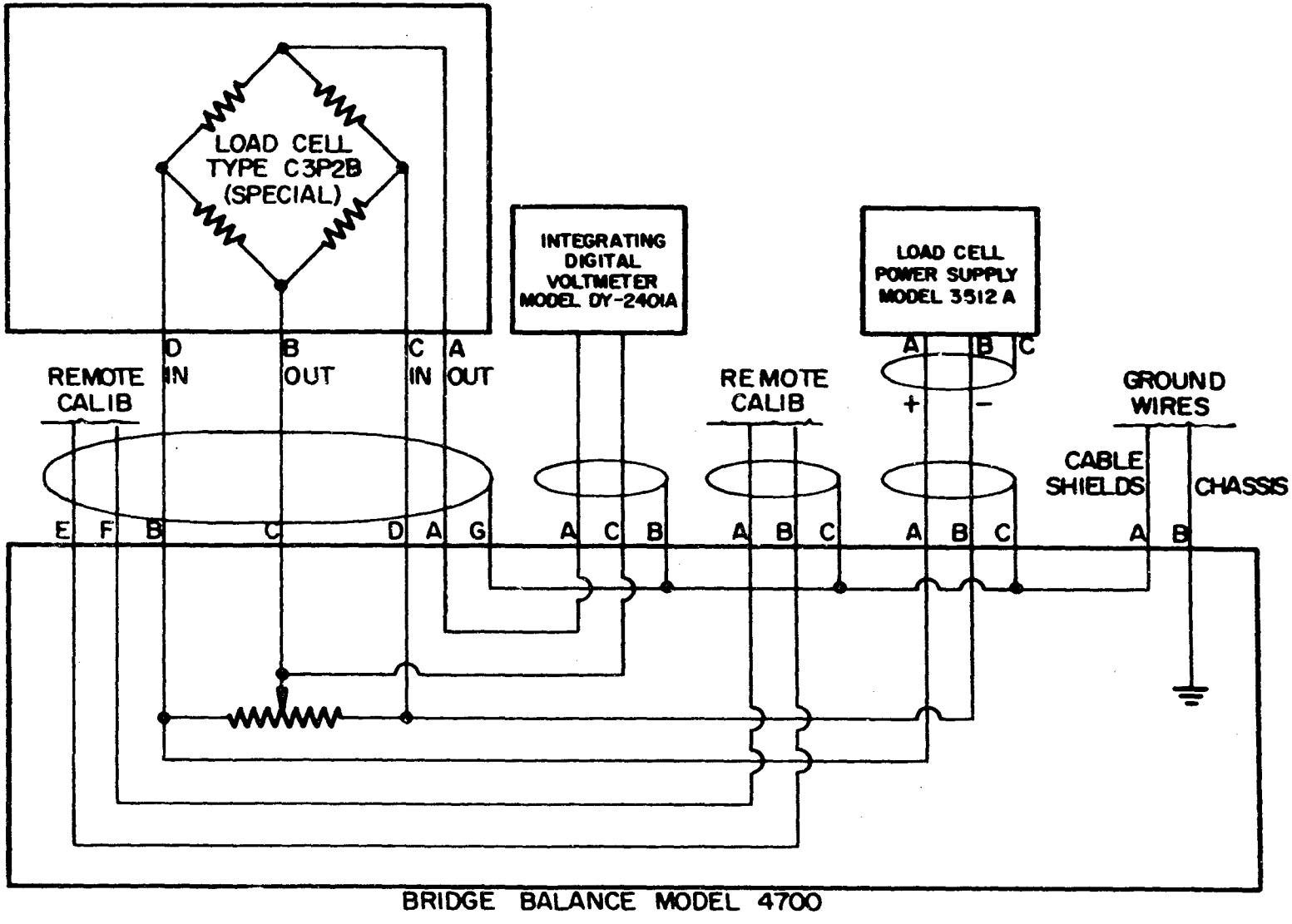

Fig. 17. Block-Schematic Diagram of Measurement Circuitry

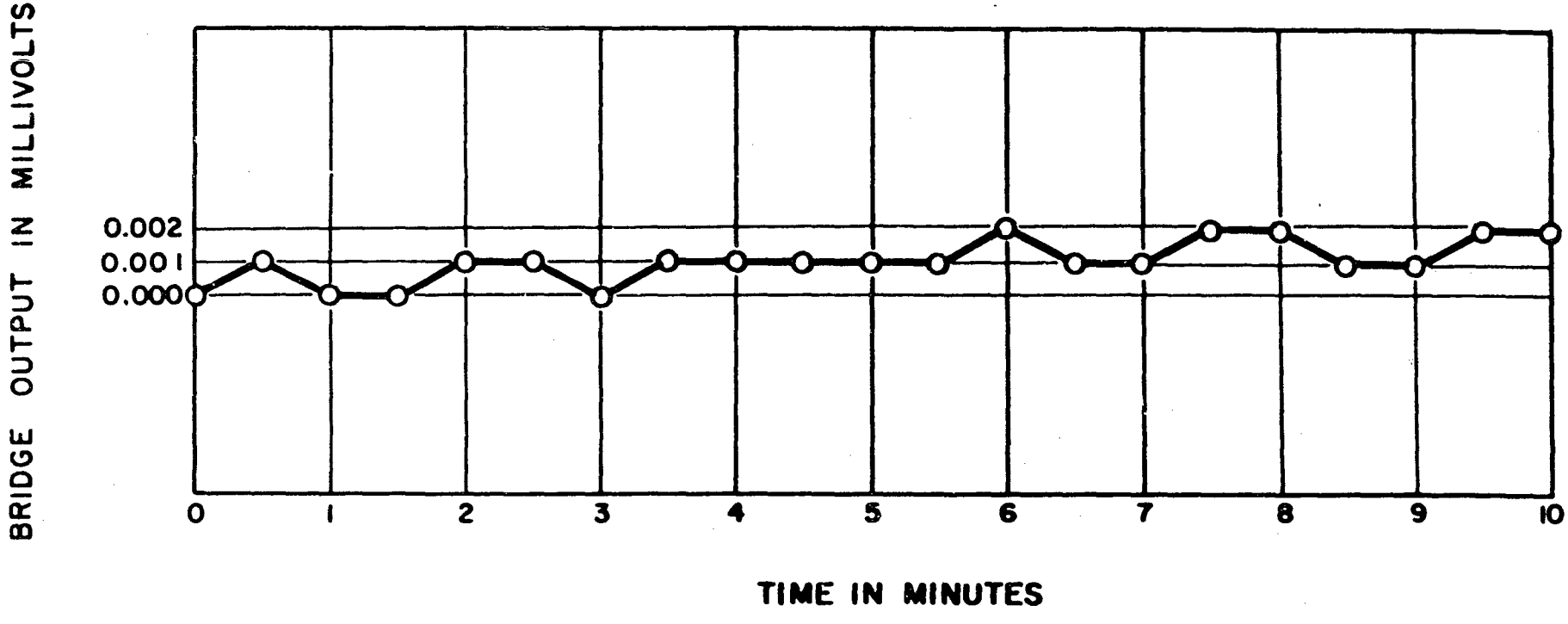

Figure 19. Zero Drift of Entire Measurement System

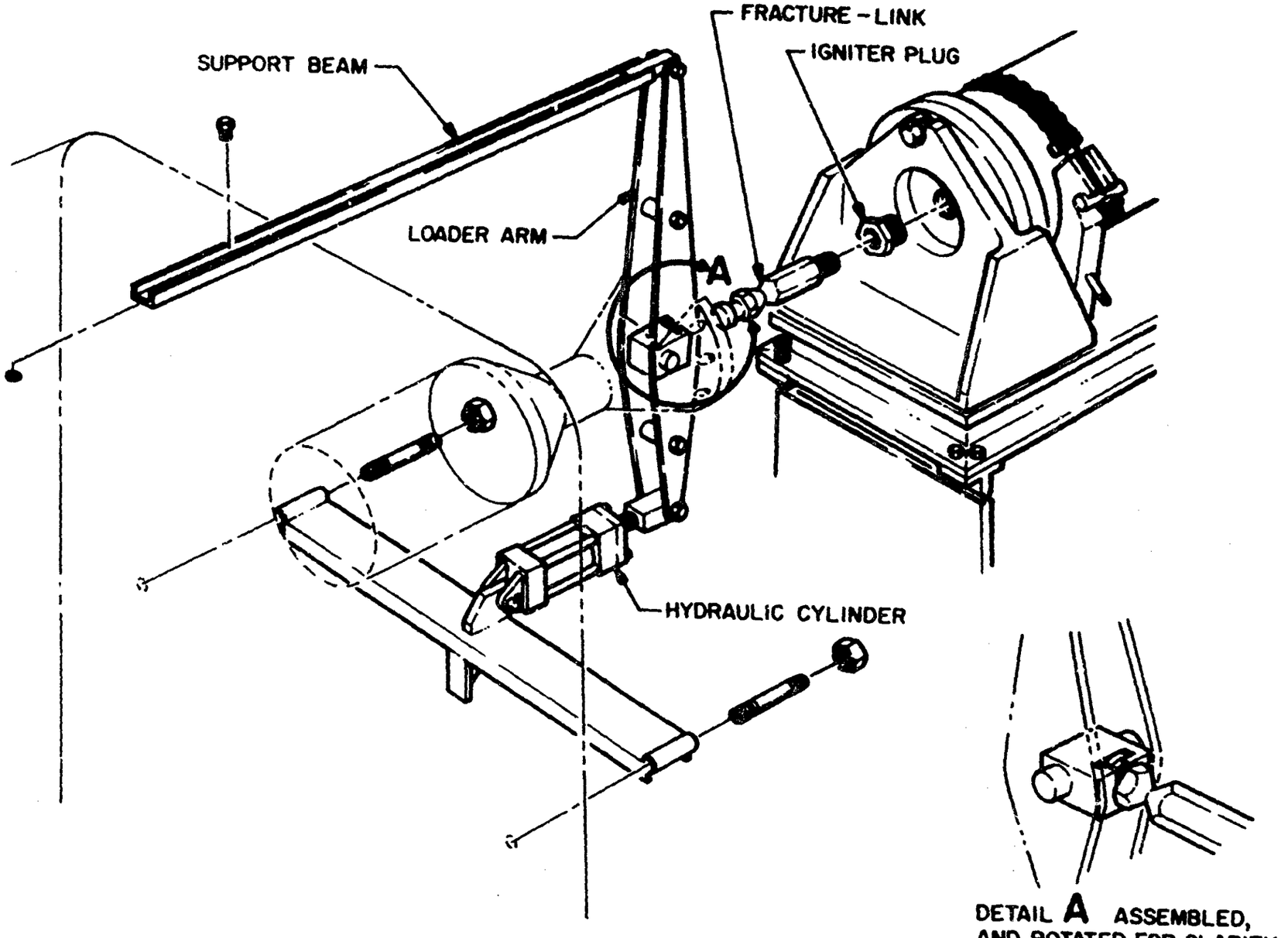

Figure 19. Dynamic Test Setup (mechanical)

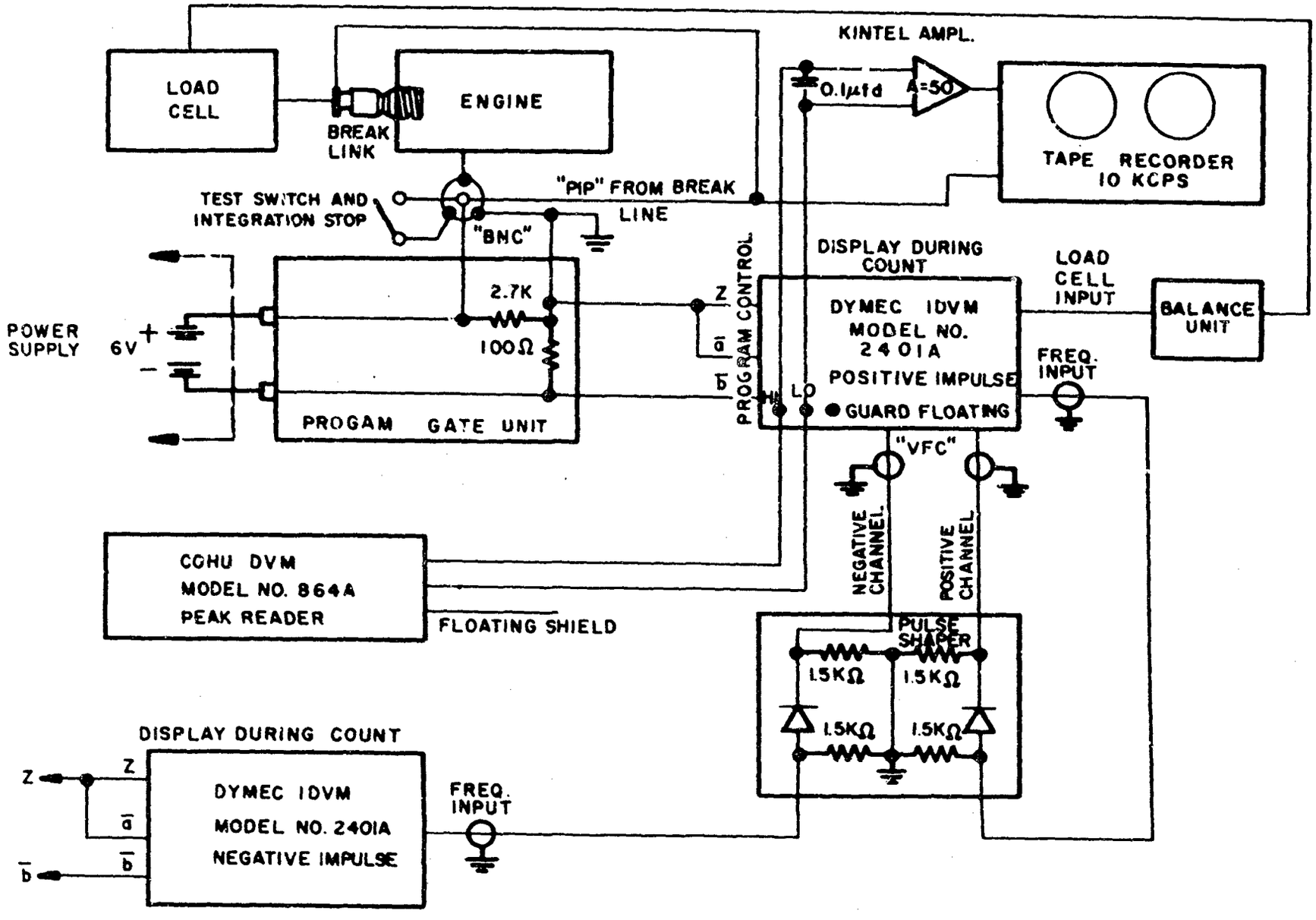

Figure 20. Dynamic Test Setup (electrical)

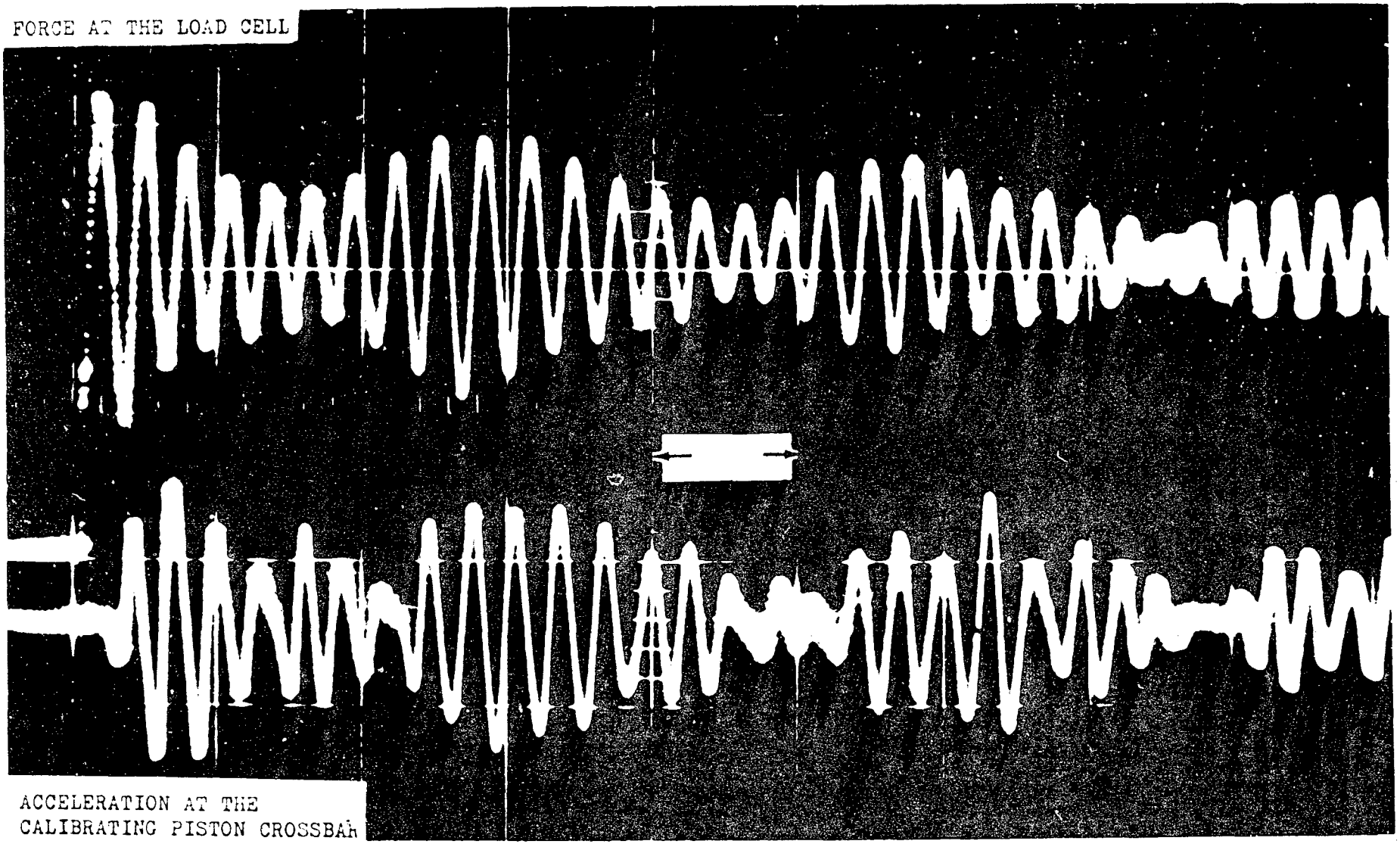

Figure 21. Oscillogram of System Response to Step Unloading (Rocketdyne)

Fig. 22. Rocketdyne Total Impulse Measurement System

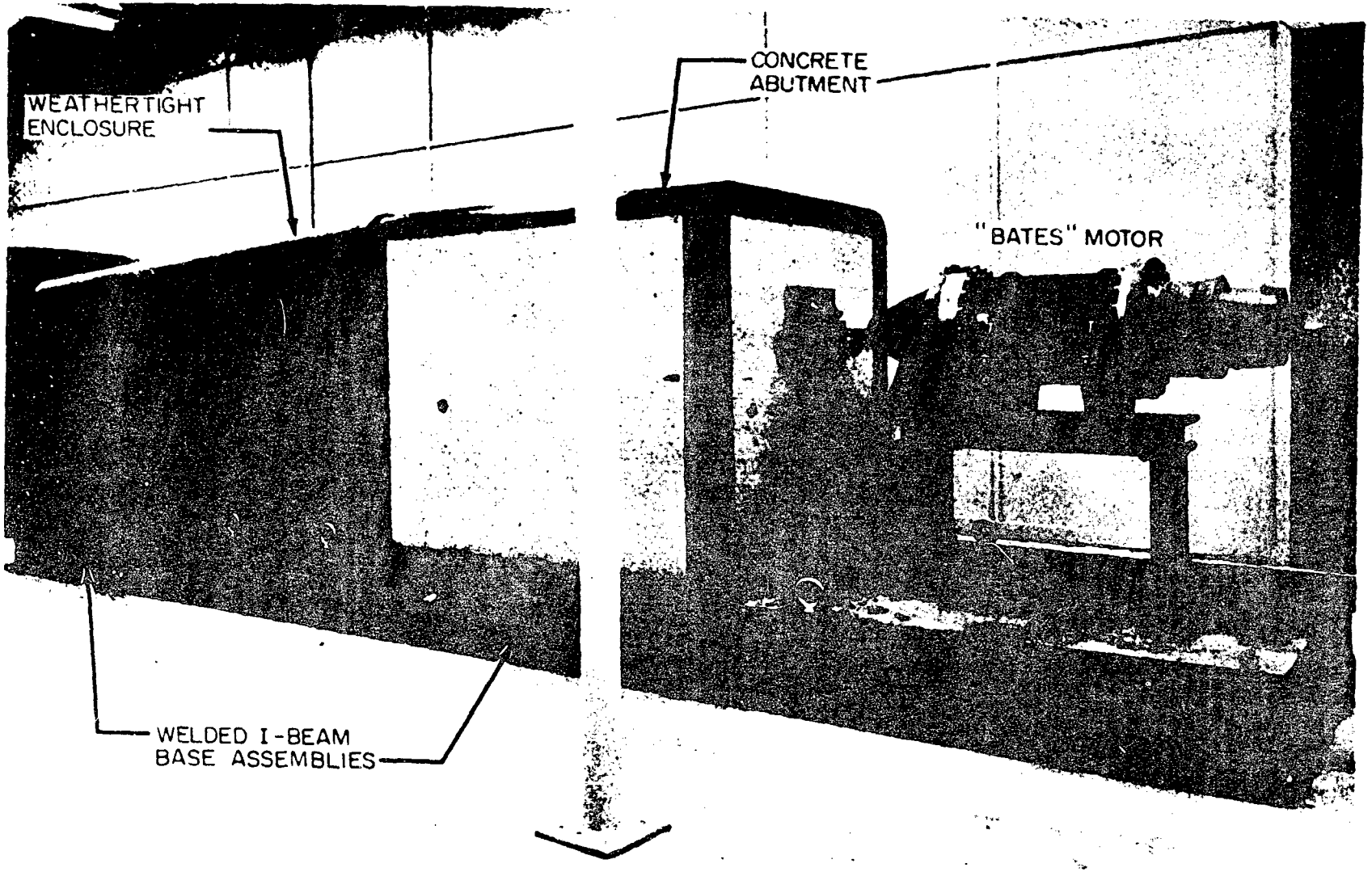

Fig. 23. Test Stand of Rocketdyne Solid Propellant Total Impulse Measurement System (Before Painting)

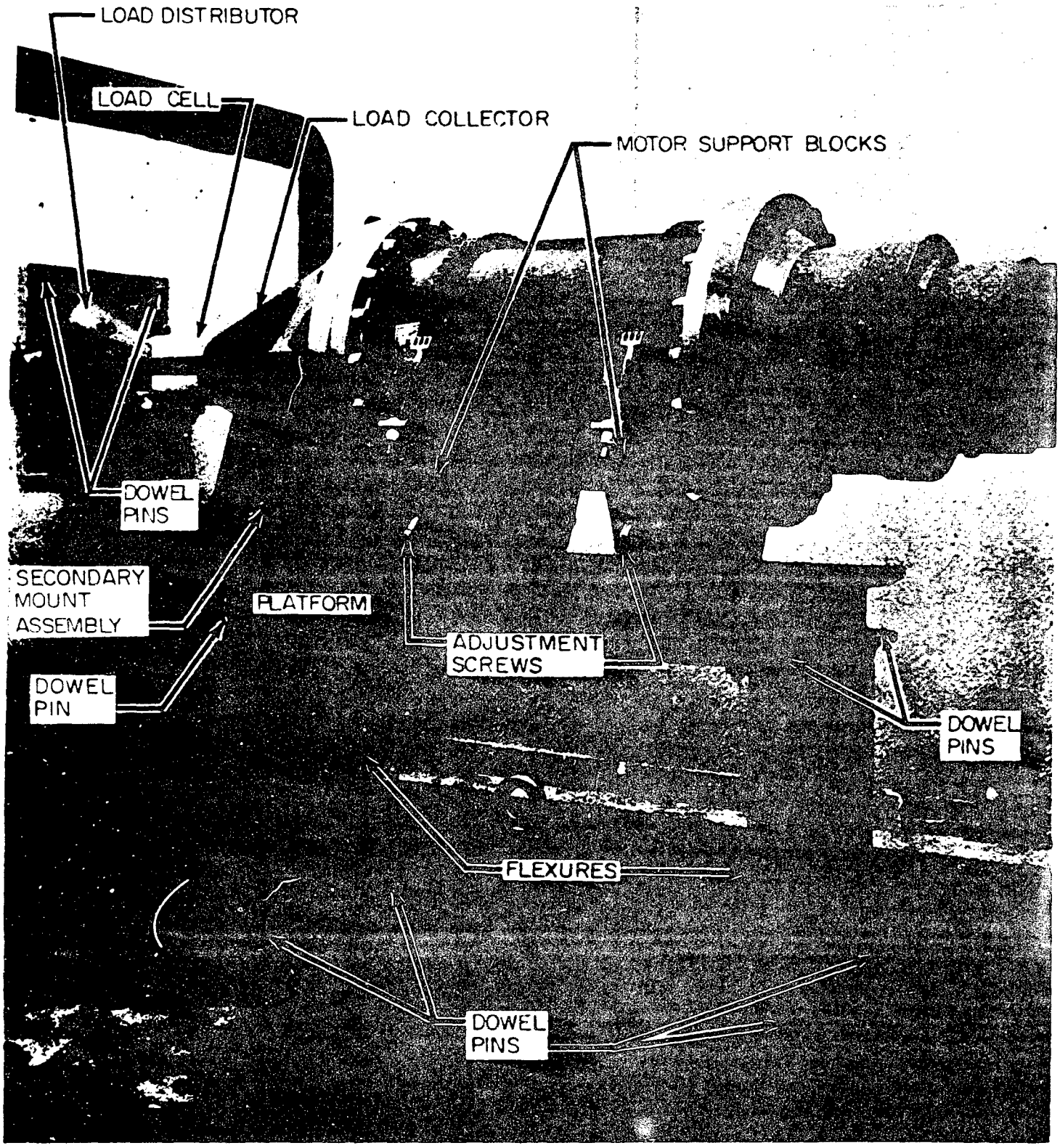

Fig. 24. BATES Motor Mount and Thrust Retainer Detail

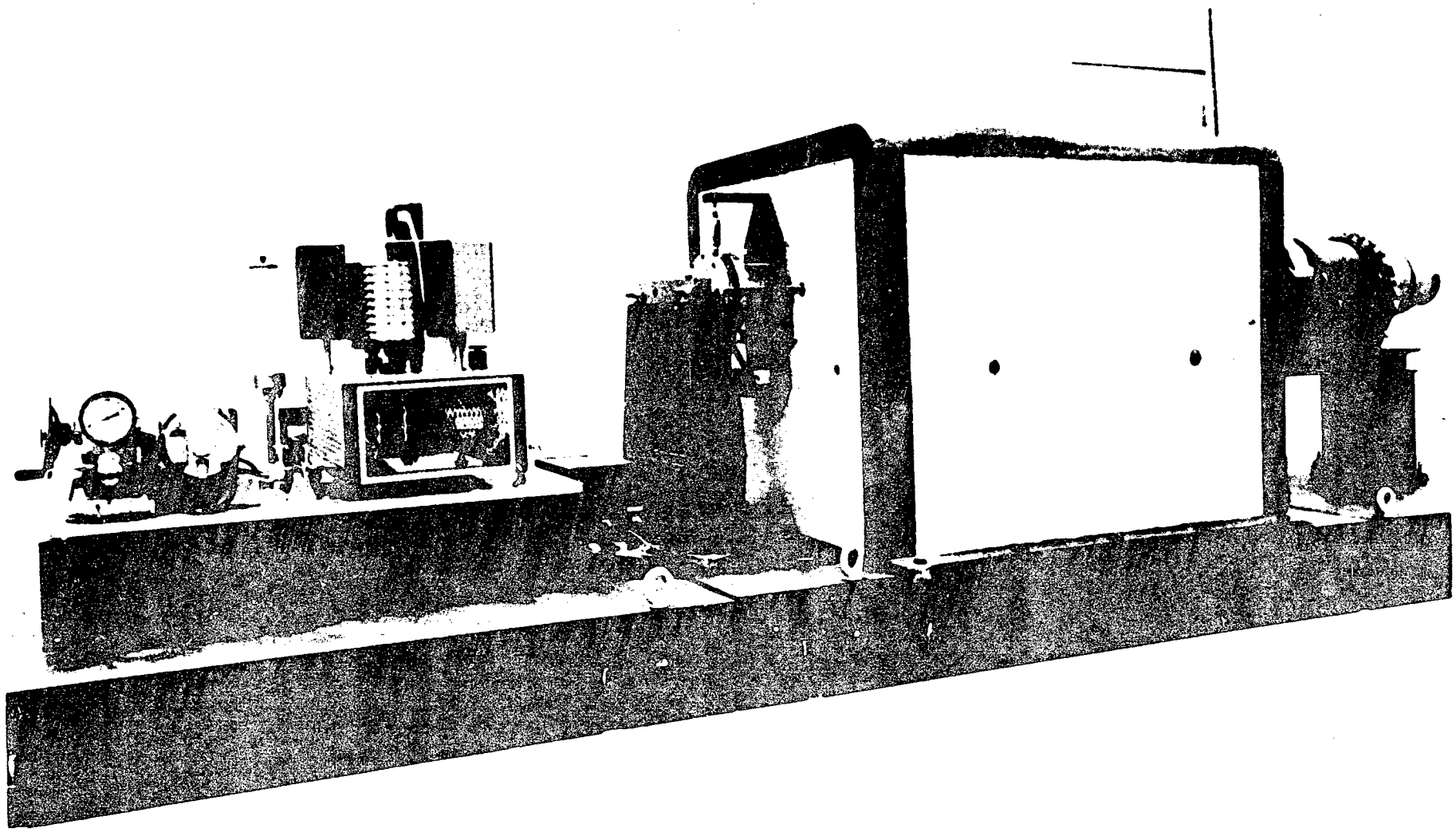

Fig. 25. Test Stand Section of Rocketdyne Total Impulse Measurement System (Weathertight Enclosure Removed)

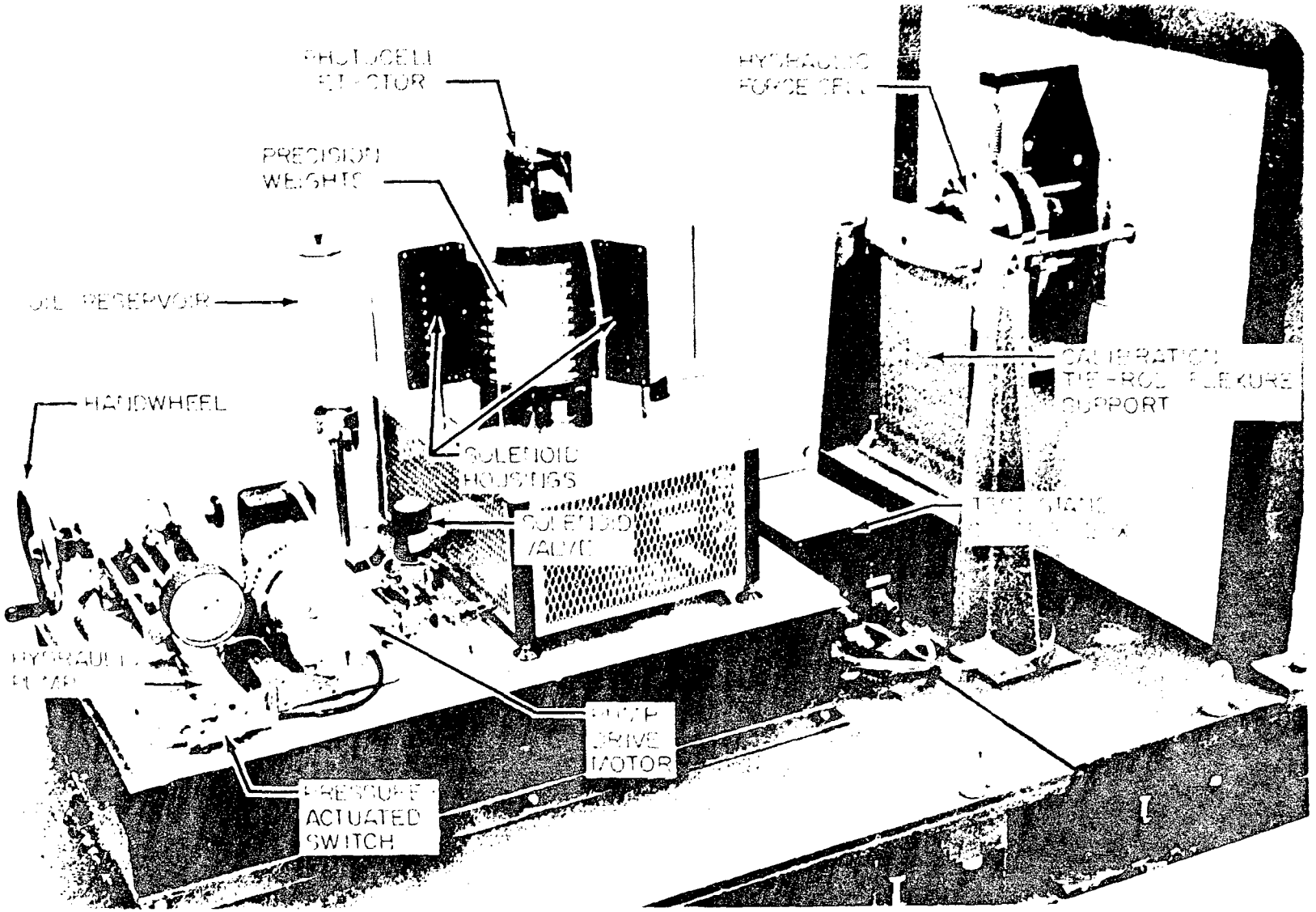

Fig. 26. Calibration System Detail

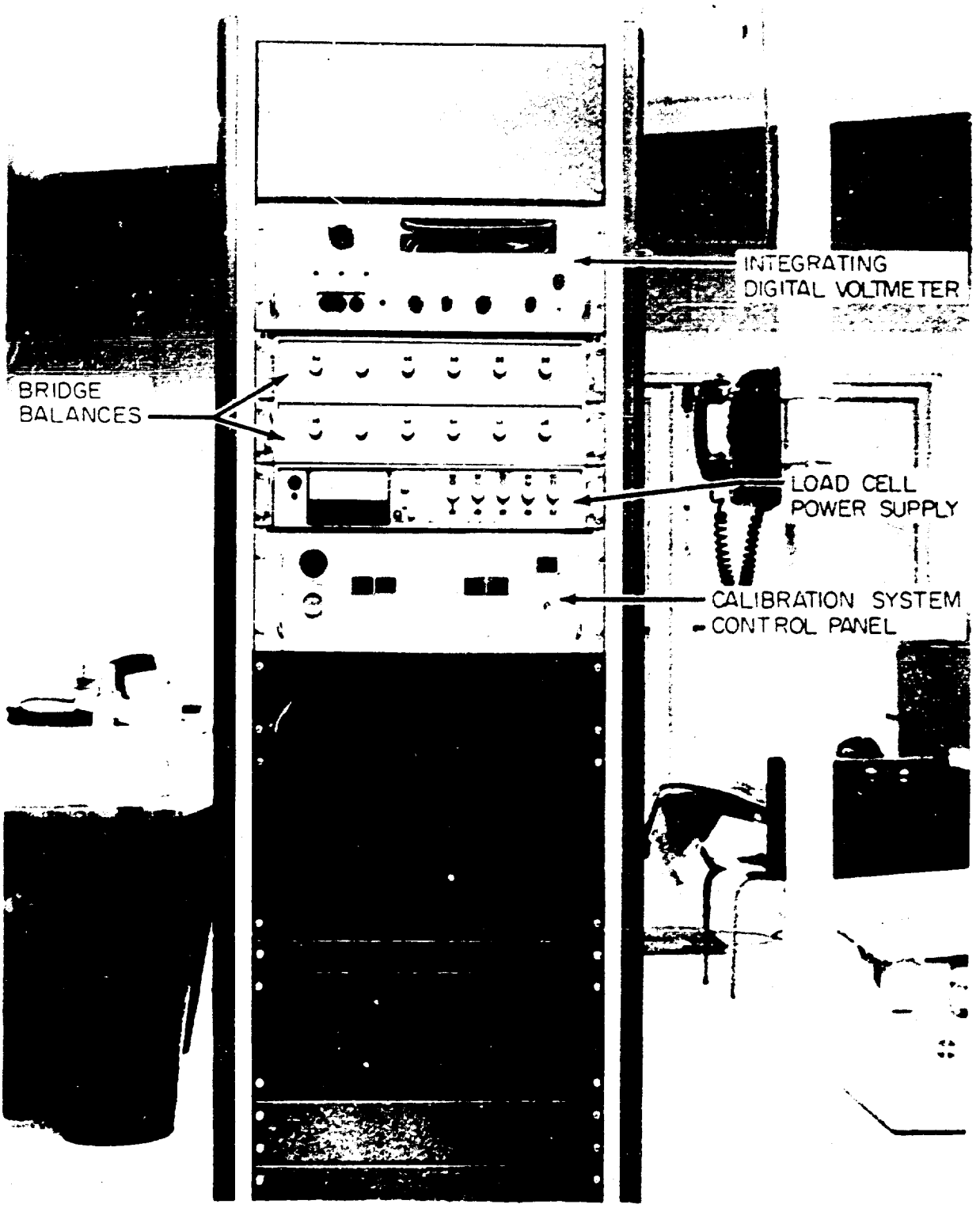

Fig. 27. Calibration Control and Measurement Equipment Section of Rocketdyne Total Impulse Measurement System

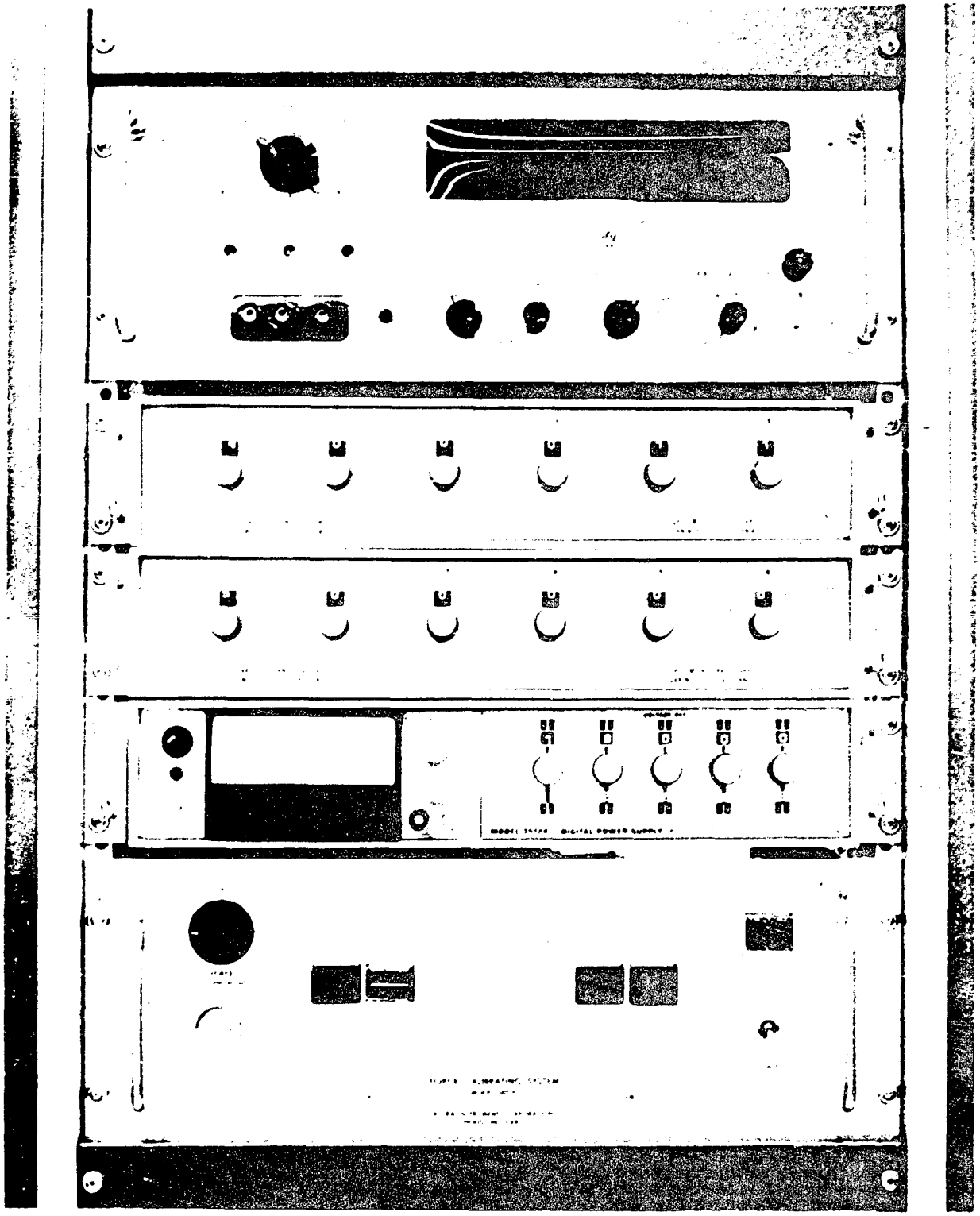

Fig. 28. Calibration Control and Measurement Equipment Detail

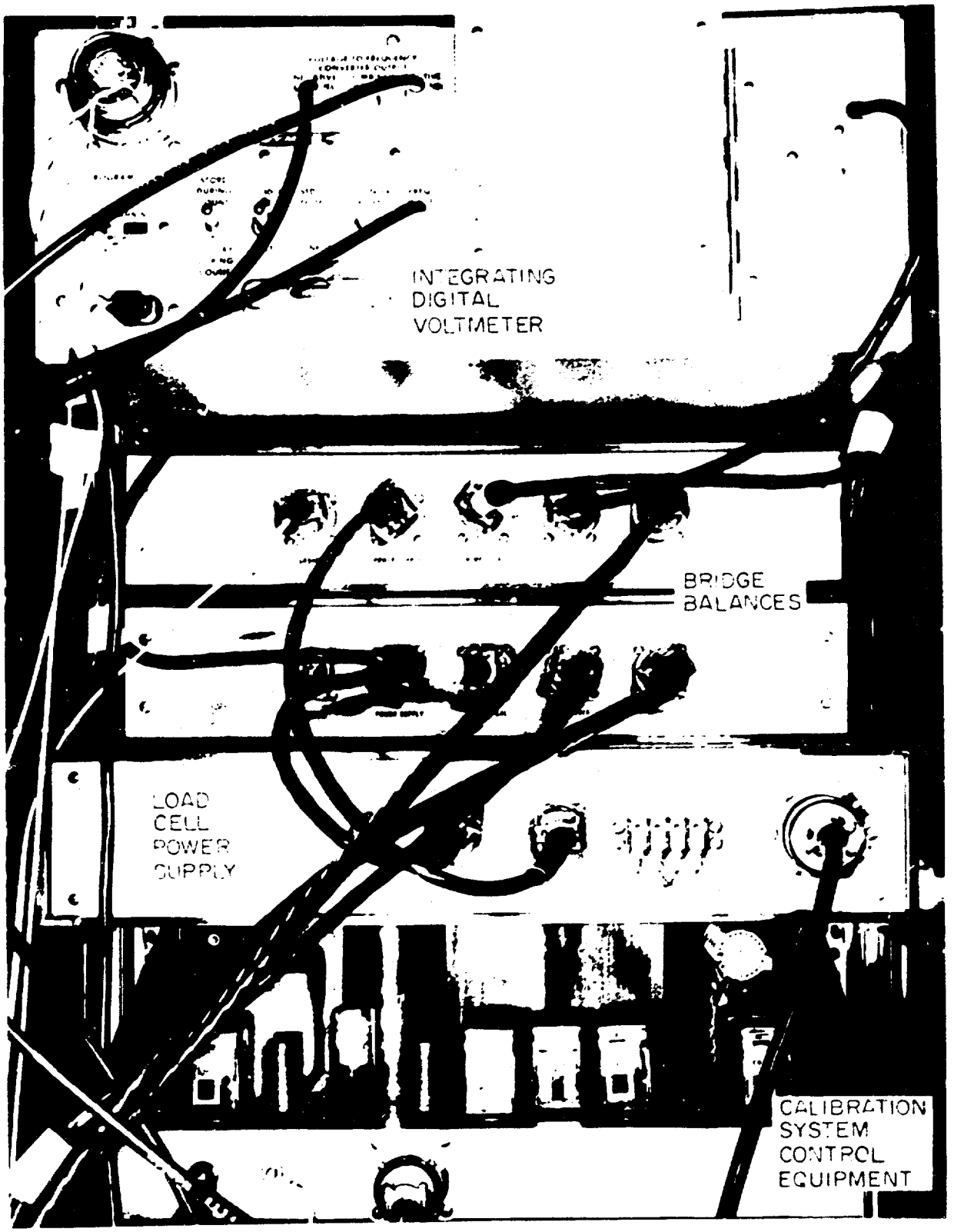

Fig. 29. Calibration Control and Measurement Equipment (Rear View)

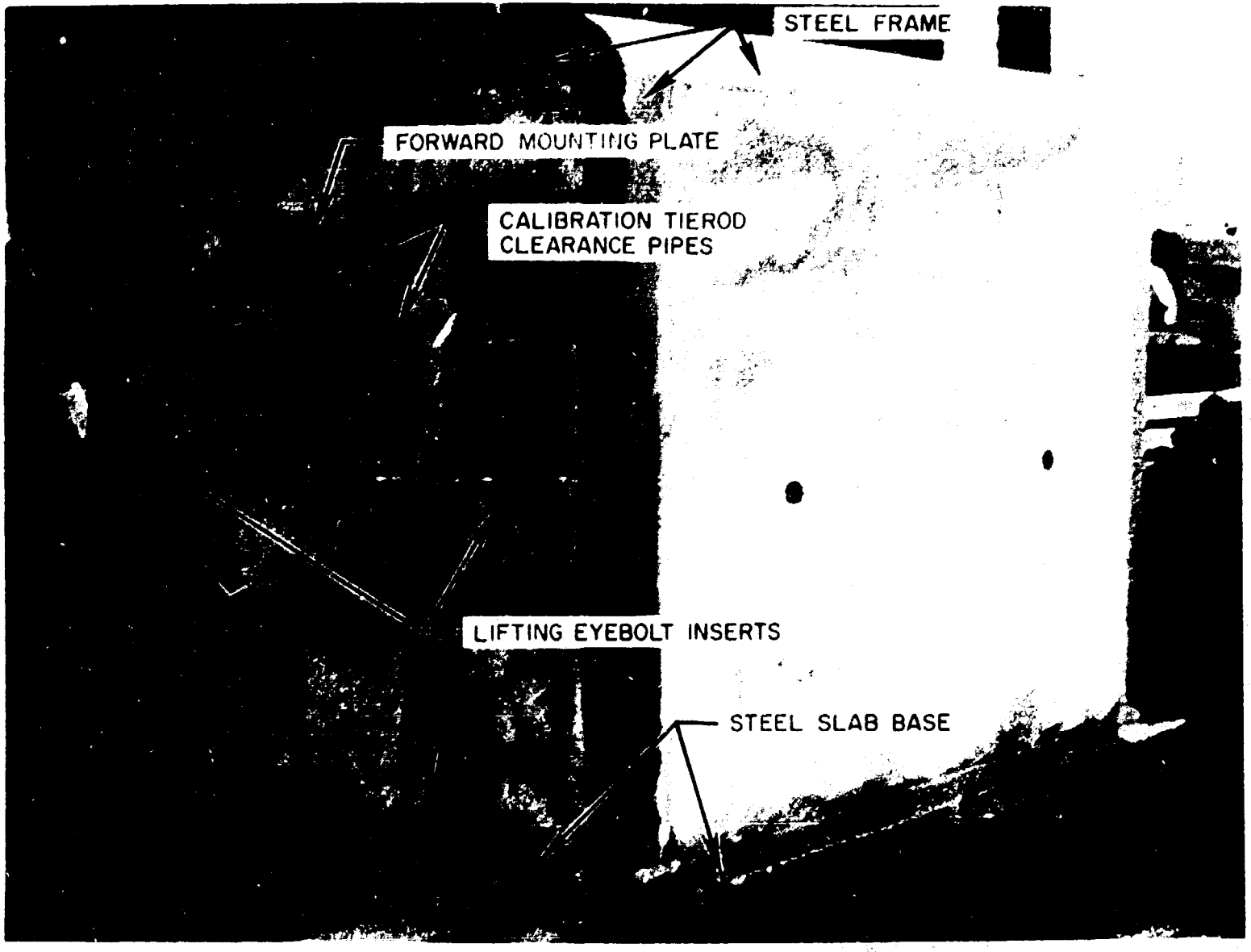

Fig. 30. Concrete Abutment During Curing

Fig. 31. Top View of Abutment Reinforcing Steel

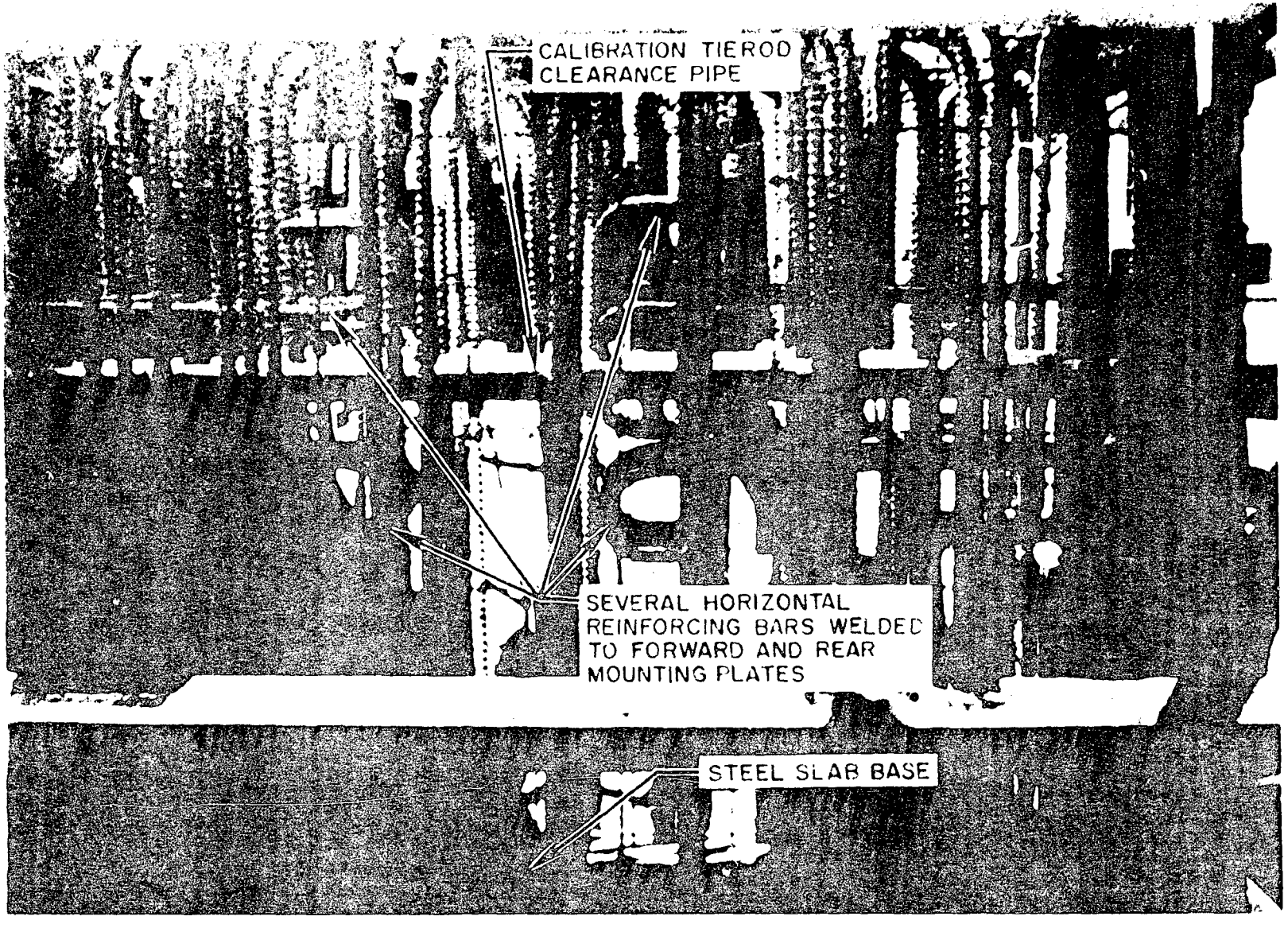

Fig. 32. Side View of Abutment Reinforcing Steel

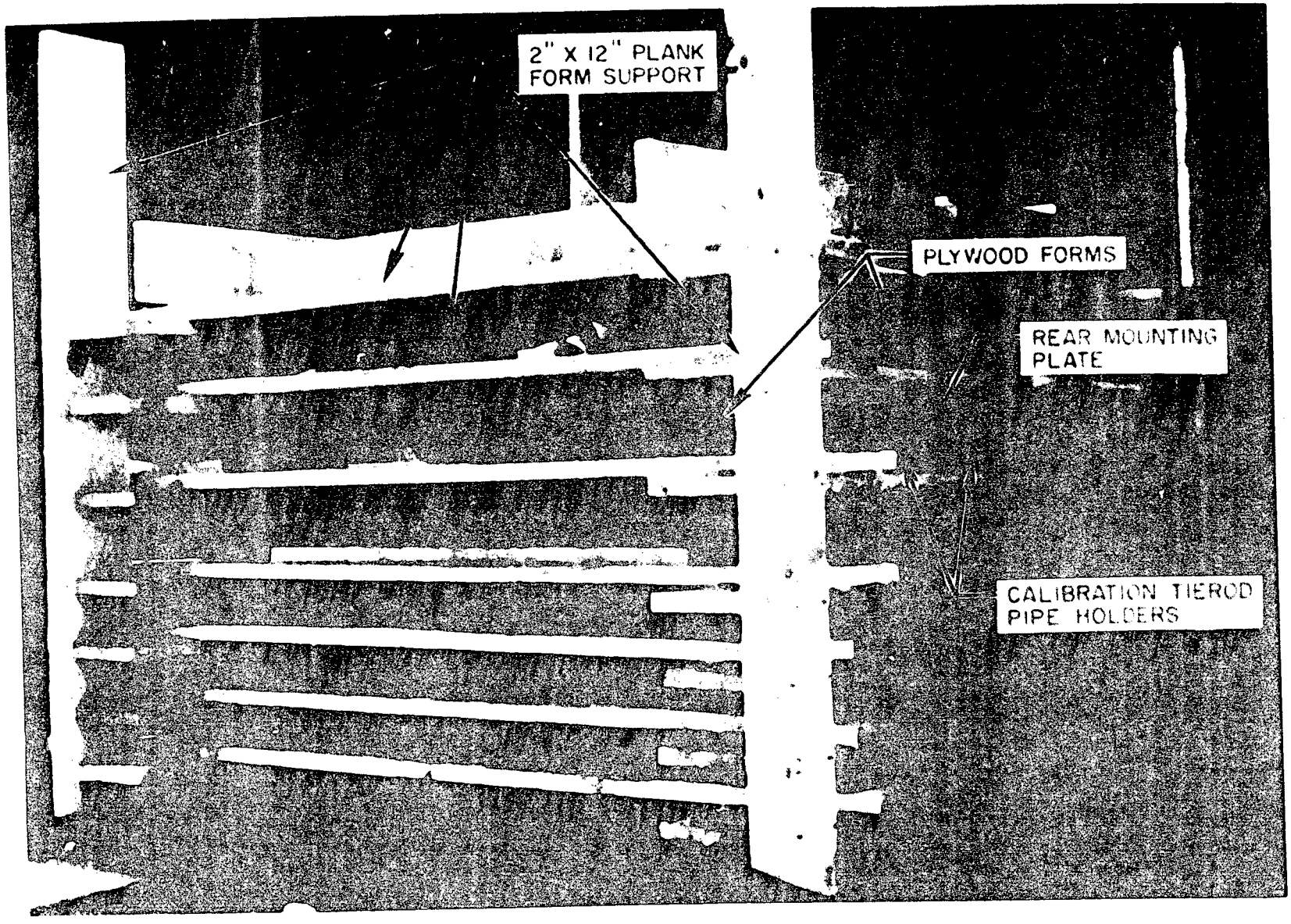

Fig. 33. Concrete Abutment Retaining Forms

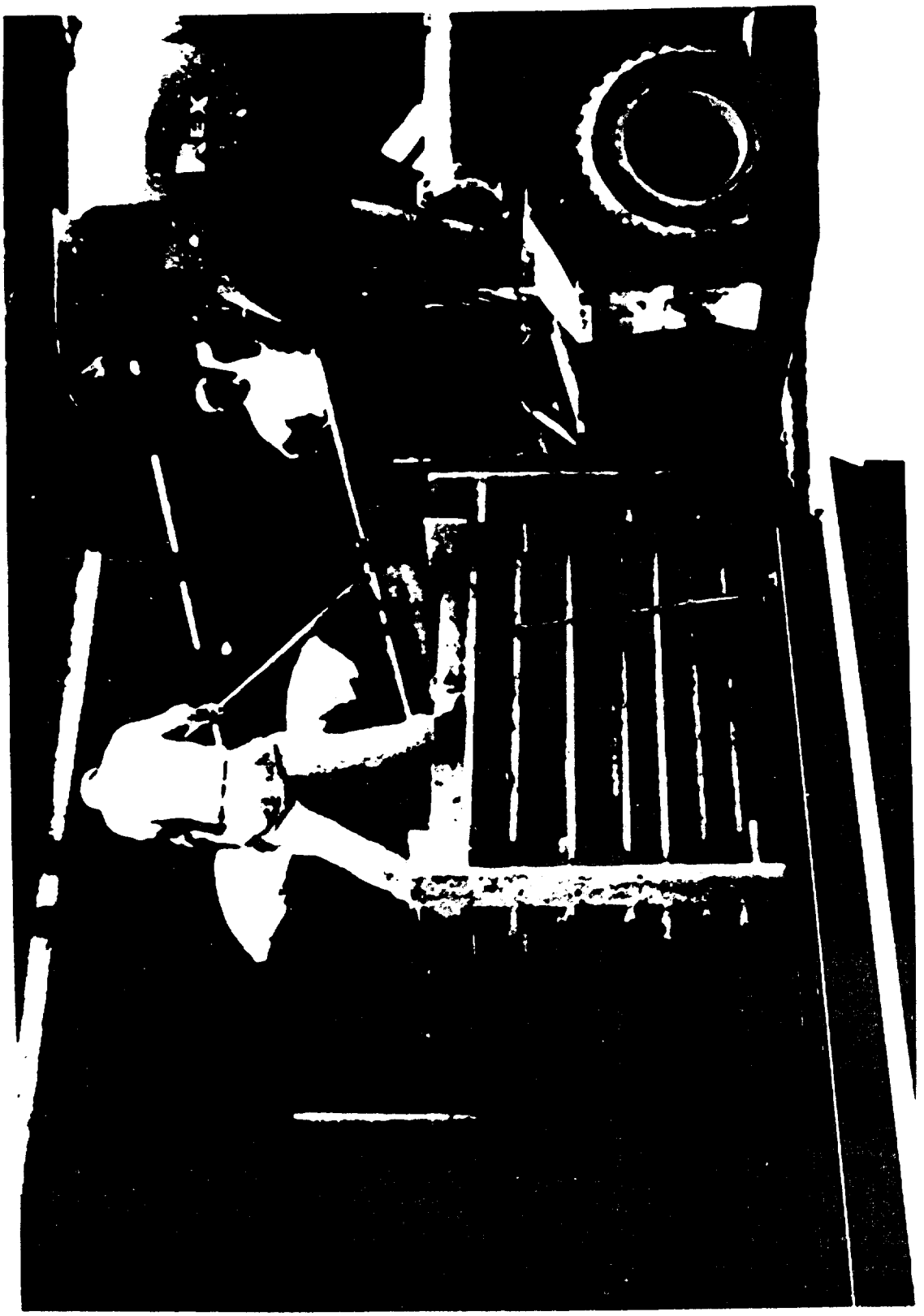

Fig. 34. Concrete Abutment Pouring

Fig. 35. Forward I-Beam Support Base

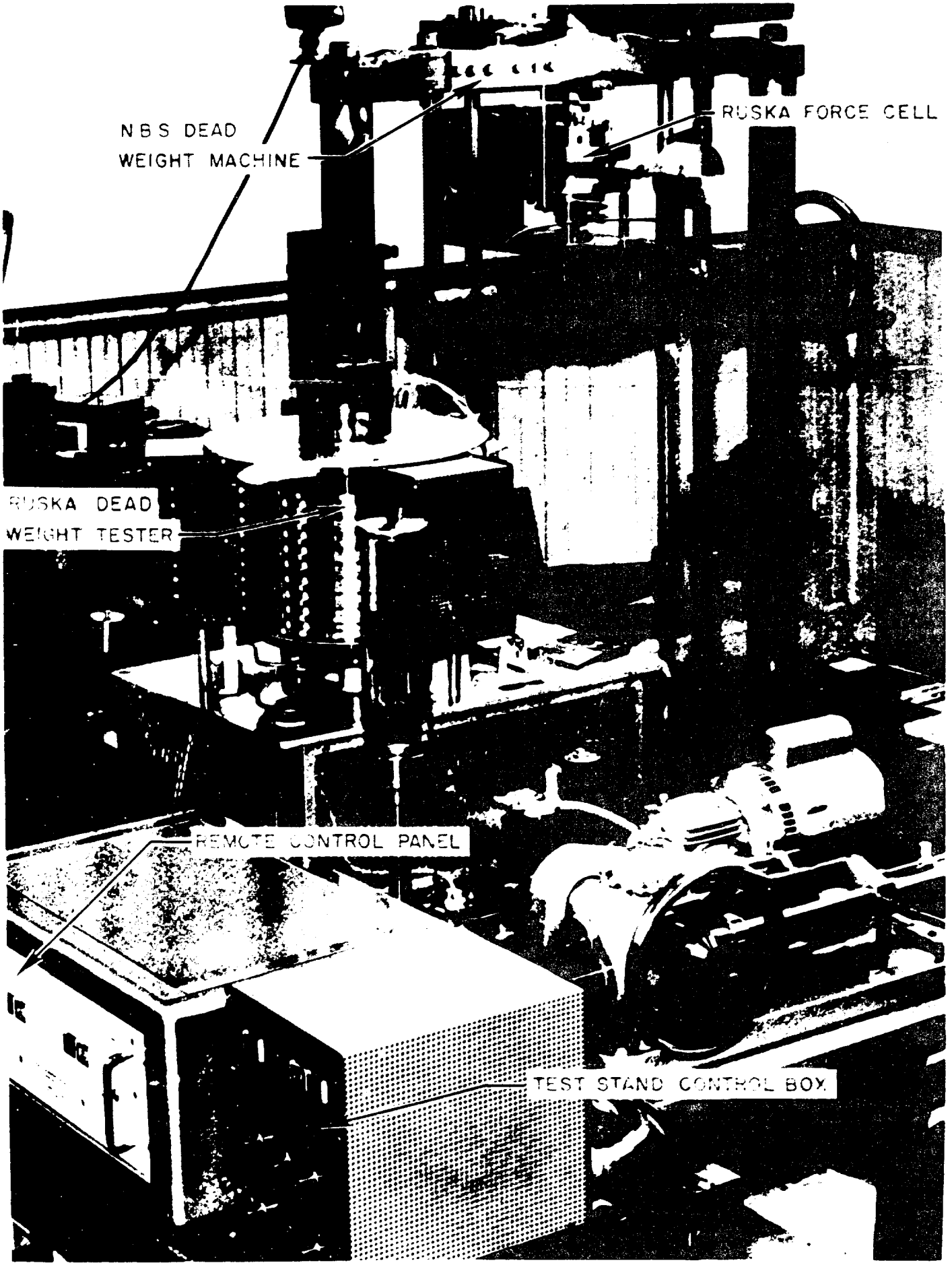

R-5638 Fig. 36. NBS Calibration of Hydraulic Calibration System

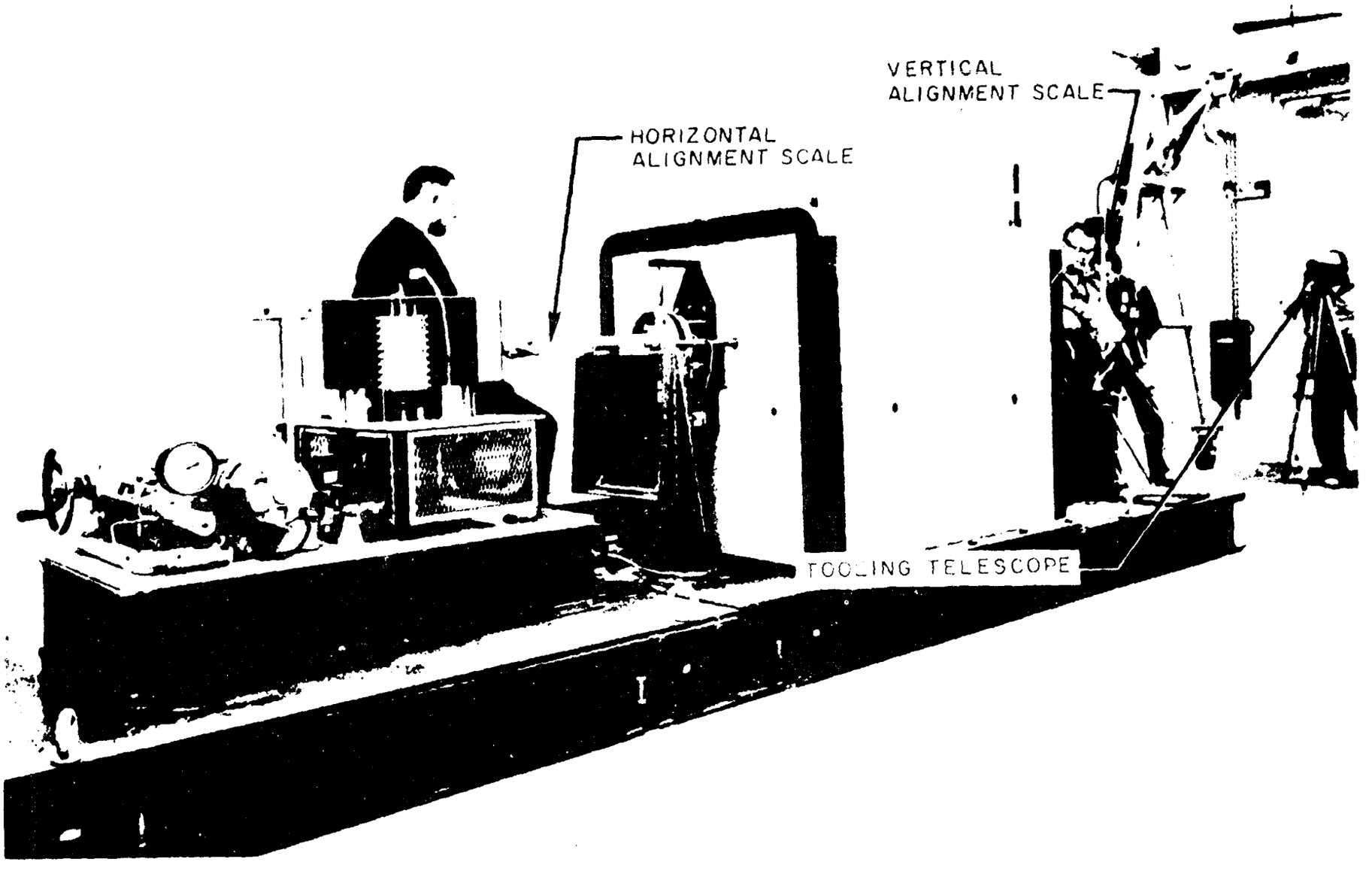

R-5638

Fig. 37. Alignment of Calibrator and Load Cell

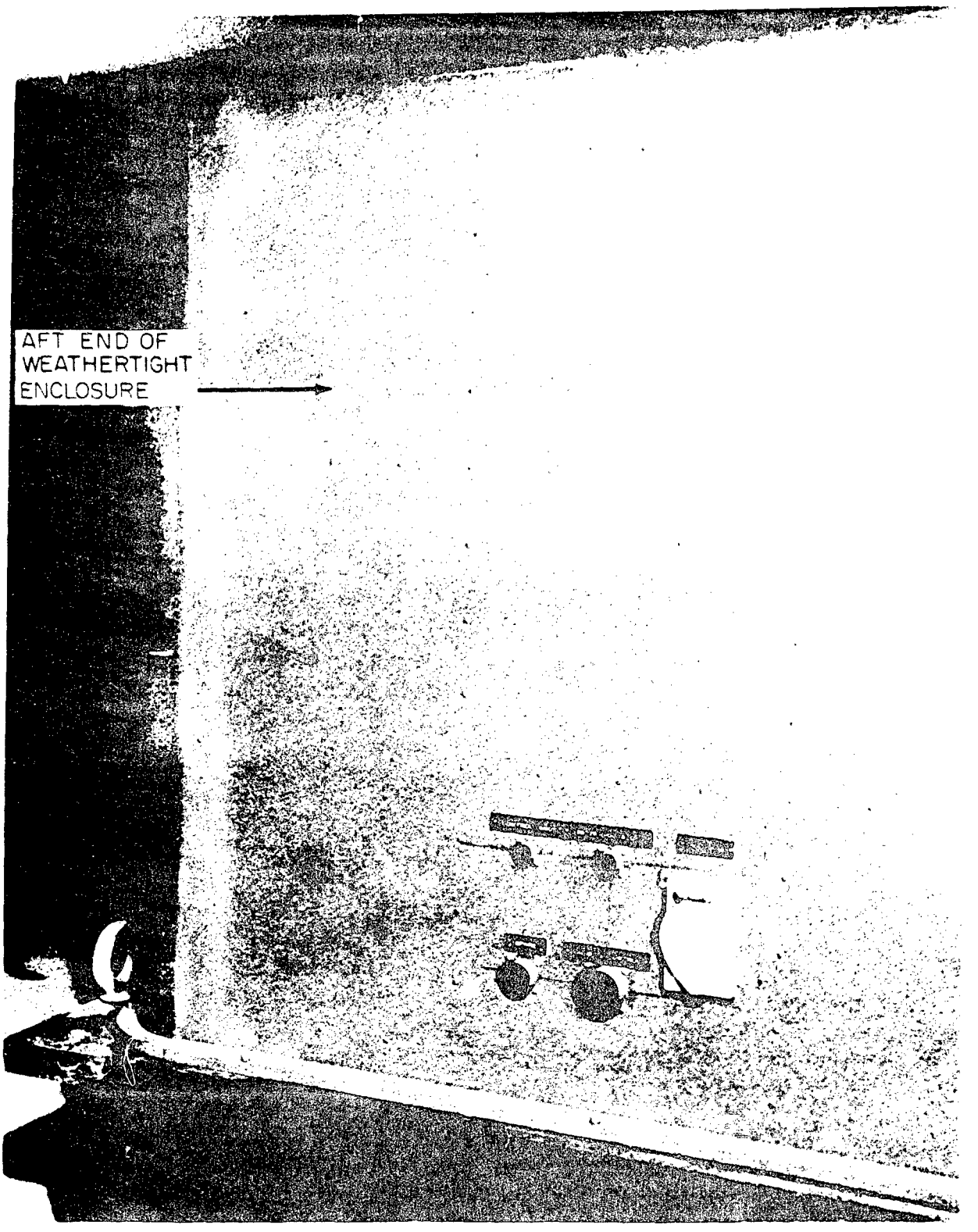

Fig. 38. Test Stand Calibration System External Wiring Connections

FIR.7 15 - MARCH 18, 1964
L/A.. 5 - MARCH 19, 1964

	1	2	3	4	5	6	7	8	9	10
FORCE K lbs.	70°F 10:00 17.066	70°F 10:15 17.066	70°F 10:30 17.066	70°F 10:40 17.066	66°F 10:50 17.066	68°F 11.00 17.066	71°F 12, 25 17.066	71°F 12:40 17.066	71°F 13:00 17.066	71°F 13:15 17.066
0	00.000	00,000	00.001	-00.00	-00.001	00 000	00.000	00.000	00.000	00.000
1	04.994	04.994	04.993	04.991	04.991	04.999	04.996	05.000	04.999	04.996
2	09.991	09.990	09.982	09.985	09.986	09.996	09.995	09.999	09.999	09.994
4	19.984	19.986	19.984	19.978	19.984	19.994	19.992	19.998	19.999	19.993
6	29.980	29.982	29.979	29.974	29.977	29.991	29.990	29.998	29.999	29.993
8	39.974	39.976	39.975	39.968	39.974	39.986	39.990	39.996	39.999	39.991
10	49.968	49.969	49.970	49.964	49.971	49.983	49.991	49.996	49.998	49.989
8	39.978	39.977	39.976	39.974	39.977	39.988	39,996	40.000	40.004	39.995
6	29.989	29.987	29.986	29.983	29.985	29.994	29,999	30.006	30.008	29.998
4	19.996	19.994	19.994	19.992	19.992	19.998	20.001	20.011	20.011	20.002
2	10.003	10.000	10.002	09.998	09.996	10.000	10.002	10.013	10.015	10.002
1	05.004	05.001	05.005	05.000	04.996	05 001	05.001	05.011	05.016	05.001
0	00.004	00.001	00.004	-00.002	-00.005	00.000	00.000	00.005	00.013	00.001
bridge balance	490540	490540	490640	490600	490720	491130	491330	491330	491460	491080
	11 71°F	12 74°F	13 74°F	14 74°F	15 74°F	16 67°F	17 67°F	18 68°F	19 68°F	20 68°F
	13:25	13.35	13.45	14:00	14:45	12:15	12:30	12:45	13:00	13:15
FORCE	17.066	17.066	17.066	17.066	17.066	17.066	17.066	17.066	17.066	17.066
0	00.001	00.001	00.000	00.000	00.001	00.000	00.001	-00.001	00.001	00.001
1	04.996	04.991	04.998	04.994	04.992	04.992	04.995	04.995	04.992	04.992
2	09.993	09.991	09.996	09.992	09.989	09.986	09.990	09.988	09.986	09.989
4	19.993	19.991	19.993	19.990	19.987	19.978	19.984	19.981	19.979	19.984
6	29.991	29.992	29.992	29.987	29.984	29.973	29.978	29.975	29.973	29.977
8	39.991	39.990	39.988	39.984	39.981	39.967	29.970	39.968	39.965	39.969
10	49.990	49.987	49.984	49.981	49.980	49.964	49.965	49.961	49.964	49.962
8	39994	39.994	39.990	39.987	39.987	39.974	39.972	39.973	39.975	39.975
6	30.000	29.999	29.995	29.993	29.995	29.984	29.979	29.985	29.986	29.985
4	20.003	20.004	20.001	20.000	20.000	19.994	19.989	19.995	19.995	19.993
2	10.006	10.007	10.003	10.003	10.005	10.000	10.001	10.002	10.002	10.004
1	05.008	05.009	05.001	05.001	05.005	05.002	05.003	05.005	05.003	05.005
0	00.006	00.008	-00.001	00.000	00.005	00.001	00.006	00.005	00.005	00.003
bridge balance	491150	491050	490830	490930	490930	490900	490900	490900	490800	490700

FIG 39 STATIC CALIBRATIONS AT EAFB.

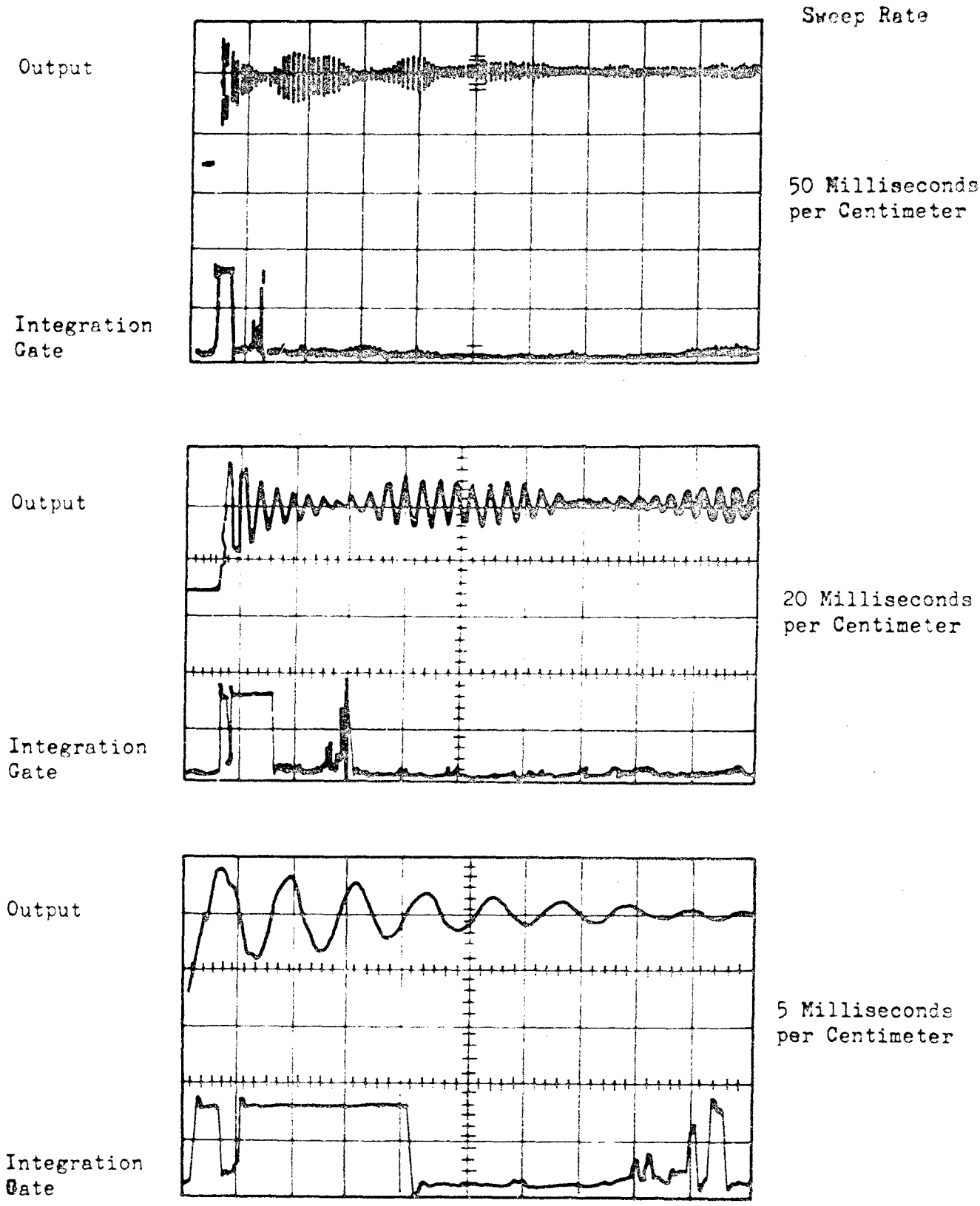

Fig. 40. Oscillogram of System Response to Step Unloading (EAFB)

APPENDIX I

AUXILIARY EQUIPMENT USED IN DATA PROCESSING

PULSE MODIFIER

During the firing of a grain in a rocket motor, the Dymec model 2401A Integrating Digital voltmeter presents the accumulating total impulse as impulse bits to its integral counter. These impulse bits are finite pulses of definite height and very short time width. The pulses are witnessed by the internal counter as a pulse train with a variable repetition rate. Access to the pulse train signal is gained via BNC connectors at the back of the Integrating Digital Voltmeter and this pulse train signal can be recorded on a tape recorder for play back and counting at a later time.

However, when a pulse of short duration is recorded on tape, the playback will distort the pulse in such a manner that the pulse will appear as though it had been acted upon by a differential transfer function. In other words, the playback pulse signal appears as a damped ringing oscillation at a frequency determined by the L-C circuits of the record and playback heads and the equalizing networks. The damping rate is determined by the combined "Q" of the circuits.

Reliable counting of these "ringing" pulses is exceedingly difficult because ambiguous counts can occur from the succeeding positive excursions. Even with careful adjustment of the trigger level, fluctuations in the zero signal level, rumble, wow, and 60 cps pickup can introduce errors in the count.

A Pulse Modifier was designed and constructed to allow the reliable counting of the pulse train output as it is expected to exist on the playback of previously recorded test firings at AFRPL. The pulse modifier assembly consists of two interconnected units, the Rocketdyne Pulse Modifier Unit and an Ad-Yu Electronics, Inc. Type 801AS, Continuously Variable Delay Line.

The Pulse Modifier removes all the generated pulses except the first one, removes base level variations, and produces sufficient amplitude of the first pulse so that the trigger level setting of a counter is not a critical limitation to the counting accuracy.

This is accomplished by phase cancellation of the ringing component of the pulses succeeding the initial pulse through the analog addition of the "ringing" pulse to a $\frac{1}{2}$ cycle-time-delayed "ringing" pulse.

Tests have shown that with a ringing frequency of 300 kc, a positive pulse of at least 6 volts is produced from the Pulse Modifier, and at

100 kc and below, at least 12 volts. With negative pulse operation the output is limited to about 5 or 6 volts regardless of the ringing frequency. A complete discussion of the principle and design of this two-unit equipment is contained under separate cover.

INTEGRATION LIMIT CONTROLLER

One of the standard practices employed in the performance evaluation of solid rocket propellants in firing tests is to cutoff the start-up and tail-off transients of the force-time-history analog; integrating only during the time the thrust history is above some pre-determined thrust level (typically from 10% maximum thrust to 10% maximum thrust for large propellant grains).

The Dymec model 2401A Integrating Digital Voltmeter of the Total Impulse Measuring System for Solid Propellant Rocket Engines, provides a pulse train output whose repetition rate is in direct proportion to the thrust level analog voltage at the input of the instrument. When recorded on tape and subsequently played back through the Rocketdyne pulse modifier, these pulses are available for gated pulse counting. Thus it is only necessary to restrict the pulse train input to a compatible counter in such a manner as to allow the counting of only those pulses which occur above a pulse repetition rate indicative of the chosen thrust level.

A rate-controlled gating device is necessary when it is required to pass pulses only when the pulse rate is in excess of some preselected value. A circuit design for an Integration Limit Controller was furnished by Rocketdyne to serve this purpose. This device is essentially a pulse rate discriminator with a timer device circuit added to accommodate integration time determinations.

The operation of the circuit is based on the principle of pulse-coincidence-adding with an internally synchronized rate-control pulse. A "breadboard circuit" model was tested and the circuit operation was shown to be entirely reliable. The design of this unit is contained under separate cover.

APPENDIX II

EXPANDED DISCUSSION OF EAFB DYNAMIC AND MOTOR FIRING TEST RESULTS RELATED TO TEST STAND PERFORMANCE

TEST STAND VIBRATIONAL MODES

Introduction

A dynamic test (step-unloading type) on the Total Impulse Measurement System test stand at EAFB on March 31, 1964 resulted in the load cell decayed response curves shown in Fig. 40. Detailed examination of these curves has resulted in substantial confirmation of deductions obtained from two-degree-of-freedom vibration theory, and constitutes additional verification of the correctness of the approach taken in the Phase I analysis and design effort of this program. A brief discussion of theory and test results is given below.

Vibration Theory

The test stand is adequately described as a two spring - two mass system with negligible damping and is pictured in the accompanying diagram.

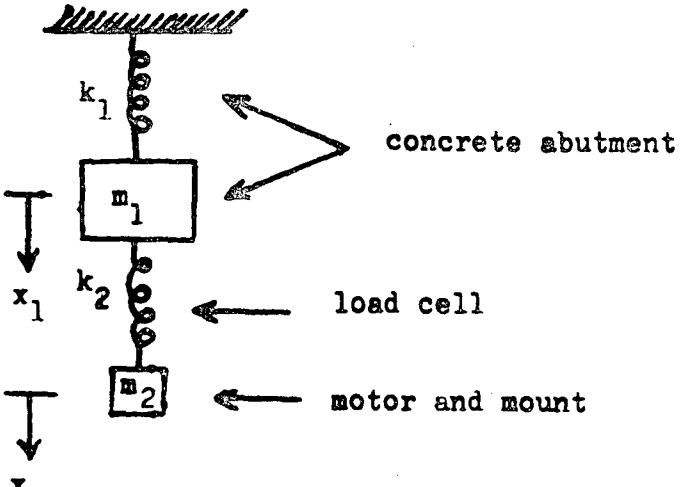

where

k_1, k_2 = abutment and load cell spring stiffnesses, respectively

m_1, m_2 = abutment and motor (and mount) masses, respectively

x_1, x_2 = displacements of the masses from their respective equilibrium positions

The method of analysis for this system is generally applicable to all types of systems with two degrees of freedom. Newton's second law for the masses can be written

$$m_1\ddot{x}_1 + k_1x_1 + k_2(x_1 - x_2) = 0$$
$$m_2\ddot{x}_2 + k_2(x_2 - x_1) = 0 \qquad (1)$$

In seeking the solutions for free harmonic vibration, note that when the frequency (circular) is ω, the maximum acceleration of m_1 is $-x_1\omega^2$, and the maximum acceleration of m_2 is $-x_2\omega^2$. This results from the fact that for harmonic motion of the type $x = X \sin \omega t$, the acceleration is $\ddot{x} = -X\omega^2 \sin\omega t = -x\omega^2$:

$$-m_1x_1\omega^2 + k_1x_1 + k_2(x_1 - x_2) = 0$$
$$-m_2x_2\omega^2 + k_2(x_2 - x_1) = 0 \qquad (2)$$

Each of these two algebraic equations can be solved for ω:

$$\omega^2 = \frac{k_1 x_1 + k_2(x_1 - x_2)}{m_1 x_1} = \frac{k_1}{m_1} + \frac{k_2}{m_1}\left(1 - \frac{x_2}{x_1}\right)$$

$$\omega^2 = \frac{k_2(x_2 - x_1)}{m_2 x_2} = \frac{k_2}{m_2}\left(1 - \frac{x_1}{x_2}\right) \tag{3}$$

Eliminating ω and rearranging terms, these equations simplify to

$$\left(\frac{x_2}{x_1}\right)^2 - \left(\frac{k_1}{k_2} - \frac{m_1}{m_2} + 1\right)\left(\frac{x_2}{x_1}\right) - \frac{m_1}{m_2} = 0 \tag{4}$$

Upon solving this quadratic equation in $\left(\frac{x_2}{x_1}\right)$ there results

$$\frac{x_2}{x_1} = \frac{\left(\frac{k_1}{k_2} - \frac{m_1}{m_2} + 1\right) \pm \sqrt{\left(\frac{k_1}{k_2} - \frac{m_1}{m_2} + 1\right)^2 + 4\frac{m_1}{m_2}}}{2} \tag{5}$$

Note that there are two solutions, each representing the ratio of displacements of the masses in a mode of free vibration, and their values can be found by the values of spring stiffnesses and masses. The values of the mode frequencies are then obtained by the use of either of the equations (3).

Test Results

The behavior of the load cell spring is observable by its electrical output signal, and when the two vibration modes of the two spring - two mass system are not far different in frequency, a motion similar to "beating" can be observed. For example, at a particular instant of time the load cell can be expanding due to the first-mode component of the vibration and compressing due to the second-mode component of the vibration. Under this combination of motions the load cell will be almost unstressed at that particular moment, while at a later moment it is uni-directionally stressed by both modes of vibration. The resulting behavior of the load cell consequently appears as shown in the following diagrams when the system is allowed to freely vibrate.

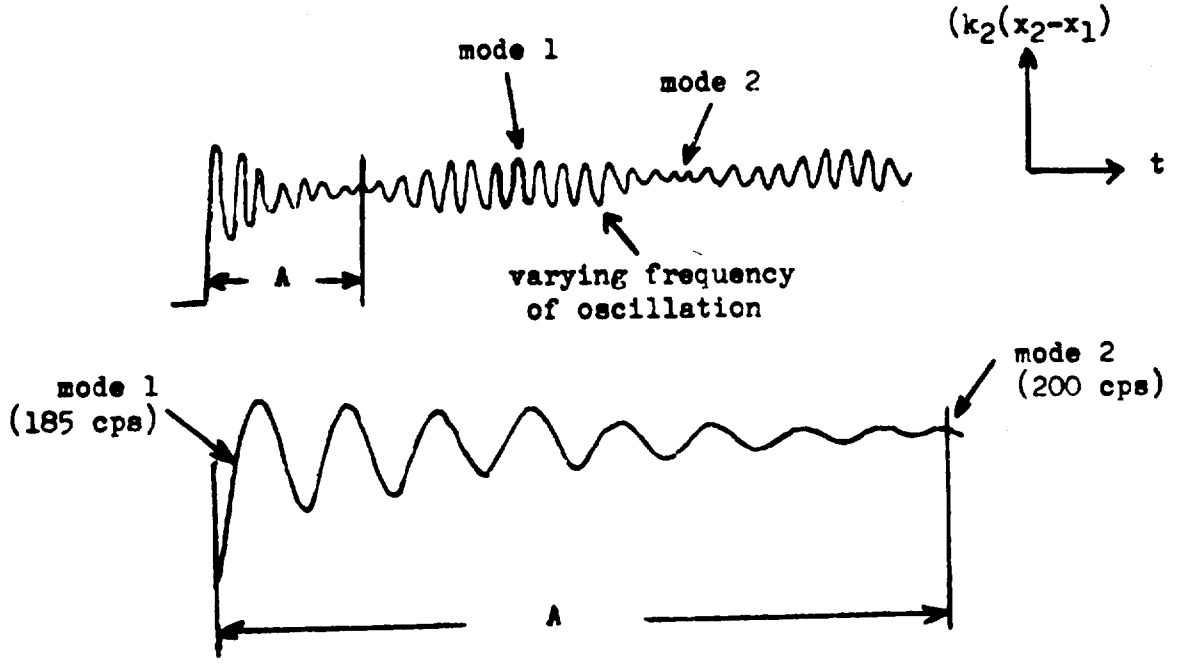

The second of the two diagrams is an expanded view of the section of time span A. The system modes are observed separately at the identified stations of the response curve in the first diagram, and the key to the verification of the presence of two coupled vibration modes is the observation of the two mode frequencies at the two stations. The frequency of oscillation of the load cell signal constantly changes with time between the two coupled mode frequencies and the observed values of the mode frequencies were in good agreement with the values obtained by calculation from system stiffnesses and masses, utilizing equations (5) and (3).

To conclude this discussion, the agreement of theory and measurements provided definite identification of the two degrees of freedom, by means of their mode frequencies, namely, the motor head and the abutment mounting face, respectively. The reference for the mathematical discussion was Vibration and Impact, Burton, 1958.

MOTOR-TEST STAND INTERFERENCE

Description of Result

As stated in the discussions of test firing results and the recommended addition to the motor installation, a post-run effect on the thrust load cell was experienced which appeared to be due to a thermal effect generated by the heat produced during a motor firing. The load cell

history during and after a motor firing is shown in the accompanying typical curve of apparent load cell force vs time, in which sections are necessarily out of scale in both coordinates.

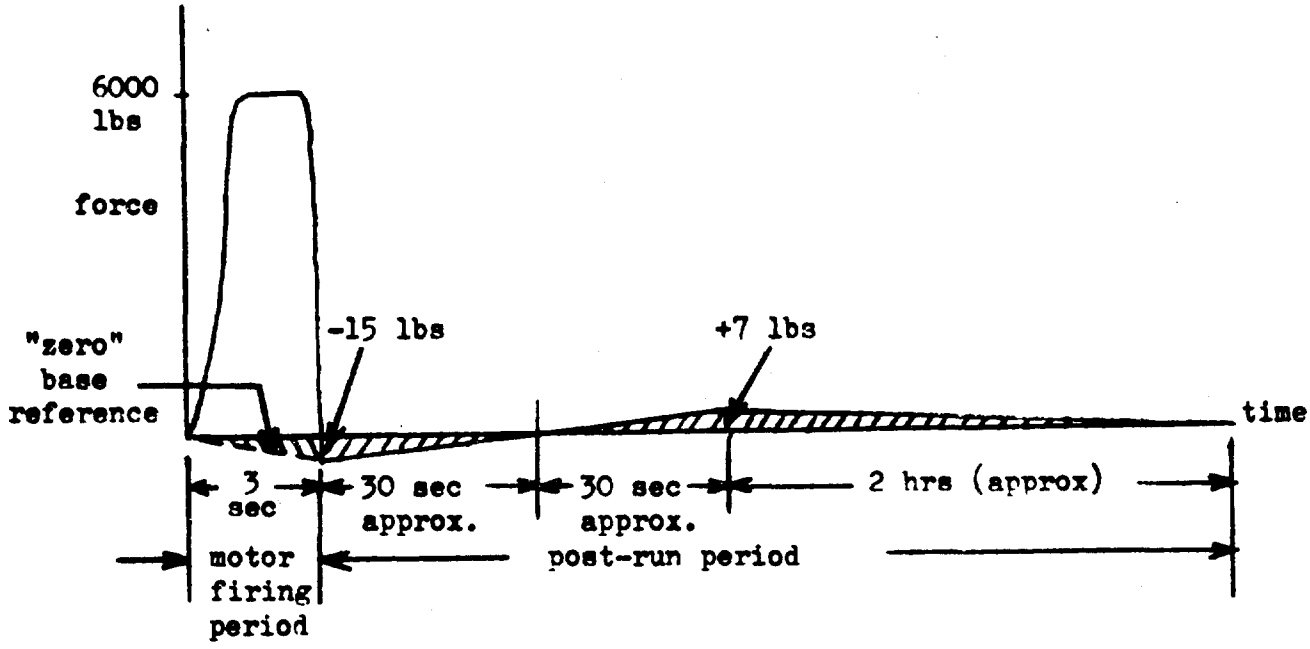

Two operationally undesirable situations result from this effect, firstly, the changing base reference which directly affects the total impulse measurement accuracy and, secondly, the interference with accurate post-run calibrations due to a shifting "zero". In the former situation, the magnitude of error, of course, depends on the manner in which the zero base reference

changes during the motor firing. Assuming a linear change of electrical "zero" with time the impulse measurement error is the area of the triangular section shown in the diagram, namely, $\frac{1}{2} \times 3 \times 15$, or $22\frac{1}{2}$ lb-sec. For a 6000 lb, 3 sec motor firing, the resulting error is 0.125%, assuming integration from "zero to zero" thrust levels. This magnitude of error is inadmissibly large when compared to the program objective of 0.1% overall measurement error.

Discussion of Possible Sources

The behavior of the resulting effect on the load cell strongly suggests that its cause is the heat produced in the motor head, wall, and/or nozzle. This belief is logically supported by the fact that the temperatures of the stated motor parts show post-run time histories which strongly resemble the load cell signal time history. The figure below is a tracing of BATES motor temperature measurements contained in EAFB Technical Documentary Report No. SSD-TDR-62-45, April 1962, page 19.

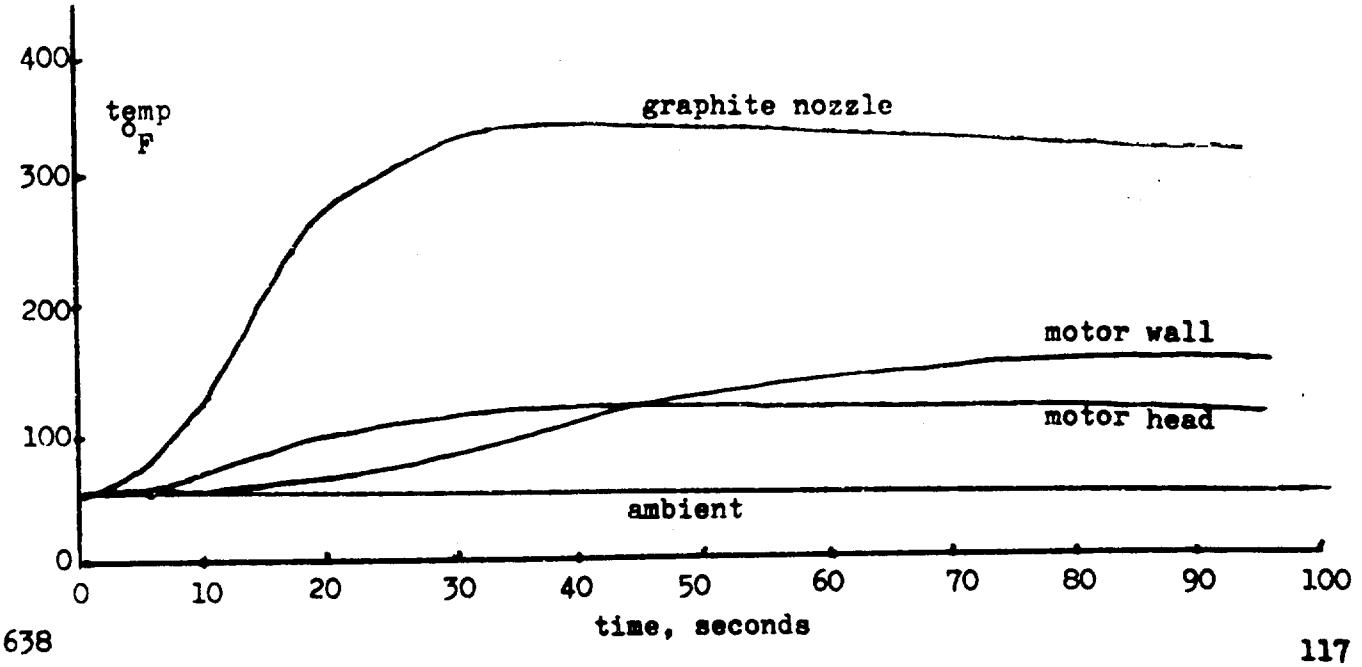

Of particular importance is the fact that the post-run temperatures follow a pattern of steady increase and leveling off in about 40 seconds for the graphite and motor head followed by a very slow temperature decrease. Comparison of these curves with the approximate apparent thrust history shows a remarkable similarity. The correlation is sufficiently close to leave little or no doubt about the cause of load cell indications. The only unresolved aspect of the effect is the exact nature of the mechanism. Two possibilities exist and are listed and discussed as follows:

1. Non-uniform heating of the load cell by conduction through the load cell collector from the motor head, to produce load cell bridge electrical unbalance.
2. Thermal expansions in the motor support table to produce flexure system displacements in the direction of the thrust axis, thereby causing a load to be applied to the cell due to the small axial stiffness of the flexure suspension system.

The latter possibility appears to be the more probable for two reasons: (1) it is difficult to conceive of appreciable heat flow through the comparatively massive load cell collector to heat the load cell non-uniformly during the 3-second run duration, and (2) localized expansions in the motor platform and secondary mount assemblies would immediately result in small axial displacements resisted by the load cell. In order to firmly establish the cause of the small post-run thrust indications, the following tests are recommended:

1. Install four strain gages on each of the two lower flexure elements of the suspension system in order to detect translation of, and expansion within, the motor platform. In order to obtain maximum sensitivity of these detector circuits, two gages should be installed in the center of each side of each lower flexure so that flexure bending will produce tension and compression on its two surfaces and result in a four active-arm bridge. Each circuit output signal should be recorded on a strip chart recorder in the control room, using D.C. amplifiers, if necessary, to obtain suitable recording pen deflections. These circuits can be easily and conveniently calibrated along with the regular system calibration, thereby relating load cell force with flexure system displacements. The post-run behavior of the flexure system circuits would immediately reveal if platform translation and/or localized expansions and stresses are occurring as a result of heat generated by a motor firing.

   Suitable radiation shields should be used during these tests to block off direct radiation from the motor exhaust to the flexures, in order that the strain gages are not unduly affected.

2. Install thermocouples on the motor platform and secondary mount assemblies, along with thermocouples on the motor wall and head, in order to determine where localized expansions are occurring in these parts, so that correlation can be made between the localized stresses and the flexure strain gage readings.

The post-run force indications of the load cell begin on the negative side of zero (opposite to motor thrust) and progress through zero to the positive side of zero (same direction as thrust). This fact, together with the behaviour of the temperature-time histories of the motor nozzle, head, and wall suggests that motor head expansion first causes displacement of the motor and its suspension in the forward direction to produce a "negative thrust" indication, and that subsequent temperature rise of the motor wall locally expands the motor platform to produce a net displacement in the thrust direction.

In any event, the strain gages on the flexure and thermocouples on the motor and its support will establish the mechanism of the effect.

If the anticipated thermal interference is demonstrated by the test results, the elimination of the effect upon the load cell can be approached in two ways, namely, (1) thermal insulation of the motor from the test stand and, (2) weakening of the flexure suspension in order that axial displacement resisting forces are reduced to a minimum. The latter of the two is the easiest to accomplish since flexure weakening is easily accommodated by drilling holes in the flexures to reduce their axial stiffness. However, it should be pointed out that flexure weakening is accompanied by increased motor axis alignment requirements if measurement accuracy requirements are to be maintained.

In the delivered configuration of the test stand to EAFB, motor axis misalignments of approximately 1/16 inch could be tolerated without undue measurement errors, and sharp reduction in the flexure system axial stiffness will correspondingly aggravate the alignment problem.

Consequently, any decision and action regarding flexure system weakening should be based on test results obtained with strain gages and thermocouples, and after all practical thermal insulation efforts have been made. A re-evaluation of motor alignment requirements should also precede any flexure weakening.

DISTRIBUTION LIST

U. S. Department of the Interior 1
Bureau of Mines
4800 Forbes Avenue
Pittsburgh, Pennsylvania 15213
Attn: M. M. Dolinar, Repts Librarian
Explosives Research Center

Central Intelligence Agency 1
2430 E Street, N. W.
Washington, D. C. 20505
Attn: OCD, Standard Dist.

Office of the Director of Defense 1
Research and Engineering
Washington, D. C. 20301
Attn: W. E. Sheehan, Office of Asst.
Dir. (Chemical Technology)

Nat'l Aeronautics and Space Admin. 1
Lewis Research Center
21000 Brookpark Road
Cleveland, Ohio 44135
Attn: Library

John F. Kennedy Space Center, 1
NASA
Cocoa Beach, Florida 32931
Attn: Library

Nat'l Aeronautics & Space Admin. 1
Manned Spacecraft Center
P. O. Box 1537
Houston, Texas 77001
Attn: Library

Nat'l Aeronautics & Space Admin. 1
George C. Marshall Space Flight
Center
Huntsville, Alabama 35800
Attn: Library

Nat'l Aeronautics & Space Admin. 3
Langley Research Center
Langley Air Force Base
Virginia 23365
Attn: Library

Nat'l Aeronautics & Space Admin. 1
Washington, D. C. 20546
Attn: Office of Technical Information
& Education Programs, Code
ETL

Scientific & Tech. Info Facility 2
P. O. Box 5700
Bethesda, Maryland 20014
Attn: NASA Representative

Nat'l Aeronautics & Space Admin. 1
Washington, D. C. 20546
Attn: R. W. Ziem (RPS)

Nat'l Aeronautics & Space Admin. 1
Goddard Space Flight Center
Greenbelt, Maryland 20771
Attn: Library

Defense Documentation Center 20
Cameron Station
Alexandria, Virginia 22314

RTD (RTNP) 1
Bolling AFB
Washington, D. C.

Arnold Eng. Development Center 1
Attn: AEOIM
Air Force Systems Command
Tullahoma, Tennessee 37389

AFRPL (RPR) 1
Edwards, California 92523

AFRPL (RPM) 1
Edwards, California 92523

AFFTC (FTBAT-2) 1
Edwards AFB, California 93523

Office of Research Analysis (OAR) 1
Attn: RRRT
Holloman AFB, New Mexico 88330

AFRPL (RPFDE) 33
Edwards, California 92523

Air Force Missile Test Center 1
Attn: MTBAT
Patrick Air Force Base, Florida 32925

Wright-Patterson AFB, Ohio 1
45433
Attn: AFML(MAAE)

Commanding Officer 1
Ballistic Research Laboratories
Aberdeen Proving Ground, Maryland
Attn: AMXBR-1
21005

Commanding Officer 1
Harry Diamond Laboratories
Washington, D. C. 20438
Attn: AMXDO-TIB

Commanding Officer 1
U.S. Army Research Office (Durham)
Box CM, Duke Station
Durham, North Carolina 27706

Commanding Officer 1
U.S. Army Chemical Research &
Development Laboratories
Edgewood Arsenal, Maryland 21010
Attn: Chief, Physicochemical
Research Division

Commanding Officer 1
Frankford Arsenal
Philadelphia, Pennsylvania 19137
Attn: Propellant & Explosives
Section, 1331

Commanding Officer 1
Picatinny Arsenal
Dover, New Jersey 07801
Attn: Library

Commanding Officer 1
Picatinny Arsenal
Liquid Rocket Propulsion Laboratory
Dover, New Jersey 07801
Attn: Technical Library

U.S. Army Missile Command 4
Redstone Scientific Info. Center
Redstone Arsenal, Alabama 35808
Attn: Chief, Document Section

Commanding General 1
White Sands Missile Range
New Mexico 88002
Attn: Technical Library

Bureau of Naval Weapons 2
Department of the Navy
Washington, D. C. 20360
Attn: DLI-3

Bureau of Naval Weapons 2
Department of the Navy
Washington, D. C. 20360
Attn: RMMP-2

Bureau of Naval Weapons 1
Department of the Navy
Washington, D. C. 20360
Attn: RMMP-3

Bureau of Naval Weapons 1
Department of the Navy
Washington, D. C. 20360
Attn: RMMP-4

Bureau of Naval Weapons 1
Department of the Navy
Washington, D. C. 20360
Attn: RRRE-6

Commander 2
U.S. Naval Missile Center
Point Mugu, California 93041
Attn: Technical Library

Commander 2
U.S. Naval Ordnance Laboratory
White Oak
Silver Spring, Maryland 20910
Attn: Library

Commander 5
U.S. Naval Ordnance Test Station
China Lake, California 93557
Attn: Code 45

Commander (Code 753) 2
U.S. Naval Ordnance Test Station
China Lake, California 93557
Attn: Technical Library

Superintendent 1
U.S. Naval Postgraduate School
Naval Academy
Monterey, California

Commanding Officer 1
U.S. Naval Propellant Plant
Indian Head, Maryland 20640
Attn: Technical Library

Commanding Officer 1
Office of Naval Research
1030 E. Green Street
Pasadena, California 91101

Director (Code 6180) 1
U.S. Naval Research Lab.
Washington, D.C. 20390
Attn: H.W. Carhart

Director 1
Special Projects Office
Department of the Navy
Washington, D.C. 20360

Commanding Officer 1
U.S. Naval Underwater Ordnance Station
Newport, Rhode Island 02844
Attn: W.W. Bartlett

Aerojet-General Corporation 1
P.O. Box 296
Azusa, California 91703
Attn: F.M. West, Chief Librarian

Aerojet-General Corporation 1
11711 South Woodruff Avenue
Downey, California 90241
Attn: Florence Walsh, Librarian

Aerojet-General Corporation 3
P.O. Box 1947
Sacramento, California 95809
Attn: Technical Information Office

Aeronutronic Div. Philco Corp. 1
Ford Road
Newport Beach, California 92600
Attn: Dr. L.H. Linder, Manager
Technical Information Dept.

Aeroprojects, Inc. 1
310 East Rosedale Avenue
West Chester, Pennsylvania 19380
Attn: C.D. McKinney

Aerospace Corporation 2
P.O. Box 95085
Los Angeles, California 90045
Attn: Library-Documents

Allied Chemical Corporation 1
General Chemical Division
Research Lab., P.O. Box 405
Morristown, New Jersey 07960
Attn: L.J. Wiltrakis, Security Officer

Amcel Propulsion Company 1
Box 3049
Asheville, North Carolina 28802

American Cyanamid Company 1
1937 W. Main Street
Stamford, Connecticut 06902
Attn: Security Officer

IIT Research Institute 1
Technology Center
Chicago, Illinois 60616
Attn: C. K. Hersh, Chemistry Div.

ARO, Inc. 1
Arnold Engrg. Dev. Center
Arnold AF Station, Tennessee 37389
Attn: Dr. B. H. Goethert
Director of Engrg.

Atlantic Research Corporation 2
Shirley Highway & Edsall Road
Alexandria, Virginia 22314
Attn: Library

Atlantic Research Corporation 1
Western Division
48-506 Easy Street
El Monte, California
Attn: H. Niederman

Battelle Memorial Institute 1
505 King Avenue
Columbus, Ohio 43201
Attn: Report Library, Room 6A

Bell Aerosystems 1
Box 1
Buffalo, New York 14205
Attn: T. Reinhardt

The Boeing Company 1
Aero Space Division
P. O. Box 3707
Seattle, Washington 98124
Attn: R. R. Barber, Lib. Ut. Ch.

Chemical Propulsion Information 3
Agency
Applied Physics Laboratory
8621 Georgia Avenue
Silver Spring, Maryland 20910

Defense Metals Information Ctr. 1
Battelle Memorial Institute
505 King Avenue
Columbus, Ohio 42301

Douglas Aircraft Co., Inc. 1
Santa Monica Division
3000 Ocean Park Boulevard
Santa Monica, California 90405
Attn: Mr. J. L. Waisman

The Dow Chemical Company 1
Security Section
Box 31
Midland, Michigan 48641
Attn: Dr. R. S. Karpiuk, 1710 Bldg.

E. I. duPont deNemours & Co. 1
Eastern Laboratory
Gibbstown, New Jersey 08027
Attn: Mrs. Alice R. Steward

Esso Research & Engineering Co. 1
Special Projects Unit
P. O. Box 8
Linden, New Jersey 07036
Attn: Mr. D. L. Baeder

General Dynamics/Astronautics 1
P. O. Box 1128
San Diego, California 92112
Attn: Library & Information
Services (128-00)

General Electric Company 1
Flight Propulsion Division
Evendale
Cincinnati, Ohio 45215

Hercules Powder Company 1
Allegany Ballistics Laboratory
P. O. Box 210
Cumberland, Maryland 21501
Attn: Library

Hercules Powder Company 1
Research Center
Wilmington, Delaware 19899
Attn: Dr. Herman Skolnik, Manager
Technical Information Division

Jet Propulsion Laboratory 1
4800 Oak Grove Drive
Pasadena, California 91103
Attn: Library (TDS)
Mr. N. E. Devereux

Arthur D. Little, Inc. 1
15 Acorn Park
Cambridge, Massachusetts 02140
Attn: W. H. Varley

Lockheed Propulsion Company 3
P. O. Box 111
Redlands, California 92374
Attn: Miss Belle Berlad, Librarian

Marquardt Corp. 1
16555 Staticoy Street
Box 2013 - South Annex
Van Nuys, California 91404

Martin Company 1
Baltimore, Maryland 21203
Attn: Science - Technology
Library - Mail 398

Minnesota Mining & Manufacturing 2
Co.
900 Bush Avenue
St. Paul, Minnesota 55106
Attn: Code 0013 R & D
VIA: H. C. Zeman
Security Administrator

Monsanto Research Corporation 1
Boston Labs., Everett Station
Chemical Lane
Boston, Massachusetts 02149
Attn: Library

New York University 1
Dept. of Chemical Engineering
New York, New York 10053
Attn: P. F. Winternitz

North American Aviation, Inc. 1
Space & Information Systems Div.
12214 Lakewood Boulevard
Downey, California 90242
Attn: W. H. Morita

Rocketdyne 3
6633 Canoga Avenue
Canoga Park, California 91304
Attn: Library, Dept. 596-306

Rohm & Haas Company 1
Redstone Arsenal Research Division
Huntsville, Alabama 36808
Attn: Librarian

Space Technology Laboratory, 2
Inc.
1 Space Park
Redondo Beach, California 90200
Attn: STL Tech. Lib. Doc.
Acquisitions

Texaco Experiment Incorporated 1
P. O. Box 1-T
Richmond, Virginia 23202
Attn: Librarian

United Technology Center 1
P. O. Box 358
Sunnyvale, California 94088
Attn: Librarian

Thiokol Chemical Corporation 1
Alpha Division, Huntsville Plant
Huntsville, Alabama 35800
Attn: Technical Director

Thiokol Chemical Corporation 1
Alpha Division
Space Booster Plant
Brunswick, Georgia 31500

Thiokol Chemical Corporation 1
Elkton Division
Elkton, Maryland 21921
Attn: Librarian

Thiokol Chemical Corporation 1
Reaction Motors Division
Denville, New Jersey 07834
Attn: Librarian

Thiokol Chemical Corporation 1
Rocket Operations Center
P. O. Box 1640
Ogden, Utah 84401
Attn: Librarian

Thiokol Chemical Corporation 2
Wasatch Division
P. O. Box 524
Brigham City, Utah 84302
Attn: Library Section

Union Carbide Chemicals Co. 1
P. O. Box 8584 (Technical Center)
South Charleston, West Virginia
25303 Attn: Dr. H. W. Schulz

United Aircraft Corporation 1
Pratt & Whitney Fla. Res. & Dev. Ctr.
P. O. Box 2691
W. Palm Beach, Florida 33402
Attn: Library

United Aircraft Corporation 1
Corporation Library
400 Main Street
East Hartford, Connecticut 06118
Attn: Dr. David Rix

General Electric Company 1
Apollo Support Department
P. O. Box 2500
Dayton Beach, Florida 32015

British Defence Staff * 4
British Embassy
3100 Massachusetts Avenue
Washington, D. C. 20008
Attn: Scientific Information Officer

Defence Research Member * 4
Canadian Joint Staff (W)
2450 Massachusetts Avenue
Washington, D. C. 20008

Commanding Officer 1
Ammunition Procurement & Supply
Agency
Joliet, Illinois 60400
Attn: Engr. Library

AFRPL (RPCS) 1
Edwards, California 93523

Callery Chemical Company 1
Research & Development
Callery, Pennsylvania 16024
Attn: Document Control

Ethyl Corporation 1
P. O. Box 3091
Istrouma Branch
Baton Rouge, Louisiana 70805

Hercules Powder Company 1
Bacchus Works
Magna, Utah 84044
Attn: Librarian

Hynes Research Corporation 1
308 Bon Air Avenue
Durham, North Carolina 27704

Walter Kidde Company 1
675 Main Street
Belleville, New Jersey 07109
Attn: Security Librarian

Olin Mathieson Chemical Corp. 1
Marion, Illinois 62959
Attn: Research Library
Box 508

Olin Mathieson Chemical Corp. 1
Research Library 1-K-3
275 Winchester Avenue
New Haven, Connecticut 06511
Attn: Mail Control Room
Miss Laura M. Kajuti

Pennsalt Chemicals Corporation 1
Technological Center
900 First Avenue
King of Prussia, Pennsylvania 19406

Purdue University 1
Lafayette, Indianna 47907
Attn: M. J. Zucrow

Rocketdyne, A Division of 1
North American Aviation, Inc.
Solid Propulsion Operations
P. O. Box 548, McGregor, Texas
76657
Attn: Library

Shell Development Company 1
1400 53rd Street
Emeryville, California 94608

Southwest Research Institute 1
Department of Structural Research
8500 Culebra Road
San Antonio, Texas 78228
Attn: Dr. Robert C. DeHart, Director

Texaco, Inc. 1
P. O. Box 509
Beacon, New York 12508
Attn: Dr. R. E. Conary, Manager

Los Alamos Scientific Laboratory 1
University of California
P. O. Box 1663
Los Alamos, New Mexico 87544

Headquarters, U. S. Air Force 1
Washington, D. C.
20330
Attn: AFRSTD

AFRPL (RPCL) 1
Edwards, California 93523

Callery Chemical Company 1
Research & Development
Callery, Pennsylvania 16024
Attn: Document Control

Chem. Research & Dev. Center 1
FMC Corporation
P. O. Box 8
Princeton, New Jersey 08540
Attn: Security Officer

Ethyl Corporation 1
P. O. Box 3091
Istrouma Branch
Baton Rouge, Louisiana 70805

Hynes Research Corporation 1
308 Bon Air Avenue
Durham, North Carolina 27704

Walter Kidde Company 1
675 Main Street
Belleville, New Jersey 07109
Attn: Security Librarian

Olin Mathieson Chemical Corp. 1
Research Library 1-K-3
275 Winchester Avenue
New Haven, Connecticut 06511
Attn: Mail Control Room
Miss Laura M. Kajuti

Pennsalt Chemicals Corporation 1
Technological Center
900 First Avenue
King of Prussia, Pennsylvania 19406

Distribution List (Cont'd) p 8

Purdue University 1
Lafayette, Indiana 47907
Attn: M. J. Zucrow

Shell Development Company 1
1400 53rd Street
Emeryville, California 94608

Southwest Research Institute 1
Department of Structural Research
8500 Culebra Road
San Antonio, Texas 78228
Attn: Dr. Robert C. DeHart, Director

Texaco, Inc. 1
P. O. Box 509
Beacon, New York 12508
Attn: Dr. R. E. Conary, Manager

* Reports prepared under a Department of the Air Force contract or project will be transmitted VIA:

Headquarters
Air Force Systems Command
Attn: SCS-41(3-1833)
Andrews Air Force Base
Washington, D. C. 20331